University of South-Eastern Norway

www.usn.no

FMH606 Master's Thesis 2023

Energy and Environmental Technology

Simulation and analysis of waterflooding oil recovery through advanced horizontal wells

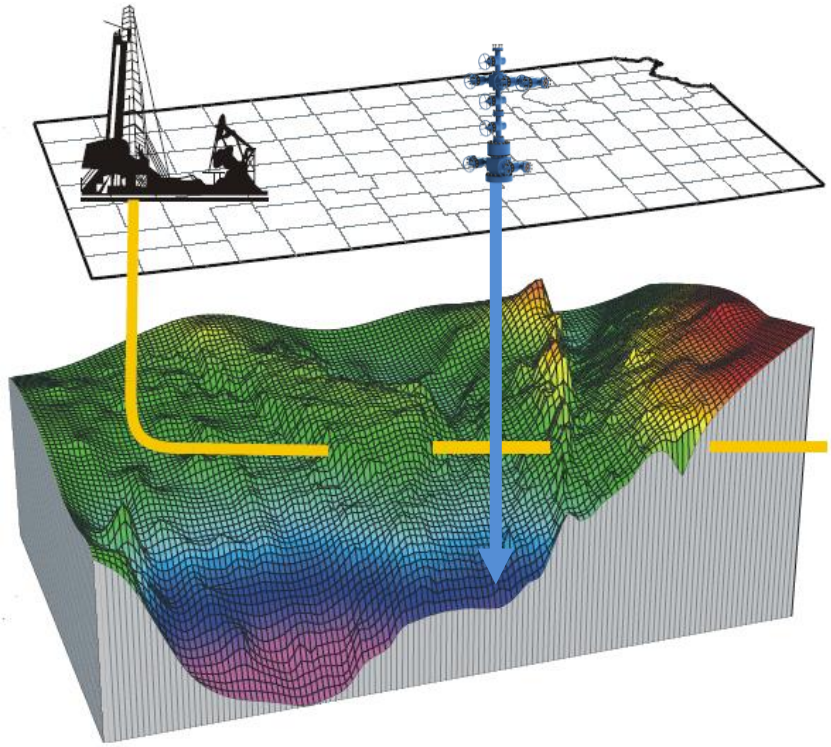

Juwan Gomasge Madhawee Anuththara

University of South-Eastern Norway

www.usn.no

Course: FMH606 Master's Thesis, 2023

Title: Simulation and analysis of waterflooding oil recovery through advanced horizontal wells

Number of pages: 122

Keywords: oil production simulation, improved oil recovery, advanced horizontal well, flow control devices, ECLIPSE, OLGA

Student: Juwan Gomasge Madhawee Anuththara

Supervisor: Prof. Birtt M.E. Moldestad, Prof. Amaranath S. Kumara, and Ali Moradi

External partner: **Equinor and SINTEF**

Summary:

The oil industry has been a significant source of energy for many years, but over 50% of oil in existing fields in NCS cannot be produced by using current enhanced and improved oil recovery technologies. Various IOR methods have been tested in the world to improve the efficiency of oil recovery methods. Long horizontal wells are commonly used in industry to maximize the oil production, but they can lead to early gas or water breakthroughs due to the water conning effect. To overcome this issue, different inflow control devices such as ICDs, AICVs, and AICDs are used in oil well completion. This thesis aims to study the performance of advanced well technologies for oil production from reservoirs with different oil viscosities using a unique approach of coupling the ECLIPSE simulator for reservoir simulation and the OLGA simulator for oil well simulation. Simulations for oil production with advanced well completions were conducted for a heavy and light oil reservoir using two vertical and one horizontal water injection wells, respectively, as the IOR method. Before the water breakthrough, AICDs and AICVs were fully open and acted like ICDs. After the breakthrough, AICD and AICV closed partially due to increasing WC. FCDs delayed the water breakthrough by 10 and 180 days for heavy and light oil reservoirs, respectively. Moreover, the cumulative oil production has increased slightly, and the cumulative water production has decreased considerably in both cases because of FCDs. Therefore, oil well completion with FCDs can potentially increase the efficiency of oil production by maximizing profit and by minimizing unwanted fluids production. Furthermore, it can be concluded that coupling the ECLIPSE/OLGA simulators has been successful at the end of the thesis.

Preface

This master's thesis shows the research work carried out in the spring of 2023 at the University of South-Eastern Norway (USN), Porsgrunn. This research work and thesis are being conducted as part of the requirement for the Master of Science degree at USN.

The main objective of this thesis was to conduct simulations for oil production with advanced inflow control technologies like ICD, AICD, and AICV by using OLGA/ECLIPSE software. This is a part of the ongoing project *Digiwell*, in corporation with Equinor and SINTEF companies.

This thesis was supervised by Prof. Britt Margrethe Emilie Moldestad, Prof. Amaranath S. Kumara, and PhD scholar Ali Moradi with whom I have learned and broadened my knowledge and skills immensely during this thesis.

First and foremost, I would like to express my sincere gratitude and appreciation to Prof. Britt Margrethe Emilia Moldestad, my thesis supervisor and co-supervisor who guided me throughout the thesis. Especially, I would like to thank them for their valuable time spent evaluating my work and giving me valuable advice. I would like to thank Ali Moradi, my thesis co-supervisor, who was always there for me whenever I needed support. His keen observations and guidance towards work always motivated me to work harder on my thesis.

I would also like to take this opportunity to thank the staff of the library and the IT department of at USN for providing me with various support whenever needed.

Finally, I would like to thank my family, who constantly encouraged and supported me to do my best in completing the thesis.

Porsgrunn, 14.05.2023

Juwan Gomasge Madhawee Anuththara

Contents

Nomenclature

Symbols and expressions		Unit
A	Area	m^2
a_{AICD}	AICD valve strength parameter	-
a_{AICV}	AICV valve strength parameter	-
A_{vc}	Vena Contracta area	m^2
A_v	Specific surface area of pores	m^2
B_g	Gas formation factor	-
B_o	Oil formation factor	-
C_D	Discharge coefficient	-
d_p	Diameter of spherical grains	m
D, d	Diameter	m
g_c	Conversion factor	-
k_H	Horizontal permeability	-
k_H	Horizontal permeability	-
k_V	Vertical permeability	-
k_{ei}	Effective permeability of that fluid i	-
k_{ri}	Relative permeability of that fluid i	-
k_{ro}	Relative permiability of oil	-
k_{rocw}	Maximum relative permiabilty of oil	-
k_{rw}	Relative permiability of water	-
k_{rwro}	Maximum relative permiabilty of water	-
k_{sp}	Geometric average permeability	-

k_x	Permeability in x-direction	-
S_o	Oil saturation	-
S_{ro}	Residual oil saturation	-
S_w	Water saturation	-
S_{wc}	Irreducible water saturation	-
T_S	Standard temperature 288.71 K	K
p_b	Bubble point pressure	Pa
γ_g	Specific gravity of gas	-
γ_o	Specific gravity of petroleum oil	-
δ_{ow}	Oil-water interfacial tension	N/m
θ_{ow}	Oil-water contact angle	-
μ_{cal}	Calibration viscosity	cP
μ_g	Gas viscosity	cP
μ_o	Unsaturated oil viscosity	cP
μ_{ob}	Satuarated (bubble point) oil viscosity	cP
μ_{od}	Dead oil viscosity	cP
ρ_{air}	Density of oil	kg/m^3
ρ_g	Density of gas	kg/m^3
ρ_o	Density of the oil	kg/m^3
ρ_w	Density of the water	kg/m^3
ϕ_a	Absolute porosity	-
ΔP_f	Frictianl pressure drop	Pa
T	Temperature	K

Z	Compressibility factor	-
K	Geometric constant	-
L	Pipe length	m
P	Pressure	Pa
Q	Volumetric flow rate	m^3/s
Re	Renolds number	-
f	Mody friction factor	-
k	Permeability	D (Darcy)
p	Reservoir pressure	Pa
r	Radius	m
α	Volume fraction	-
ε	Absolute roughness	m
μ	Viscosity	cP
v	Velocity	m/s
ρ	Density	kg/m^3
τ	Tortuosity	-
ϕ	Effective porosity	-

Abbreviations		**Unit**
AICD	Autonomous inflow control devices	
AICV	Autonomous inflow control valves	
AMW	Advanced multilateral wells	
BC	Before christ	-

C-C	Carbon-carbon	-
C-H	Carbon-hydrogen	-
CO_2	Carbon dioxide	-
EJ	Exajoule	EJ
EOR	Enhanced oil recovery	-
EOS	Equation of state	
FCD	Flow control devices	
FD-AICD	Fluidic diode autonomous inflow control devices	
GLR	Gas-liquid ratio	
GOR	Gas-oil ratio	
ICD	Inflow control devices	
IOR	Improved oil recovery	-
LPG	Liquefied petroleum gas	-
MSW	Malti segment well	
MW	Molecular weight	
N_2	Nitrogen	-
NCS	Norwegian continental shelf	-
NPD	Norwegian Petroleum Directorate	-
OG21	Oil and Gas for the 21st century	-
PVT	pressure-volume-temperature	
RCP-AICD	Rate controlled autonomous inflow control devices	
scm	Standard cubic meters	Sm^3
WAG	Water altering gas	-
WC	Water cut	

Overview of figures and tables

List of figures

List of tables

1 Introduction

This thesis addresses the new technological approaches for effective oil recovery. The introduction chapter focuses on the background that motivated this study, problem description, objectives, and report structure.

1.1 Background of the study

The creation of the kerosene lamp in 1854 sparked a significant increase in the need for petroleum. This demand led to Edwin L. Drake's historical drilling of the first oil well in Titusville, Pennsylvania, in 1859, which marked the start of the contemporary oil industry [1], [2]. Since then, the oil industry has been a dominant force in the energy sector for many decades, providing a significant portion of the world's energy supply. Figure 1.1 illustrates the historical and projected global energy supply by primary energy sources.

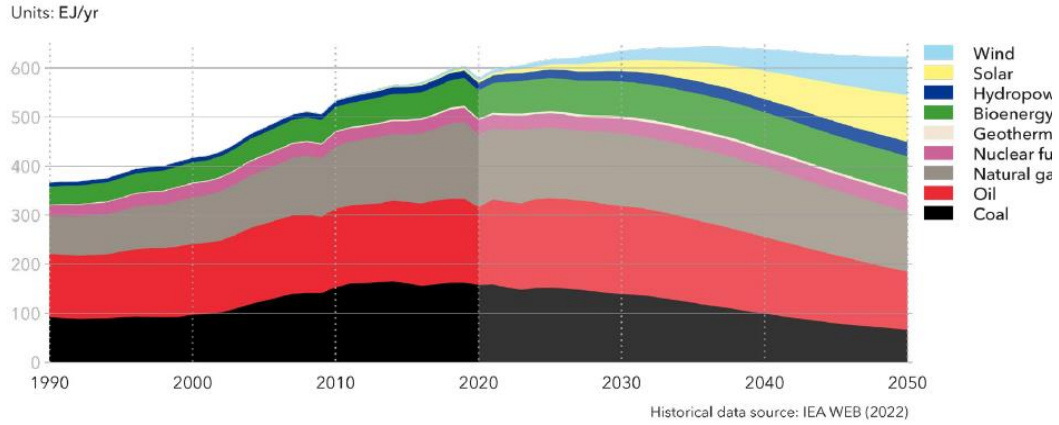

Units: EJ/yr

Source	2020	2030	2040	2050
Wind	6	20	44	79
Solar	5	21	57	95
Hydropower	15	21	27	29
Bioenergy	57	73	74	76
Geothermal	4	5	5	5
Nuclear	28	29	33	31
Natural gas	149	149	143	123
Oil	159	179	156	118
Coal	157	139	99	66
Total	**579**	**635**	**638**	**623**

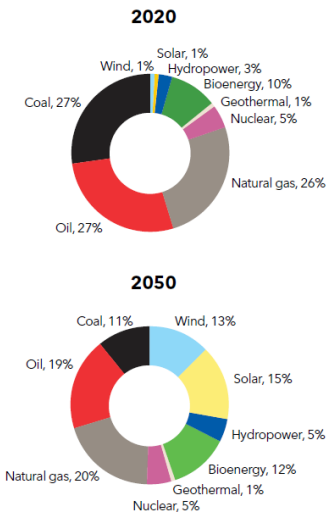

Figure 1.1: World primary energy supply by source [3].

As per the DNV Energy Transition Outlook 2022 [3], the consumption of oil and gas accounted for 53% of the world's energy requirement in 2020. Primary energy supply is predicted to peak in 2036 at 643 EJ per year, which is 8% higher than the current level. It is then expected to remain relatively stable until 2050. Despite the increasing adoption of renewable energy sources, it is projected that oil and gas will still fulfill 39% of the world's energy needs in 2050. This suggests that oil and gas will continue to be a significant contributor to the global energy mix for the foreseeable future, even as efforts are made to transition to more sustainable and cleaner energy sources.

Moreover, in an energy transition period, improving the efficiency of oil recovery methods is important for several reasons. The improved efficiency of oil recovery methods can represent cost savings for companies, which will contribute to the economic viability of projects and provide an incentive for continued investments. And also, enhancing oil recovery methods are important to maximize the amount of oil that can be extracted from existing fields so that resources can be utilized as efficiently as possible.

Norway's contribution to the oil industry has been significant, both in terms of production and technology development. Currently, Norway supplies about 2% of the world's oil consumption [4]. The Norwegian Continental Shelf (NCS) is globally recognized for its advanced petroleum technology. In 2001, the Ministry of Petroleum and Energy established a board with the mandate of developing a strategic plan known as OG21 (Oil and Gas for the 21st century) [5]. The purpose of this strategy was to help NCS sustain its competitive position in the global market by staying ahead in the adoption of the latest technological innovations. The goal was to ensure that the NCS could continue to create value from its oil and gas resources in an efficient, secure, and environmentally friendly manner that would benefit present and future generations [5].

According to the Resource Report 2022 by the Norwegian Petroleum Directorate (NPD) [6], figure Figure 1.2 illustrates the oil reserves and resources of the largest oil fields in the Norwegian Continental Shelf (NCS). The gray column represents the volume of oil that has already been extracted from these fields. The dark green column shows the amount that is planned to be produced with available technology before the fields cease operations. The column colored in light green represents the unrecoverable oil resources that are presently impractical to extract due to factors such as high expenses or technological constraints. This indicates that the recovery of over 50% of oil in existing wells cannot be produced with available technology [6], [7].

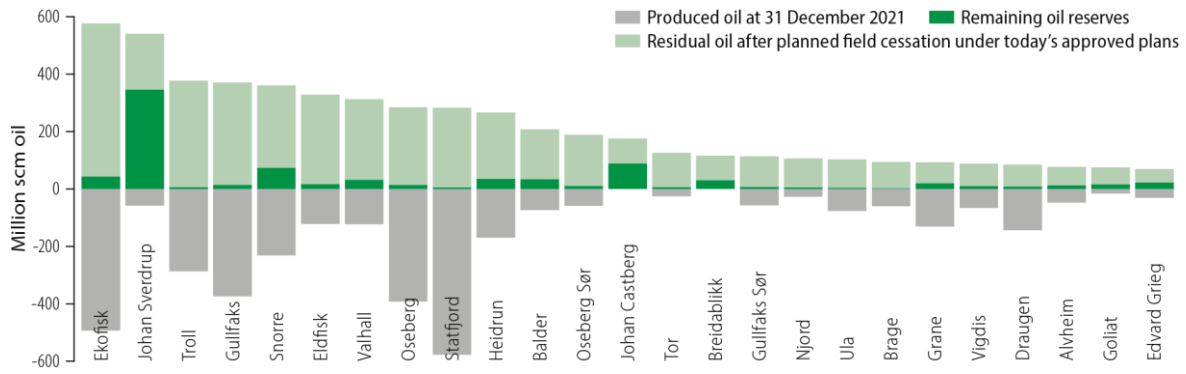

Figure 1.2: Oil reserves and resources for the largest oil fields in NCS by 2022 [6].

The Resource Report 2022 by NPD states that the implementation of improved oil recovery projects can enhance oil production. These methods include water injection, gas injection, thermal recovery through steam injection to increase pressure and displace oil, and chemical flooding techniques such as polymer and surfactant flooding to reduce viscosity and improve oil mobility. Figure 1.3 displays project data about 184 improved oil and gas recovery methods for various fields. The data predicts that the adoption of 13 projects for injection and advanced methods can increase oil recovery by approximately 10 million standard cubic meters (scm) [6].

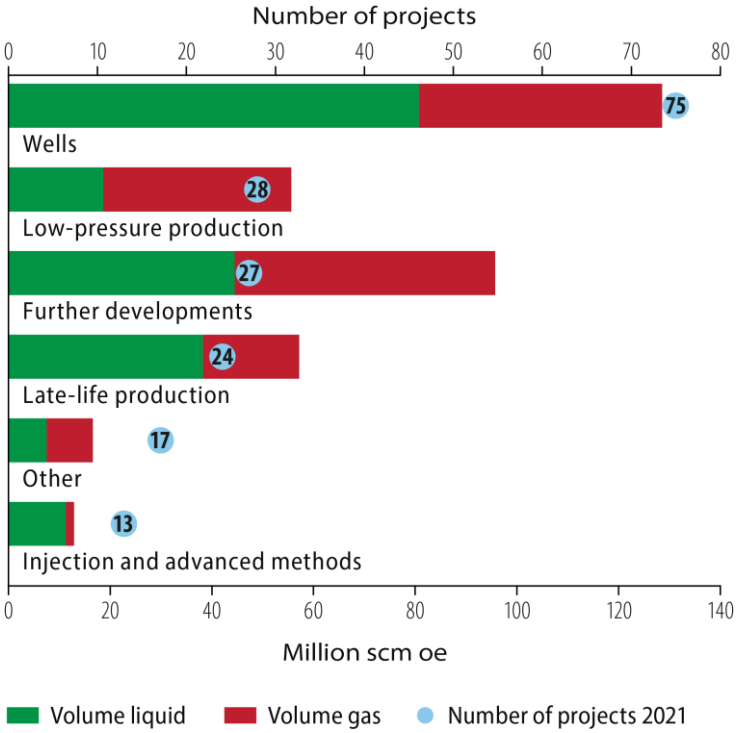

Figure 1.3: Specific projects for improved oil and gas recovery from fields, numbers, and resources [6].

Overall, these trends imply that further innovations and improved technology are needed for a cost-effective and efficient oil industry. To maximize oil production and recovery, it is important to obtain maximum reservoir contact and to prevent the negative effects of early gas or water breakthroughs [8]. Long horizontal wells can be used to achieve this goal, especially in reservoirs with thin oil columns. However, there are some challenges associated with horizontal wells, such as early gas/water breakthrough. This is caused by the water conning effect towards the heel due to the heel-toe effect and heterogeneity along the horizontal well. To address this issue, passive inflow control devices (ICDs), autonomous inflow control valves (AICVs), and autonomous inflow control devices (AICDs) are widely used in oil well completion. ICDs can balance the drawdown pressure along the horizontal well, thus preventing an early water breakthrough, but they cannot choke the water once it eventually enters the well. The use of AICDs will provide both a delay in the early water breakthrough as well as the possibility of partially choking back water automatically, thereby reducing any adverse effects associated with early water breakthrough. AICD's good performance is limited

to medium and light viscosity oil reservoirs, while AICDs can provide better performance for heavy viscosity oil reservoirs [7], [9]–[11]. The appropriate selection of inflow control technologies is dependent on the reservoir characteristics, such as the permeability of the formation, the fluid properties, and the reservoir pressure.

Multilateral wells are another well-completion technique utilized to enhance oil recovery. This advanced drilling method involves a single mother bore and several horizontal sections, also known as laterals, which connect to it. Multilateral wells enable access to multiple areas of the reservoir without the need for constructing additional wells, resulting in reduced total costs for well construction [12]. This design provides several advantages, such as accessing multiple zones and increasing the contact area between the wellbore and the reservoir. However, the use of a multilateral well completion is only suitable for reservoirs that exhibit certain characteristics, such as good connectivity between different zones or layers and high permeability.

Consequently, applying inflow control technologies in multilateral well completions and using EOR/IOR technologies would have significant potential to extract non-recoverable oil resources cost-effectively. Effective oil well completion and the appropriate selection of inflow control technologies are essential to maximize oil recovery from a reservoir. The selection of these technologies depends on more accurate knowledge of the reservoir characteristics and conditions. With such knowledge, it is possible to predict the optimal water injection flow rates, operating conditions, and maximum potential oil production over a specific period. For that, computer-based modeling and simulation software are commonly used. These software packages use complex algorithms to simulate reservoir performance under various scenarios, allowing for optimizing production rates and identifying potential issues. OLGA, ROCX, and ECLIPSE are among the most widely used well and reservoir modeling and simulation software packages. OLGA is a dynamic multiphase flow simulator that can simulate complex well configurations and flow regimes, while ROCX and ECLIPSE are reservoir simulation software that provide accurate predictions of production rates and reservoir performance. By coupling OLGA with either ROCX or ECLIPSE, more advanced and effective oil recovery models can be developed, which is a promising approach for technological advancement in the future.

1.2 Problem description

The use of water flooding to improve oil recovery is a well-established method in the industry. However, the effectiveness of various water flooding methods varies depending on several factors specific to the reservoir. Maximizing well reservoir contact using long horizontal wells is a fundamental principle to achieve cost-effective and efficient oil recovery. However, a major challenge associated with the use of such wells is the occurrence of early water/gas breakthroughs caused by the heel-to-toe effect and reservoir heterogeneity. To overcome this challenge, inflow control devices are widely used in the oil industry. Inflow control technologies have shown an improvement in the oil recovery in horizontal wells, an area of ongoing research and development. ICDs, AICDs, and AICVs are the three main categories of flow control devices. The efficiency of flow control devices can be influenced by the unique properties of each reservoir. Prior to implementing these technologies in an existing reservoir, it is customary to perform oil production simulations to determine the most effective methods for increasing oil recovery. Various simulation tools, including OLGA, ECLIPSE, and ROCX,

are used in the industry for this purpose. OLGA is a production well simulator, and ECLIPSE and ROCX are mainly used for reservoir simulation. Several research studies have been carried out on the OLGA/ROCX software combination. However, there is a research gap regarding the use of OLGA/ECLIPSE software combinations for oil production simulations of advanced wells. This thesis aims to address this gap.

1.3 Objective

The main objective of the thesis is to study, model, and simulate oil production from synthetically designed heavy and light oil reservoirs by coupling ECLIPSE and OLGA, which are reservoirs and well simulators, respectively. Oil is produced from advanced horizontal wells, and water flooding is used as an improved oil recovery method. This project will aim to achieve the following goals in order to achieve its main purpose.

- Literature study for the evolution of oil recovery, application of improved oil recovery methods, and for various inflow control technologies.
- Synthetically designing the reservoirs based on required reservoir properties.
- Location optimization for vertical water injections.
- Development of reservoir model in ECLIPSE and well model in OLGA. And coupling them to develop a dynamic model of oil production.
- Implementation of the autonomous function of AICD and AICV in OLGA.
- Analyzing the impact of FCDs and water flooding method on early water breakthrough.
- Comparing the functionality of ICD, AICD, and AICV with the OPENHOLE case.
- Discussing the challenges in water flooding oil recovery and suggestions for further works.

1.4 Thesis structure

The report contains seven chapters. The first chapter of the thesis provides an overview of the study's background, the problem description, and the thesis' objectives. Chapter 2 is the literature review for the evolution of oil recovery methods, how water flooding oil recovery method has been used specifically used in industry, horizontal well technology, different inflow control technologies, and various modeling and simulation tools used. Chapter 3 introduces the necessary theories, principles, and equations for the study. In Chapter 4, all methods, procedures, and calculations involved in the development of the OLGA/ECLIPSE model are described. It is explained in Chapter 5 how the OLGA/ECLIPSE model was developed and how simulations were conducted for different cases. Chapter 6 presents and discusses the simulation results, discusses the challenges in water flooding, and offers some suggestions for future research. And at the end, chapter 7 concludes the study.

2 Literature review

In this chapter, the evolution of conventional oil recovery methods through decades, a detailed review of some new technological innovations, and the use of computer-based modeling and simulation in oil recovery will be discussed based on information from numerous research studies.

2.1 Evolution of oil recovery methods

The use of crude oil dates to ancient times, with records of oil seeps being used by the Babylonians for medicinal purposes and evaporated seep oil (bitumen) was used in the construction of boats, plumbing, and bricks, waterproofing agents as early as the 18th century BC [1]. However, the commercial exploitation of crude oil did not begin until the mid-19th century. The invention of the kerosene lamp in 1854 led to the first large-scale demand for petroleum [1]. In 1859, Edwin L. Drake drilled the first oil well in Titusville, Pennsylvania, marking the beginning of the modern oil industry [2]. Initially, oil was recovered through manual digging and the use of hand pumps, but these methods were soon replaced by more efficient techniques.

The first major technological breakthrough in crude oil recovery was the introduction of rotary drilling in the early 1900s [13]. This involved drilling a hole into the ground with a rotating drill bit and using mud to lubricate and cool the drill bit. The use of mud reduced the friction and prevented the well from collapsing, allowing for deeper and more efficient drilling. After drilling and opening the first well for production, trapped hydrocarbons begin to flow towards the well due to the over-pressure in the reservoir. This technique is called primary oil recovery which only recovers around 5% to 15% of the total potential of the well potential.

As the reservoir pressure decreases, the flow of hydrocarbons also decreases. To maintain pressure and to enhance the production of more profitable hydrocarbons, water or gas was injected into the reservoir from separate injection wells, in the mid-20th century [14]. In this method, injected liquid displaces the oil and pushes it toward the production well, allowing for more oil to be recovered. This is called *secondary oil recovery*, which enhances the recovery of up to 45% of oil in the reservoir [15].

Even though oil recovery efficiency generally has been at around 30% to 50%, it has increased quite significantly in recent decades. At this point, *tertiary oil recovery* processes come into play, which can recover oil beyond primary and secondary methods. During tertiary oil recovery, fluids other than conventional water and immiscible gas are injected into the formation to enhance oil production. And also, advanced technologies such as hydraulic fracturing (fracking) and horizontal drilling have revolutionized the oil industry in recent years. Fracking involves injecting a high-pressure mixture of water, sand, and chemicals into the rock formation to create fractures and allow oil and gas to flow more easily to the wellbore [16], [17]. Horizontal drilling involves drilling a wellbore at an angle and then turning it to follow a horizontal path through the oil-bearing formation, allowing greater access to the oil reservoir [17]. These new advanced technologies used to optimize oil recovery can be categorized into two methods named enhanced oil recovery (EOR) and improved oil recovery (IOR).

2.1.1 Improved oil recovery (IOR)

Improved oil recovery has not been defined properly, and most of the research articles and books mention that IOR is a synonym for EOR to some extent [18]–[20]. But according to George (2003) [21],

"IOR refers to any practice to increase oil recovery beyond primary production. That can include EOR processes as well as all secondary recovery processes, such as water flooding and gas pressure maintenance. [21]*"*

This definition of IOR encompasses a diverse range of production technologies [18],

- **Secondary recovery methods:** Waterflooding and gas flooding.
- **EOR:** Thermal recovery, miscible flooding, and chemical flooding
- **Complex well drilling:** Horizontal wells, multilateral wells.
- **Well stimulation**: Hydraulic fracturing.

This definition of IOR permits the utilization of additional vertical wells to enhance well coverage also, which may not have been included in the initial development plan.

2.1.2 Enhanced oil recovery (EOR)

Enhanced oil recovery (EOR) is a technique that involves injecting fluids or energy into an oil reservoir to recover the oil that can't be extracted by conventional recovery methods [18]. But this technique can be utilized at any stage of oil recovery, whether it be primary, secondary, or tertiary recovery. In cases where EOR is applied after a waterflooding or an immiscible gas injection, it is considered a tertiary process. Alternatively, if EOR is employed directly following primary recovery, it can be classified as a secondary process [19]. The applicable EOR methods for a given reservoir depend on the nature and the characteristics of the reservoir and containing fluid [18]. Generally, EOR methods can be categorized into 3 as follows [22], [23].

2.1.2.1 Thermal recovery

Thermal recovery is a term used to describe heat injection processes into a reservoir to produce thick, viscous oils with API gravities of less than 20. To flow toward the producing wells, oil must be heated so that its viscosity can be reduced. In the process of thermal recovery, crude oil undergoes physical and chemical changes because of heat introduction. Consequently, physical properties such as viscosity, specific gravity, and interfacial tension change, as well as chemical changes such as cracking and dehydrogenation occur. It involves a variety of chemical reactions, including cracking, which involves the destruction of C-C bonds to form lower molecular weight compounds, and dehydrogenation, which involves the rupture of C-H bonds [24]. Thermal recovery can be mainly subdivided into two methods as follows,

- **Hot fluid injection:** Steam flooding, hot water flooding
- **In-situ combustion process:**

This involves injecting a gas with oxygen, like air, into the reservoir to generate a fire. The heat generated from burning the heavy hydrocarbons in the reservoir causes hydrocarbon cracking, vaporization of light hydrocarbons and reservoir water, and deposition of heavier hydrocarbons (coke). As the fire moves, the burning front ahead a mixture of hot combustion gases, steam,

and hot water. This can reduce the oil viscosity and then displaces oil towards production wells. In situ combustion is also called fire flooding or fire-flood [25]. Figure 2.1 represents the schematic diagram of in-situ combustion oil recovery process.

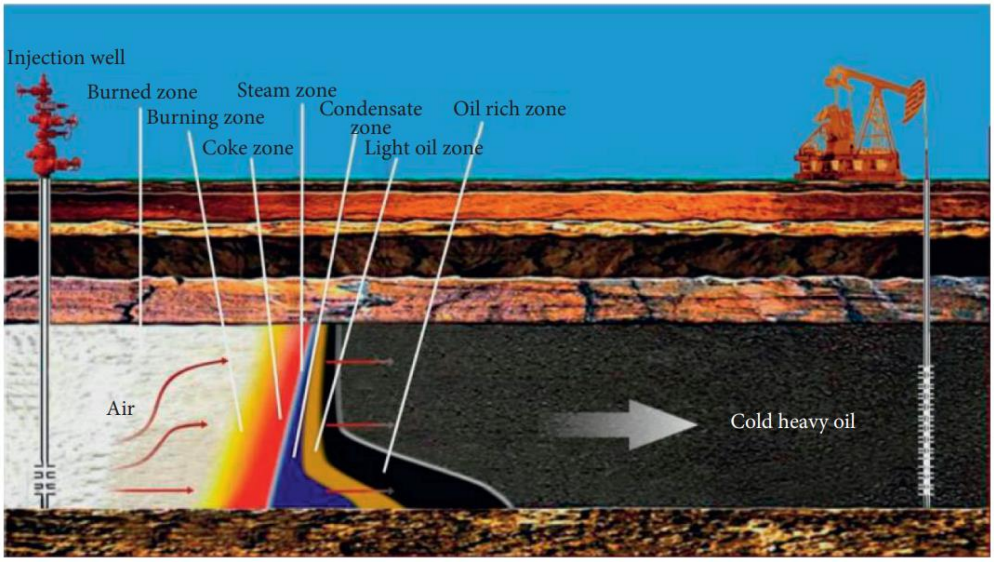

Figure 2.1: Schematic diagram of in-situ combustion oil recovery process [26].

2.1.2.2 Miscible flooding

Miscible flooding is a very popular EOR method due to its high effectiveness. In this process, a gas that is miscible (i.e., capable of forming a homogeneous mixture) with oil is injected into the reservoir. The gas and oil mixture becomes a single-phase fluid with uniform properties, which helps to reduce the interfacial tension between the oil and the rock surfaces. This makes it easier for oil to flow through the porous rock and into production wells. The injected gas also helps to "push" the oil towards the production wells by maintaining high pressure in the reservoir. The injected gas is usually carbon dioxide (CO_2) or nitrogen (N_2), liquefied petroleum gas (LPG), methane, ethane, and propane. But the most common gas is CO_2 due to its low cost and ability to reduce the oil viscosity [27]. However, it is also a relatively expensive process and is generally used only in mature oil fields where the cost of the process can be justified by the increased oil recovery.

2.1.2.3 Chemical flooding

Generally, in this method, chemical solutions are injected into the reservoir to increase the amount of oil that can be extracted. The chemicals used in chemical flooding are typically surfactants, polymers, and alkalis.

- **Surfactants**: Surfactants are used to reduce the surface tension of the oil, allowing it to flow more easily through the reservoir.
- **Polymers**: Polymers are used to increase the viscosity of the injected fluid, which helps to displace the remaining oil from the reservoir. Increased viscosity reduces water breakthrough towards the production wells. Consequently, polymer flooding increases the sweep efficiency of the oil in the reservoir. Polymer flooding is more suitable for viscous reservoir fluids. Figure 2.2 illustrates this phenomenon.

- **Alkalis**: Alkalis are used to react with and neutralize acids that may be present in the reservoir, which can improve the performance of the other chemicals.

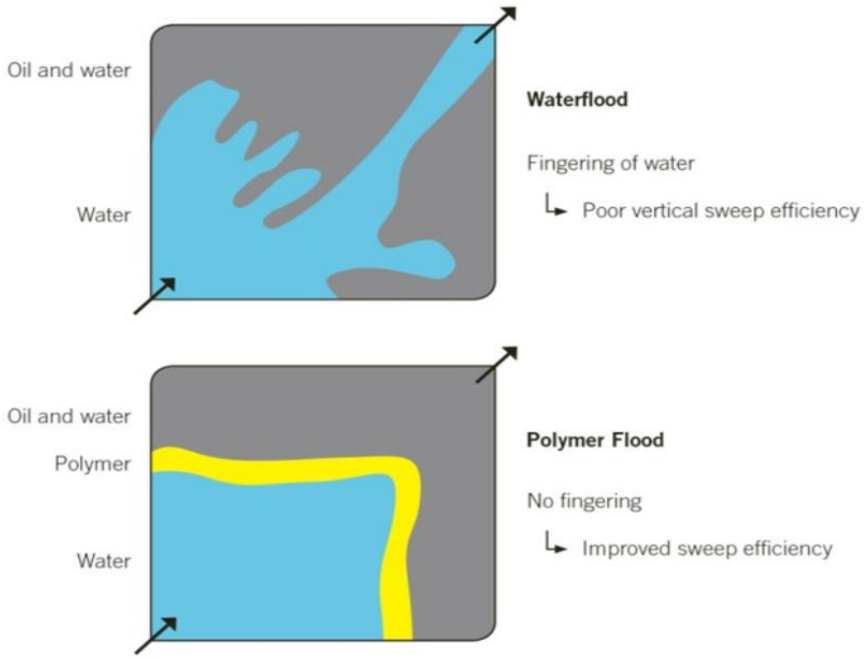

Figure 2.2: An illustration of typical polymer flooding operation [28].

Chemical flooding is mostly used in combination with other EOR techniques, such as water flooding or gas injection. However, it can be a complex and expensive process, and the success of the method depends on numerous factors, including the type of reservoir, the characteristics of the oil and rock, and the specific chemicals used [22].

2.1.3 The potential of different oil recovery methods in NCS

According to the Resource Report 2022 of the Norwegian Petroleum Directorate (NPD) [6], they have identified substantial potential for oil production related to various EOR methods, as shown in Figure 2.3. This analysis is based on 27 fields in NCS, including the 25 largest oil fields in Figure 1.2. According to this analysis, miscible WAG (Water Altering Gas) with hydrocarbon gas and law salinity water injection has the highest technical potential for enhanced oil recovery.

Miscible WAG with hydrocarbon gas: This is a combined method of miscible flooding and waterflooding. This involves alternating injections of hydrocarbon gas and water that are miscible with the oil in the reservoir. The gas is injected to help sweep the oil towards the production wells, while the liquid injection maintains reservoir pressure and helps to maintain the miscibility of the gas and oil [29].

Low salinity waterflooding: This is a waterflooding technique that involves injecting water with reduced salt content into an oil reservoir to improve oil recovery. It is based on the concept that the interaction between the injected water and the reservoir rock alters the rock's wettability

and reduces the capillary forces that trap the oil in the rock pores. This makes immobile oil more mobilized, allowing the oil to flow more easily and be produced at a faster rate [29].

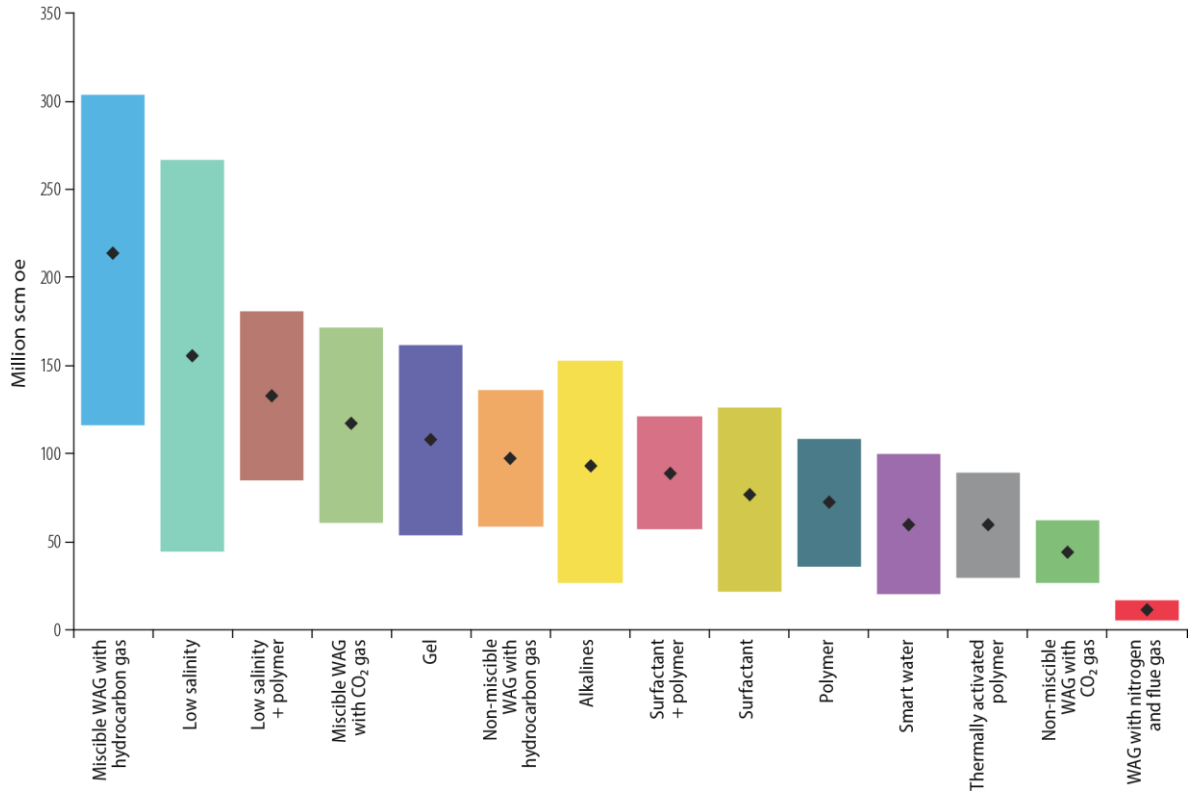

Figure 2.3: Oil recovery potential with different EOR methods for oil fields in NCS by 2022 [6].

Compared to conventional methods, offshore EOR projects typically require a significant amount of investment in terms of capital and operational costs, but they can yield extra oil recovery. The total capital cost of EOR projects depends on numerous factors, including the size of the oil field and the geological complexity of the reservoir. As well pilot testing to determine the recovery potential and technical feasibility is also included in the capital costs. However, due to the equipment and infrastructure requirements, EOR methods that require miscible gases (hydrocarbon gas) or low salinity water injection have the highest capital costs. In addition to the high capital costs, operation costs are higher due to the use of expensive chemicals. In order to determine the most cost-effective EOR method for an oil field, a comprehensive cost estimation that addresses technical, financial, and operational factors is needed [7], [29].

2.2 Waterflooding oil recovery

Generally, waterflooding is injecting water into the oil reservoir to enhance oil recovery. Although this method was recognized in 1880, it was not applied field-wide until 1930 [30]. Figure 2.4 illustrates how displacements happen in both the pore level and the larger scale. As explained in the earlier sections, several complex and advanced techniques have been developed over the years to enhance the recovery of oil reserves left behind by inefficient primary recovery methods.

While some of these processes have the potential to recover more oil than waterflooding in a particular reservoir, the waterflooding process remains the most widely used fluid injection technique. This is mainly due to the following reasons [30],

- Water is generally easily accessible.
- Water injection is relatively low cost compared to other injection fluids.
- Injecting water into a formation is straightforward.
- Water is highly efficient in displacing oil during the recovery process.

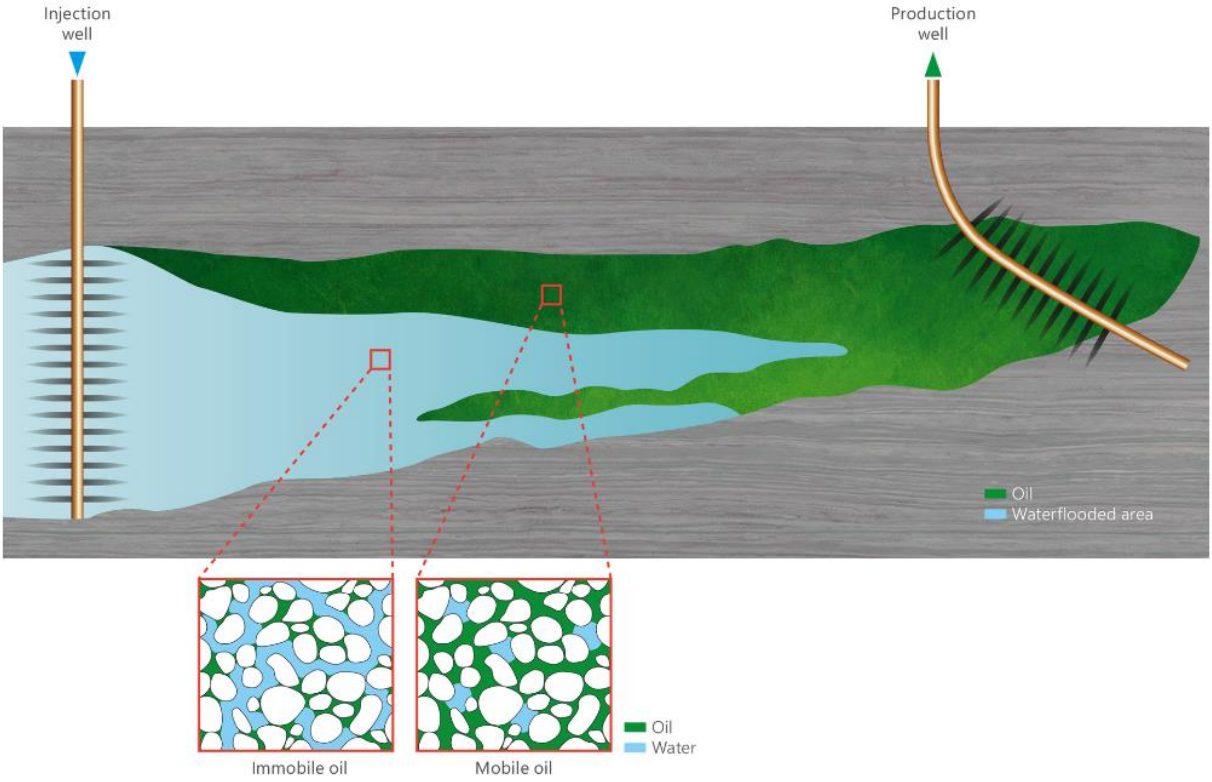

Figure 2.4: An illustration of oil displacement caused by waterflooding, both in large scale and pore level [31].

For determining whether a reservoir is suitable for waterflooding improved oil recovery, the following are the main characteristics that must be taken into account [32].

Reservoir geometry: Geometrical characteristics of the reservoir will affect both the location of wells and the number of platforms that will be required. In order to determine whether there is a natural water drive and whether it should be enhanced or not, it is important to analyze the reservoir geometry and previous reservoir performance. In the case of water-drive reservoirs classified as active water drives, the injection may not be required.

Fluid properties: Oil viscosity and density are the most important fluid properties which determine the oil mobility ratio, which in turn determines its sweep efficiency. The higher the oil viscosity, the more difficult it will be to displace oil with water. Similarly, if the density of the injected water is higher than the oil, it may not effectively displace the oil from the reservoir.

Reservoir/rock properties: The characteristics of the reservoir, such as permeability, porosity, and reservoir pressure, are essential factors in determining if waterflooding is a viable option. The reservoir needs to have sufficient permeability to allow the injected water to flow through the rock and displace oil from the reservoir rock. Additionally, the porosity of the reservoir must be high enough to hold and release sufficient amounts of water.

Reservoir depth: The depth of a reservoir is important in both the technical and economic aspects of oil recovery projects. It will be difficult to tolerate the maximum economic water-oil ratios in very deep wells, which will reduce the ultimate recovery factor and increase overall project operational costs. On the other hand, shallow reservoirs have a limited injection pressure since the pressure must be less than the fracture pressure. The critical pressure gradient of water flooding operation is approximately 0.23 bar/m in depth. If the operational pressure gradient exceeds the critical value, this causes fractures and results in injected water channeling. To prevent this, the operational pressure gradient of 0.17 bar/m is usually set as a safe margin.

Fluid saturations: In order for waterflooding operations to be successful, a reservoir must have a high oil saturation that provides sufficient recoverable oil. As shown in Figure 2.5, in terms of oil recovery potential, waterflooding is not as effective as polymer flooding (chemical) methods, and a part of immobilized oil may remain in the well even after the injection. This implies that the use of water flooding is suitable for high oil-saturated reservoirs.

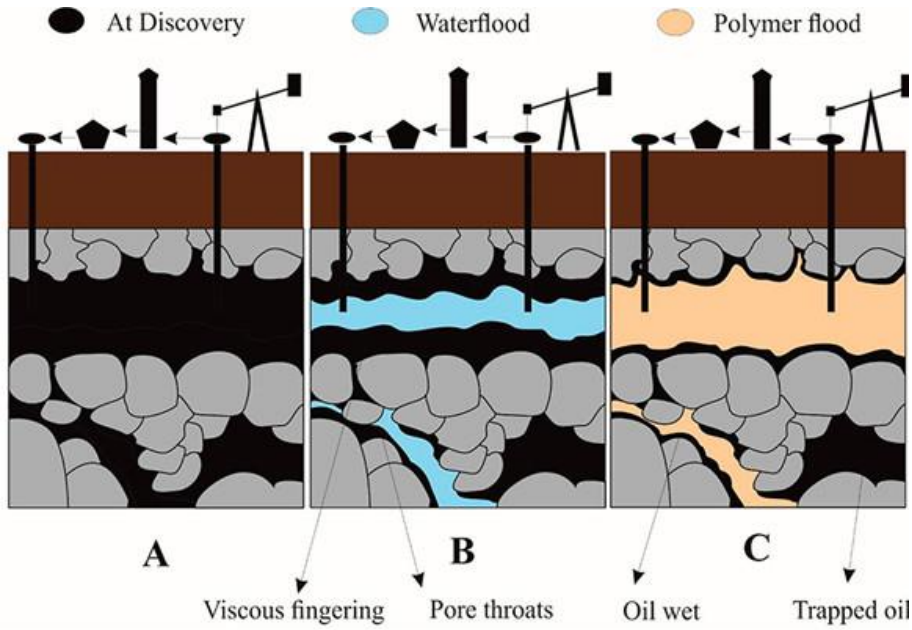

Figure 2.5: An illustration of the oil recovery potential of waterflooding and polymer flooding techniques [33].

Reservoir Heterogeneity: Reservoir heterogeneity refers to the variation of rock and fluid properties within the reservoir. When a reservoir is heterogeneous, some parts of the reservoir may be more accessible to the injected water, and others may be less accessible, leading to uneven oil displacement and reduced oil recovery.

2.3 Horizontal wells

Horizontal wells are a type of multi-directional drilling technique that drills the well with an incline of at least 80 degrees in order to enhance the performance of the reservoirs. Typically, horizontal wells are used as an alternative method of drilling for oil and gas in situations where vertical wells are not possible or reservoir shapes are difficult to access. Because, vertical wells have a limited exposure to oil layers and require several wells to produce oil effectively from the reservoir. In contrast, horizontal wells have a larger contact area with the reservoir, resulting in higher oil production despite their higher capital cost [32]. Although horizontal well efforts date back to 1927, the major thrust of this technology started in 1985. Initially wells were in short length, with a length of approximately 76 m. Throughout history, horizontal wells have been used to produce thin zones, fractured reservoirs, formations with water and gas coming problems, water flooding, heavy oil reservoirs, gas reservoirs, and in methods such as thermal and CO_2 flooding for enhanced oil recovery [34].

2.3.1 Advantages of horizontal wells

Horizontal wells have several advantages over conventional vertical wells as follows [32], [35]–[37], while Figure 2.6 illustrates some of them.

Increased productivity: Horizontal drilling enables a higher production rate compared to vertical drilling because a larger portion of the reservoir pay zone is accessible. This is because the greater wellbore length can intersect multiple fractures and flow channels, increasing the contact area between the wellbore and the reservoir.

Reduced water/gas coning: Because of the lower pressure drawdown for a given production rate, water and gas coning reduces, while delaying the water/gas breakthrough. This minimizes the remedial actions required to delay the breakthrough.

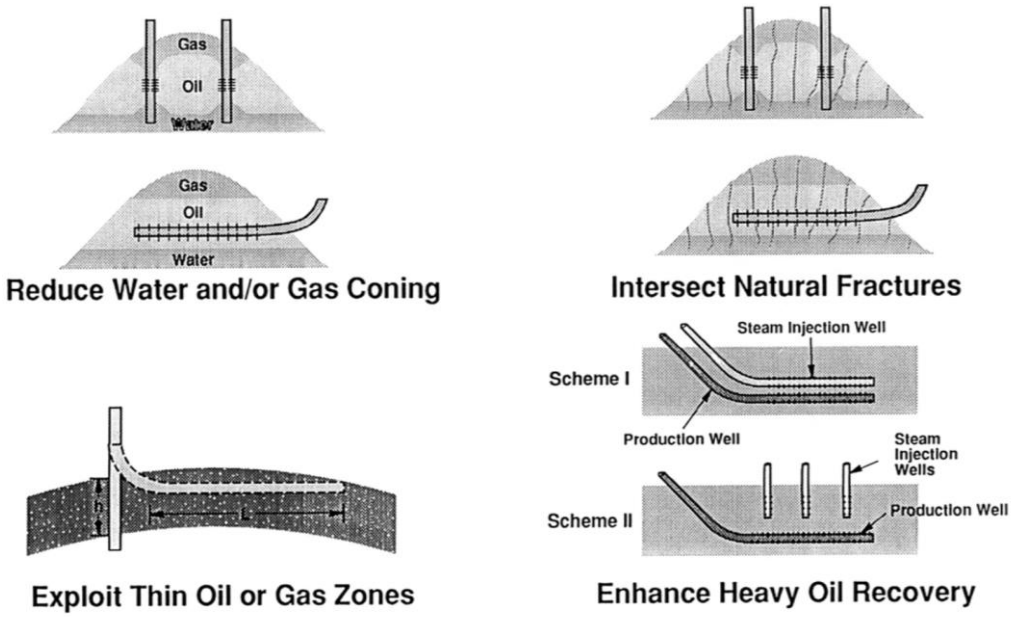

Figure 2.6: Illustration of applications of horizontal wells due to its advantages over vertical wells [38].

Reduced velocity around wellbore: Reduced pressure drawdown leads to lower pressure drop around the wellbore. This lowers the fluid velocities around the wellbore causing the reduction of sand production.

Enhanced oil recovery: In secondary and enhanced oil recovery applications (ex. water/gas flooding), long horizontal injection wells can significantly increase the injectivity rate, improving oil recovery significantly.

Reduced footprint on surface: Since the horizontal wells can hit the inaccessible targets over vertical wells, the required number of offshore platforms can be reduced.

Reduced environmental impact: Produced water often contains contaminants and can be difficult to dispose of safely. As water protection can be delayed this impact can be reduced.

2.3.2 Limitations of horizontal wells

In comparison with vertical wells, horizontal wells cost between 1.4 and 3 times more limiting the application of horizontal well technology for promising revenue with matured oil reserves [37]. The horizontal well is drilled almost parallel to the stratification plane of the reservoir, and its productivity will be influenced by the length of the well. When selecting a well length that will fit a reservoir block, the turning radius of the well will be a limiting factor [39]. Figure 2.7 shows the classification of horizontal wells according to turning radius.

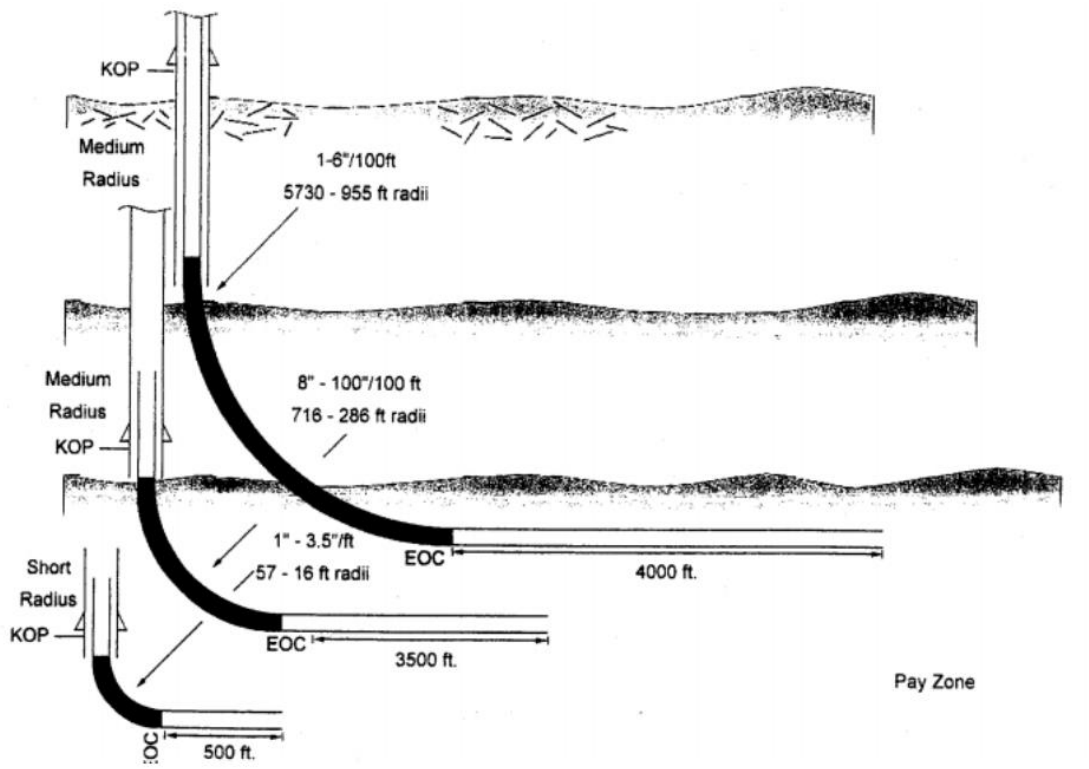

Figure 2.7: Classification of horizontal well based on drilling radius [40].

2.3.3 Gas and water coning

As the name implies, *coning* refers to the mechanism for the upward movement of water or/and the downward movement of gas into the perforations of an oil production and then into the wellbore.Figure 2.8 illustrates these movements of water beneath oil and gas over oil.

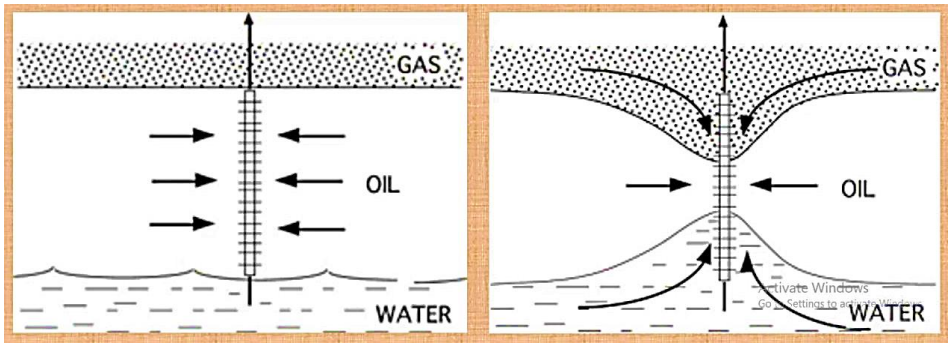

Figure 2.8: Schematic diagram of oil production before the water & gas coning (left) and after the water & gas coning (right) [41].

Fluid flow distributions around wellbores are influenced by three basic forces, capillary forces, gravitational forces, and viscous forces. Generally, these forces create an equilibrium, which determines the distribution of fluid movement across the wellbore. Due to the lower density of gas and the higher density of water, gas remains above the oil zone and water remains below the oil zone. However, as oil production continues, the pressure gradient changes over time. As a result, the gas-oil contact surface moves downward and the water-oil contact surface moves upward in the vicinity of the well in order to maintain equilibrium. Due to the counterbalancing of these forces, these water-oil and gas-oil contacts eventually bend into a cone like shape, as shown in figure 2.8. This developing coning effects lead to water and/or gas breakthrough and once it happens water and/or gas production drastically increases by reducing the oil production [7], [32]. This phenomenon is a major problem in oil refinery because this effect can reduce the productivity of the production well. Post processing costs to remove the gas and water added to producing oil and reducing total field recovery are main problems associated with this. Delaying the water and gas breakthrough can result in ultimate recovery of oil from field [7], [32]. The heel-to-toe effect and heterogeneity of reservoir along the well, are main factors that encourage the early water and/or gas breakthrough in horizontal wells at higher drawdown areas [9], [42].

2.3.3.1 Heel-toe effect

In horizontal wells, pressure-drawdown refers to the pressure difference (drop) between the well and the reservoir. When the oil is produced from a horizontal well, the flowing oil through the horizontal part loses its pressure along the wellbore length, from toe to heel, due to friction between the oil flow and the very long well boundaries. As a result, the pressure in the tubing at the heel becomes lower than the pressure at toe, resulting in a higher pressure-drawdown at the heel section than at the toe section. This is called the heel-to-toe effect. As a result of this, the area of the reservoir closest to the heel section of the well drains oil quicker than the area closer to the toe section, making the flow rates into the wellbore uneven along the length as

shown in Figure 2.9. This encourages water or gas to enter with oil via the heel section, causing an early water breakthrough. This heel-to-toe effect is stronger in longer horizontal wells [7], [43], [44].

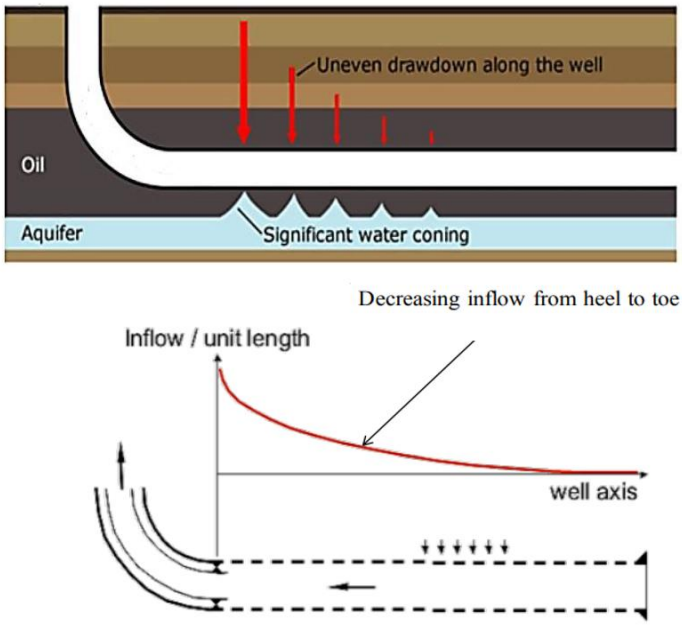

Figure 2.9: Heel-to-toe effect in horizontal wells [7], [43].

2.3.3.2 Heterogeneity of reservoir along the well

The reservoir's heterogeneity can significantly impact pressure drawdown and early water breakthrough in a horizontal well. Heterogeneous reservoirs have variations in permeability, porosity, and other properties over time and space. The flow of fluids (oil, gas, and water) through the reservoir will be uneven, because of the major contribution of permeability variations in reservoir. As a result, pressure drawdown in a horizontal well may vary along its length, resulting in early water and/or gas breakthrough in various locations along the length [9] as shown in Figure 2.10.

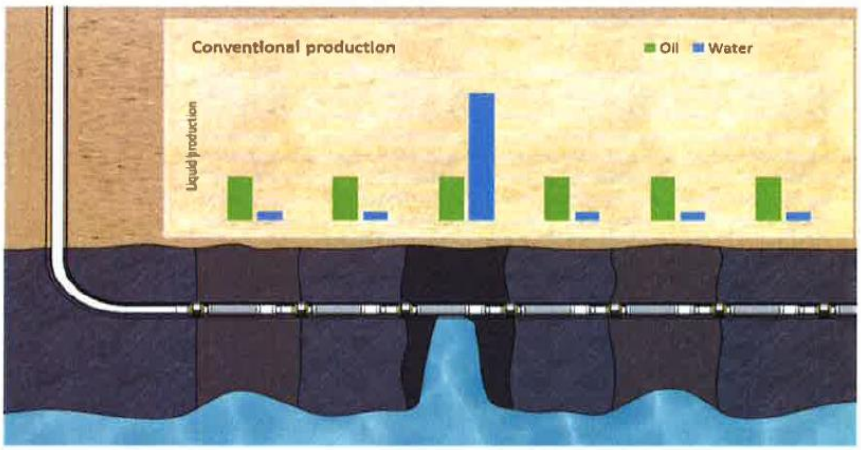

Figure 2.10: Liquid flow variations in heterogeneous reservoir [9].

2.3.4 Advanced multilateral wells (AMW)

The horizontal well has proven to be an efficient method for the development of oil fields. However, in some cases, the construction of single horizontal wells may result in high total costs and a low compensation for oil production. In complex bedding structures, oil and gas can be contained in small or isolated pockets. A multilateral well is a type of oil or gas well that has two or more branches or lateral boreholes that extend from the main vertical wellbore. Each lateral borehole is drilled horizontally in a different direction, typically in a parallel or radial orientation to the main wellbore, to increase the contact area between the well and the hydrocarbon reservoir. Figure 2.11 provides a visual representation of different configurations of multilateral wells used in the oil industry.

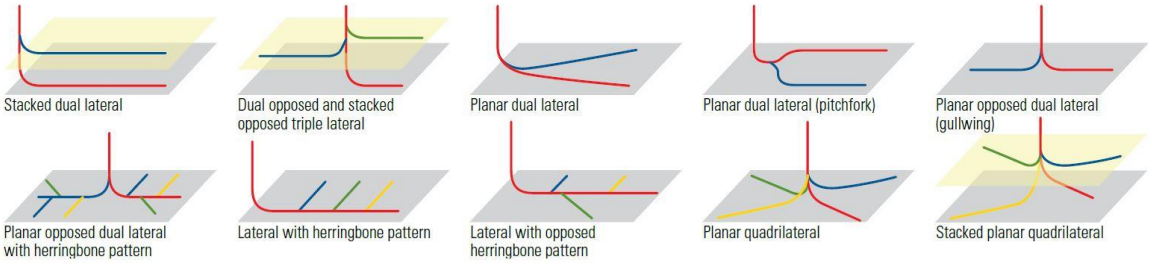

Figure 2.11: Different multilateral well configurations [45].

Multilateral wells offer several advantages over conventional vertical wells [46].

- They can access more reservoir volume than a single vertical well by intersecting multiple zones of production.
- They can reduce drilling costs by allowing multiple wells to be drilled from a single surface location.
- They can improve the overall production efficiency by providing multiple drainage points in the reservoir, which can help to reduce pressure drawdown and improve recovery rates.

Multilateral wells can be more complex to design and drill than conventional vertical wells, requiring specialized equipment and expertise. However, advances in technology and drilling techniques have made multilateral wells more feasible and cost-effective in recent years, making them a popular option for oil and gas companies looking to increase production and reduce costs.

2.4 Inflow control technologies

The use of horizontal wells in the oil and gas industry has resulted in high productivity due to large contact area, but it poses challenges related to uneven fluid flow rates and early breakthroughs due to the heel-to-toe effect and, permeability changes in heterogeneous reservoirs. Inflow control technology has been developed since 1990 to ensure uniform production along the length of a horizontal wellbore by limiting the inflow rate of fluids from high-permeability zones and encouraging inflow from low-permeability zones [42]. Initially,

passive flow control devices such as screens and gravel packs were used, but these methods were not always effective due to blockage by fine particles in the reservoirs.

2.4.1 Passive inflow control devices (ICD)

Inflow control devices (ICDs) have the purpose of equalizing inflow regardless of the location and permeability variation along the length of the wellbore. This technology enables the entire wellbore to contribute to total production, thus maximizing hydrocarbon recovery. Weatherford, Schlumberger and Baker Huges are some of main companies that manufacture ICDs [9]. Once installed at the desired depth, these inflow control devices start and continue to work based on their initial design. They are relatively inexpensive devices and any control from the ground surface is not required. Therefore, they are also known as passive inflow control devices.

ICD is based on the principle of restricting the flow by creating an additional pressure drop to achieve an evenly distributed flow profile along a horizontal well as shown in Figure 2.12. This pressure drop is a function of liquid flow rate and is dependent upon the specific design of the ICD, the density of the fluid, and the viscosity of the fluid, though the viscosity plays a less important role. As a result of an even production rate along the well, water/gas breakthrough could be delayed significantly. Specifically, they are designed to apply a specific differential pressure at a specified flow rate. Based on the method of creating the pressure drop, there are different types of ICDs: channel type, nozzle (orifice) type, tube type and hybrid type [9]. But the most common ICDs are channel type and nozzle (orifice) type which are illustrated in Figure 2.13 [42].

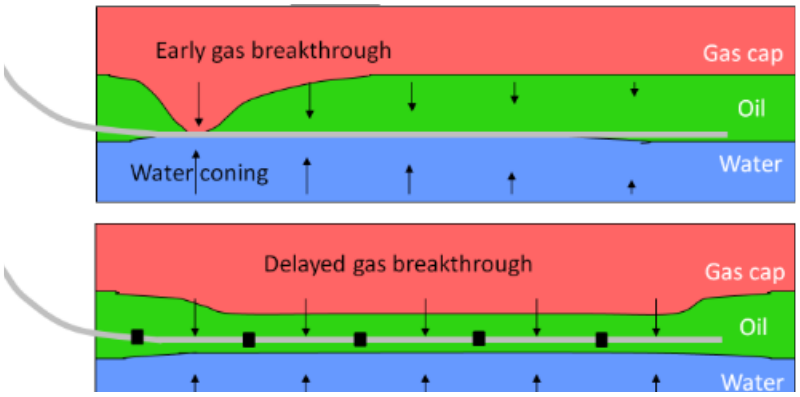

Figure 2.12: Early water & gas breakthrough without ICDs (top) & delayed water & gas breakthrough with ICDs (bottom) [47].

Channel type ICDs use surface friction to generate a pressure drop. As the arrows shown in Figure 2.13, channel ICDs allow inflow to enter the base pipe through a multi-layered screen. Then it travels in a helical pattern through the annulus of the well before ultimately entering the main production well. Friction is exerted against the fluid flow direction by the changing flow direction and roughness of the multilayered screens and helical passage. This generates the necessary pressure drop required to delay water breakthrough. These devices are fixed once installed underground. This has the advantage of creating less velocities leading to erosion and plugging. But it caused problems in larger viscosity fluid differences [42].

Orifice/nozzle type ICDs create a resistance when the fluid tries to enter the well, by forcing the flow through a set of small-diameter nozzles or orifices. This means that instead of changing the direction of the incoming flow to achieve the desired pressure drop, they create the necessary pressure drop by squeezing the fluid through an orifice. In contrast to channel type ICDs, orifice ICDs function based on differences in fluid density (density sensitive ICDs). This can be explained using Bernoulli's equation. Since the pressure drop is highly depend on the density and velocity (and less on viscosity), this is ideal for wells that produce fluids with large viscosity differences [42].

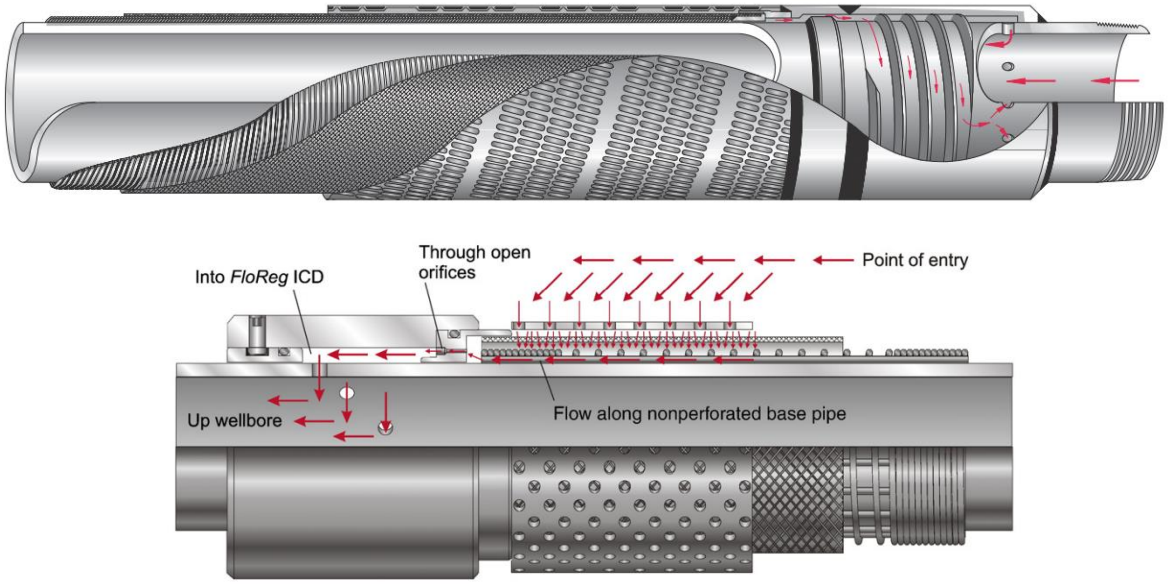

Figure 2.13: Channel type ICD (top) and Nozzle (orifice) type ICD (bottom) [48].

Overall, Inflow Control Devices (ICDs) are effective in delaying the water and gas breakthrough in oil wells. However, ICDs are not designed to choke or close off water and gas inflows once a breakthrough occurs. Consequently, if a water and gas breakthrough occur, the entire well must be choked to prevent their production. Unfortunately, this action also restricts the flow of oil, reducing overall production [9].

2.4.2 Autonomous inflow control devices (AICD)

To address the limitations of ICDs that cannot control the water and gas production after breakthrough, efforts have been made to develop a new device that can function as an ICD until a breakthrough occurs, and then automatically control and reduce water and gas production. This innovation aims to minimize separation costs and environmental impact, as well as enhance oil recovery by reducing pressure decline in the reservoir. The autonomous inflow control device (AICD) combines passive inflow control with an active control element to produce a pressure drop, while autonomously restricting the flow of the unwanted fluid. AICD valves restrict flow of low-viscous fluids and favours viscous fluids.

Mainly, there are two types of AICDs used in industry, based on their operating principle [49].

Fluidic diode (FD-AICD): This uses the vortex principle, where the less viscous water travels a longer path to reach the nozzle, experiencing a greater pressure drop than the more viscous oil which travels directly to the nozzle. By using this method, Hilliburton has developed an AICD with the trade name of Equiflow [9], [50], which is shown in Figure 2.14.

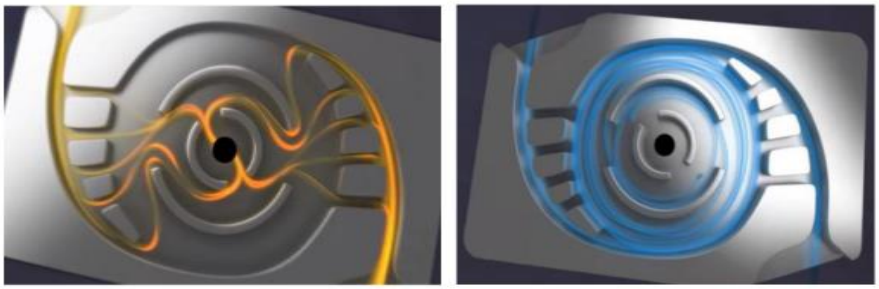

Figure 2.14: Equiflow's streamlines for oil flow (left) and streamlines for water flow (left) [51].

Rate controlled production (RCP-AICD): Working method is based on the Bernoulli's principle (along a streamline; static pressure + dynamic pressure + frictional pressure = constant). In this device, fluids pass through a valve containing a floating disc that alters the flow path geometry according to changes in the fluid's properties. By using this method, Statoil developed an AICD called RCP [9], [52].

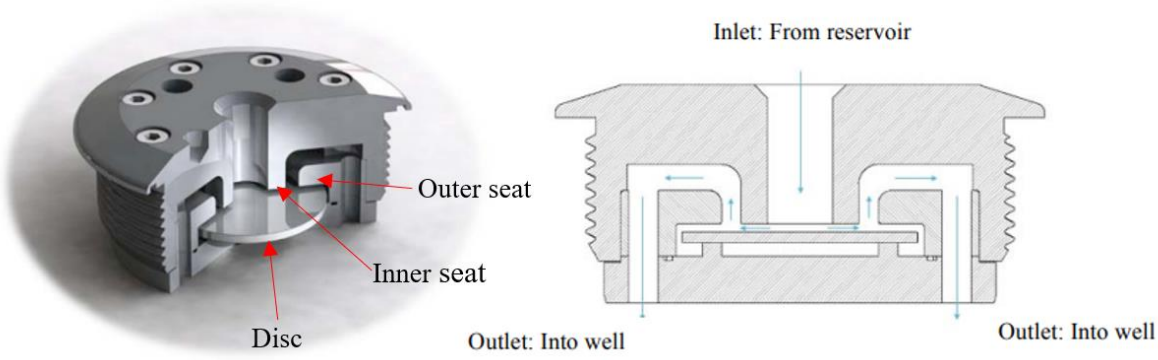

Figure 2.15: Schematic diagram of Statoil's RCP valve [52].

As shown in Figure 2.15, the RCP valve consists of 3 parts, free-floating disc, inner seat, and outer seat. The outer and inner seats create the flow path of fluid passing through the AICD, whereas the disc controls the amount of fluid passing through. When the valve is in operation, the force acting on the disc is the sum of the pressure forces acting on both sides of the disc. When a low viscous fluid like water/gas flows through the valve, its high velocity results in a decrease in pressure on the downstream side of the disc. This creates a force on the disc which moves it towards the inlet, reducing the flow area and subsequently the flow rate. However, when more viscous fluids pass through the valve, the friction loss increases, and the pressure recovery of the dynamic pressure decreases. This means that the pressure on the rear side of the disc, which is on the outlet side of the valve, will decrease, resulting in a lower force acting

on the disc towards the inlet. As a result, the disc moves away from the inlet, increasing the flow area, and thus the flow rate. Thus, the RCP valve can delay the early breakthrough and selectively choke low viscous fluids after breakthrough.

Studies conducted in Troll fields have shown that Statoil's RCP valve can increase the production of oil by 20% compared to ICDs [9]. The experiments conducted for Statoil's RCP at laboratory Porsgrunn, have proved its significant potential in fields with highly viscous oils. Experimental results for oils with different viscosities are shown in the Figure 2.16, and it can be observed that the higher the viscosity, the higher the volumetric flow through the RCP valve [52].

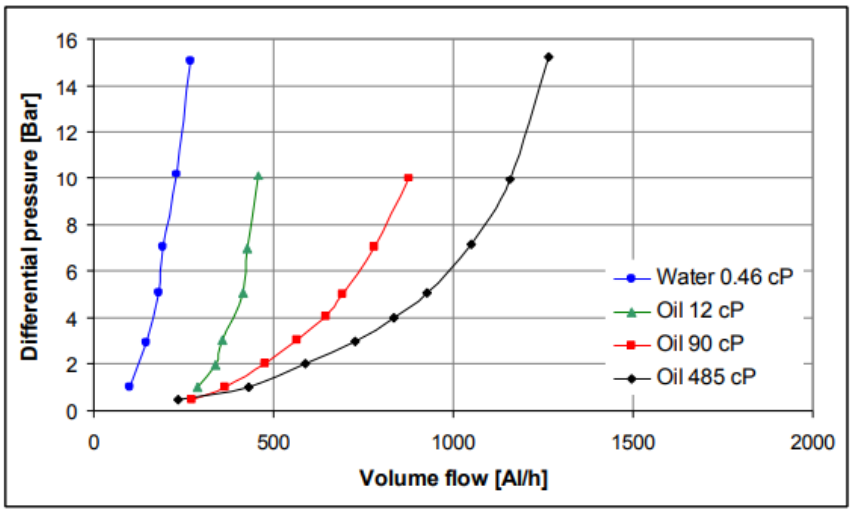

Figure 2.16: Differential pressure vs volume flow for water and oils with different viscosities [52].

2.4.3 Autonomous inflow control valves (AICV)

Autonomous inflow control valve (AICV) is a new type of inflow control device developed by InflowControl AS [9]. It is placed along the well in the same manner as the ICDs. AICV can equalize the inflow before the breakthrough and, it can almost completely shut off unwanted fluid production, after breakthrough occurs. At the same time, oil can be produced from the other inflow zones along the well, ensuring maximum oil production and recovery. AICVs are completely self-regulating and do not require any form of external control, thus making it possible to mount large numbers of valves in the well in a simple and robust manner. This results in a significantly greater level of efficiency in oil recovery. And AICV technology allows for the drilling of longer wells and maximizes reservoir contact. Furthermore, AICV eliminates the need for separation, transportation, and handling of unwanted fluids, thereby reducing risk, cost, and time. By using this technology, it is possible to maximize well production in a far more efficient manner than ever before [53].

AICV technology is designed to achieve its autonomous functionality by distinguishing between fluids based on their density and viscosity. It utilizes a minor pilot flow that runs parallel to the main flow, as shown in Figure 2.17, to control AICV's function. The pilot flow passes through a laminar flow restrictor and a turbulent flow restrictor in series. The main inflow from the reservoir enters from 'A', and P1 represents the reservoir pressure. When the pilot flow passes through the laminar flow element, the pressure drops to P2 (pressure in

chamber ‘B’). It then proceeds to pass through the turbulent flow elements until it reduces the pressure to the inside well pressure P3. The AICV functions according to acting pressure in chamber ‘B’ (P2).

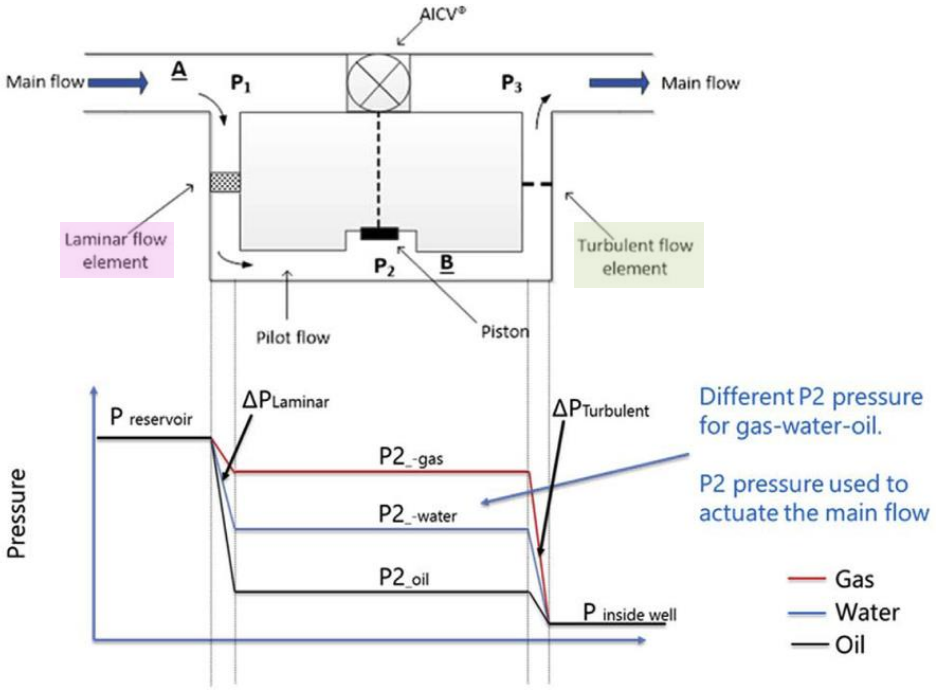

Figure 2.17: Simplified sketch of the flow paths on AICV and pressure changes inside for different fluids [54].

The laminar flow restrictor can be considered as a pipe segment, and pressure drop across $\Delta P_{Laminar}$ can be expressed by equation (2.1), as a relation of fluid viscosity μ, velocity v, pipe length L and pipe diameter D [53].

$$\Delta P_{Laminar} = \frac{32 \cdot \mu \cdot \rho \cdot v \cdot L}{D^2} \tag{2.1}$$

The turbulent flow restrictor can be considered as an orifice plate, and pressure drop across $\Delta P_{Turbulent}$ can be expressed by equation (2.2), as a relation of fluid density ρ, velocity v and geometric constant K [53].

$$\Delta P_{Turbulent} = K \cdot \frac{1}{2} \cdot \rho \cdot v^2 \tag{2.2}$$

According to these relationships, ΔP across the laminar flow restrictor depends on the viscosity and the velocity of the fluid, while ΔP across the turbulent flow restrictor depends on the density and the velocity of the fluid. Consequently, P2 depends on fluid properties such as density and viscosity. As the plot shown in Figure 2.17, P2 for oil is low due to high oil viscosity, and this keeps the valve in open position producing more oil. P2 for water is high due to low viscosity in water. Due to the high pressure, a piston in chamber 'B' will be actuated, closing the valve. The open and closed positions of the AICV is illustrated in Figure 2.18.

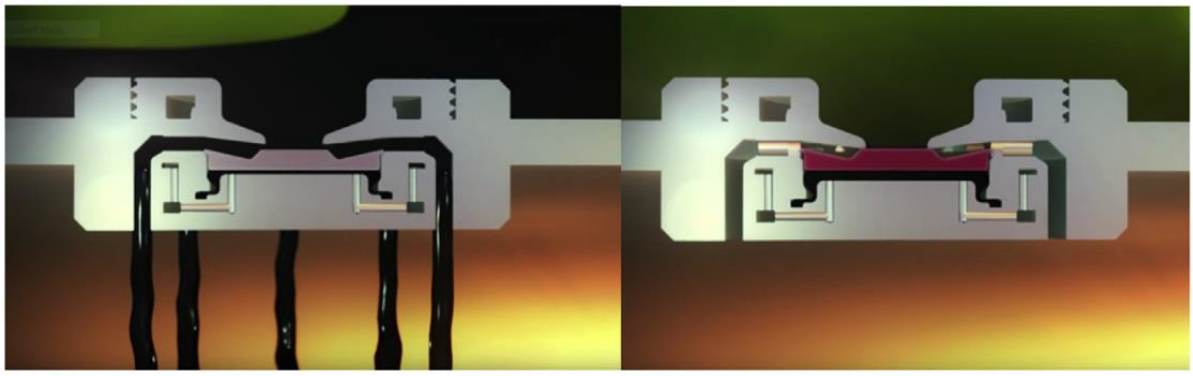

Figure 2.18: AICV open position (left) and closed position (right) [54].

The position of the piston is decided by the force balance around the piston. Figure 2.19 shows the cross section of AICV representing the forces acting on the piston.

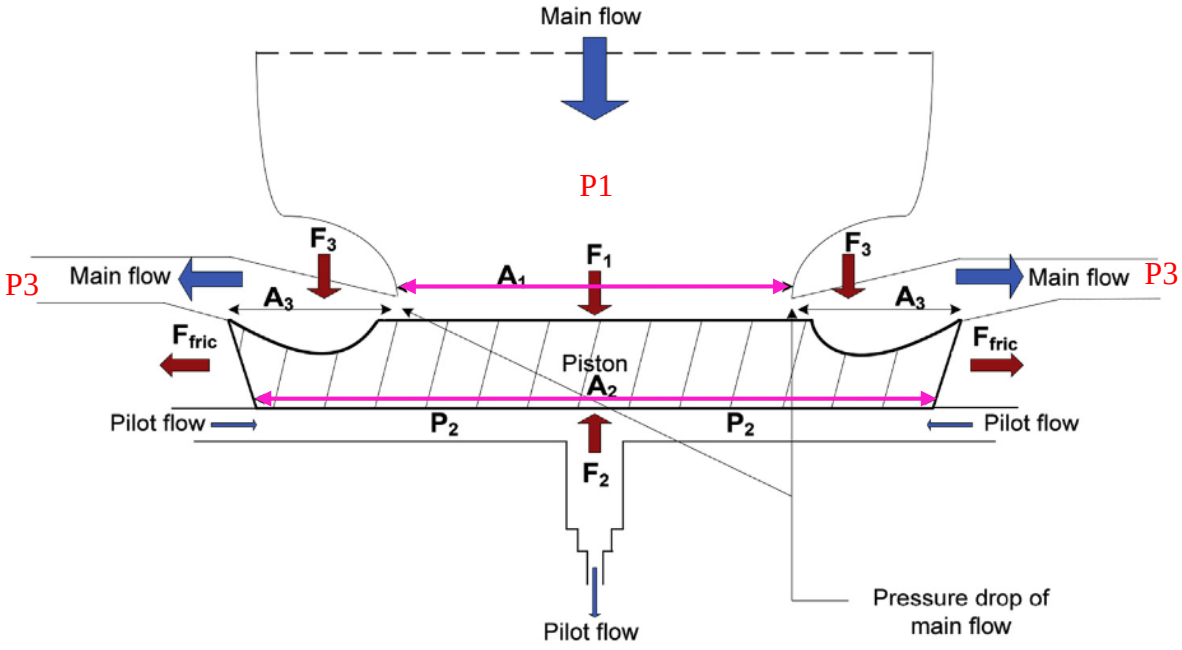

Figure 2.19: AICV cross section and forces acting on the piston [54].

On the upper part of the piston, F1 (=P1.A1), the force acts downwards, and on the lower part of the piston, F2 (=P2.A2), the force acts upwards. F3 force acts downwards on the outer part of the piston. There is a friction force, F_{fric} that acts against the flow direction of fluid, and it is normal to F1, F2 and F3. If the net force (F1- F2 + F3 + F_{fric}) is positive, the valve is in the open position, and if it is negative, the valve is in the closed position. As P1 is obtained from the reservoir side, it is regularly higher than the pressure in Chamber B, which is behind the piston P2. Because of the higher pressure P1, the area A2 must be larger than the area A1 to close the valve. A1 and A2 are the design parameters for the valve, dependent on the properties of the fluids [54].

Figure 2.20 shows simulated results of AICD and ICD, conducted for horizontal well using OLGA and ROCX tools. Results indicates that AICV valve can shut-off 95% of gas at gas breakthrough, implying that AICV is much more effective in stopping low viscous fluids compared to ICD [53].

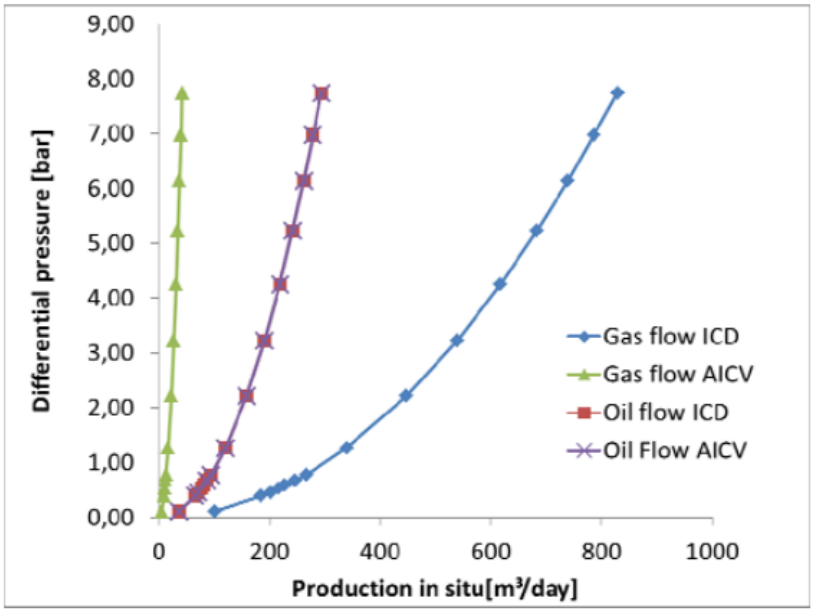

Figure 2.20: Oil and gas flow rates through AICD and ICD at differential pressures [53].

2.5 Modeling and simulation of oil production

Oil production simulation is important for several reasons. Firstly, simulating oil production can help exploration companies to determine the viability of an oil field before drilling. By analyzing geological data and running simulations, companies can estimate the amount of oil that may be present, the expected production rate, and the potential profitability of the field. Secondly, oil production simulation helps in identifying potential problems and mitigating risks. By simulating different scenarios, potential issues such as water production, and gas breakthrough can be predicted. This information can help in designing production processes to minimize these issues, optimizing oil production, thus reducing production costs. Therefore, numerous commercial software products for the oil industry have been developed in recent years and OLGA, ROCX, and ECLIPSE are some of powerful software.

OLGA (Oil and Gas Analysis) is a commercial software developed by Schlumberger for simulating multiphase flow in oil and gas production systems. OLGA has been widely used in the oil and gas industry for several decades, and it is mainly used for modeling and simulating fluid flows in pipelines, specifically for the operation in production well. ROCX and ECLIPSE are three-dimensional transient near well simulation software products designed to model and simulate the reservoir. The total oil production is typically modeled and simulated by coupling multiphase flow simulation software with reservoir simulator software like OLGA+ROCX/ECLIPSE.

The OLGA-ROCX combination is one of the most widely used transient reservoir flow models commercially available today. OLGA simulator calculates and sends wellbore pressure

information to ROCX to simulate three phases of flow near the wellbore in three dimensions. ROCX then determines the flow rate of each phase of the reservoir fluid and sends that information back to OLGA. Combining OLGA and ROCX can have a variety of applications in modeling and simulation, including liquid loading, wellbore slugging, well testing, shut-in and startup, water and gas coining, etc. [7], [53], [55]. In the studies [55] and [56], OLGA+ROCX combination has been used to simulate oil production from heavy oil reservoirs with water drive, for well completions with ICD and AICV.

2.5.1 ECLIPSE and OLGA-ECLIPSE combination

Oil and gas reservoir simulator ECLIPSE was developed originally by Exploration Consultants Limited (ECL) in the late 1970's. But now it is owned, developed, marketed, and maintained by Schlumberger. Due to its comprehensive, more accurate and faster simulation capabilities ECLIPSE has become the reservoir simulator choice in Europe [57]. In [58], ECLIPSE has been used to determine the optimal arrangement for vertical and horizontal waterflooding. ECLIPSE has 3 editions,

1. Eclipse 100 (Black Oil Simulator)
2. Eclipse 300 (Compositional Simulator)
3. Eclipse 500 (Thermal Simulator)

The ECLIPSE Black oil simulator treats oil and gas phases as a single “component” over time, and properties of the component changes with pressure and temperature, but composition does not change [57]. In [59], ECLIPSE Black oil simulator has been used to investigate hybrid enhanced oil recovery. In [51] study, ECLIPSE has been used for cases with horizontal wells completed with ICDs, AICDs, and AICVs for four different numerical reservoir models including heavy oil reservoir, thin oil reservoir, low viscous oil reservoir, and homogeneous reservoir.

In Compositinal simulator, oil and gas phases are represented by “multi-component” mixtures, assuming that compositions can vary with pressure, temperature and time, and EOS are used for calculations. The ECLIPSE Compositional Simulator can track each component of the oil and gas in the reservoir (ex: C1-methane, C2-ethane,...). Using this method, fluid behavior can be modeled near the critical point, where pressures and temperatures change dramatically, resulting in significant deference in fluid behavior [57].

Although various oil and gas production simulation studies have been conducted with OLGA-ROCX combination, reported studies for OLGA-ECLIPSE simulations are almost not available in accessible research hubs. OLGA user manuals published by Schlumberger clearly mention the capability of coupling OLGA with ECLIPSE [60]. If ECLIPSE compositional simulator (Eclipse 300) is integrated with OLGA, it can be predicted that it may lead to more precise and advanced simulations of oil and gas production due to the comprehensive nature of Eclipse 300.

3 Theoretical background

This chapter focuses on the fundamental concepts and equations required for simulating oil production, which involves understanding the characteristics of the reservoir rock and fluid, as well as the design principles for horizontal well completion. To model and simulate the oil production accurately, a thorough understanding of these concepts is essential.

3.1 Reservoir rock properties

Reservoir rocks are underground rocks that contain porous and permeable formations capable of holding fluids such as oil, gas, or water. Petroleum reservoir rocks can have a diverse composition ranging from loosely packed sand to dense sandstone, limestone, or dolomite. Silica, calcite, and clay are among the substances that bind these rock grains together. To understand and evaluate a reservoir's performance, it is vital to understand how the hydrocarbon system interacts with the rock. To determine the rock properties, cores samples taken from the reservoir rock are tested in the laboratory [32].

3.1.1 Porosity

The rock of a reservoir looks solid from the ground, but when examined under a microscope, it is revealed to have tiny void spaces called pores. This property is important in understanding the storage potential of a rock for fluids such as oil and gas. Total or absolute porosity ϕ_a is calculated as the ratio of the total pore volume to the total or bulk volume of the rock as shown in equation 3.1 [61].

$$\phi_a = \frac{\text{Total pore volume}}{\text{Total or bulk volume}} \tag{3.1}$$

It has been observed that some void spaces developed during the formation of rocks during the past geological period and became isolated from other spaces because of excessive cementation. Therefore, some pores are interconnected, while others are completely isolated, as illustrated in Figure 3.1.

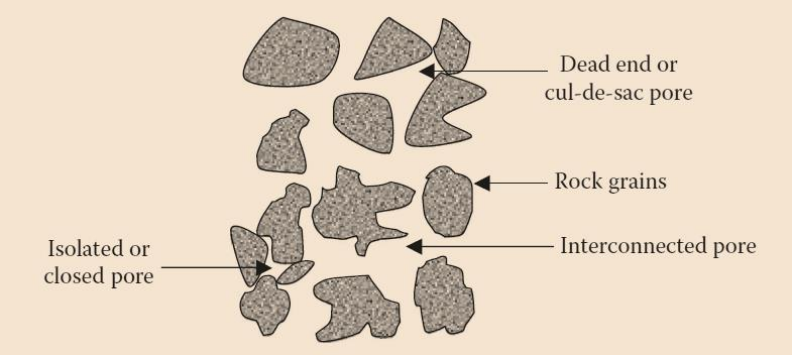

Figure 3.1: Different types of pores in reservoir rocks [61].

A reservoir rock may have a high total porosity, but due to the lack of interconnectivity, fluids trapped inside isolated pores cannot be recovered. These pores are present in all reservoirs,

which makes a large portion of the oil unrecoverable. The term *effective porosity* ϕ is defined to represent the pore volume with recoverable oil, indicating the dead-end pores and interconnected pores, as shown in equation 3.2 [61].

$$\phi = \frac{\text{Vol. of interconnected pores} + \text{Vol. of dead} - \text{end pores}}{\text{Total or bulk volume}} \tag{3.2}$$

3.1.2 Fluid saturation

When the porosity measures the total storage capacity of a reservoir rock, fluid saturation quantifies the amount of pore space occupied by oil, gas, or water. Fluid saturation is the ratio of the volume of a fluid phase to the effective pore volume of the rock sample and can be expressed as a fraction or percentage. The general relation for fluid saturation is expressed by equation 3.3 [61].

$$\text{Fluid saturation} = \frac{\text{Total volume of the fluid phase in pore volume}}{\text{Effective pore volume}} \tag{3.3}$$

Since reservoir pores contain 3 different fluid phases, oil, gas and, water, fluid saturations can be specifically defined for each fluid phase by equations 3.4, 3.5, and 3.6 [61]. Parameters S_o, S_g, and S_w are saturations of oil, gas, and water respectively.

$$S_o = \frac{\text{Volume of oil}}{\text{Effective pore volume}} \tag{3.4}$$

$$S_g = \frac{Volume\ of\ gas}{Effective\ pore\ volume} \tag{3.5}$$

$$S_w = \frac{Volume\ of\ \text{water}}{Effective\ pore\ volume} \tag{3.6}$$

The summation of all the fluids saturations equals to one, since each saturation is defined as a fraction of the effective pore volume [61].

$$S_o + S_g + S_w = 1 \tag{3.7}$$

3.1.3 Wettability

In reservoir engineering, wettability refers to the ability of a fluid (typically oil or water) to spread over and adhere to the surface of a solid material (typically a rock). Since fluids are distributed and moved in the rock pores, wettability is an important parameter in the study of crude oil recovery from reservoirs. Based on the degree to which the rock surface is wetted by oil or water, wettability is typically classified into three categories:

- Oil-wet
- Water-wet
- Intermediate-wet

Oil-wet reservoirs have a rock surface that is preferentially wet with oil, which makes it challenging for water to displace the oil and recover the oil. A water-wet reservoir has a rock surface that is preferentially wetted by water, which enhances oil displacement and improves oil recovery. Figure 3.2 illustrates the oil-wet and water-wet conditions. Intermediate-wet reservoirs exhibit both oil-wetting and water-wetting characteristics, and the wettability can vary according to the properties of the fluids and the surface of the rocks [32], [61]. Therefore, in enhanced oil recovery techniques such as water flooding, surfactant flooding, and gas injection, wettability is important.

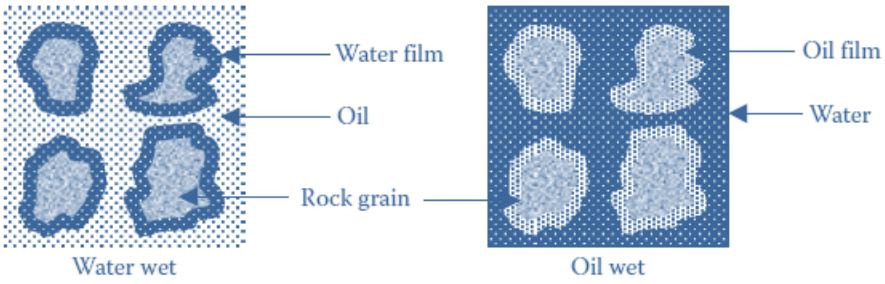

Figure 3.2: representation of oil-wet and water-wet cases in a porous medium [61].

There are numerous methods to determine the wettability and the most common method is Amott-Harvey wettability test. Simply, the Amott method involves saturating a rock sample with oil, then removing the oil from the surface of the rock using a vacuum. The rock is then placed in contact with water, and the rate at which the water displaces the oil is measured. This displacement rate is used to calculate a *wettability index*, which ranges from 1 (completely water-wet) to -1 (completely oil-wet) [7], [61], [62].

3.1.4 Permeability

While having a large porosity is important for storing significant quantities of oil, it alone is not enough to facilitate oil production. This is because the reservoir fluids must have flow ability to reach the surface. Permeability of a reservoir rock denoted by k, is a measure of this flow ability through the rock, but this is affected by the trapped fluid type. Term *absolute permeability* refers its ability to transmit a single phase fluid when the void space is completely filled with that fluid (at saturation of 100%), while *relative permeability* is used, when the same rock is filled with two or more fluids (multiple fluids) [63]. Thus, the permeability of petroleum reservoir rock is one of the most important parameters affecting oil production.

3.1.4.1 Darcy's law

In 1856, Henry Darcy defined a mathematical expression for permeability, after conducting experiments for water flow through a sample from porous medium (core plug), and still this expression is used in petroleum industry [32]. Figure 3.3 illustrates the schematic representation of cylindrical core plug used by Darcy, where Q is the volumetric flow rate through the core plug (m^3/s), A the cross-sectional area (m^2), h_1 and h_2 hydraulic head at inlet and outlet, P_1 and P_2 pressures at inlet and outlet, and L the length of core plug (m).

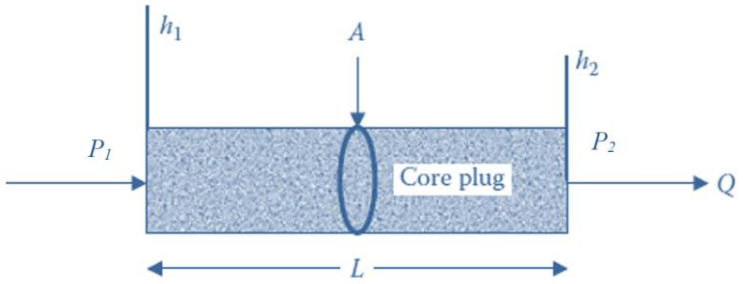

Figure 3.3: Illustration of fluid flow through a core plug [61].

Darcy expressed the equation 3.8 for flow through the core plug using the pressure gradient dP (N/m^2) over the section dL (m). K is a proportional constant [32].

$$Q = -KA\frac{dP}{dL} \tag{3.8}$$

Darcy's expression was limited for water flow through a core plug, but later investigations found that equation 3.8 can be modified for other fluids, by adjusting the proportional factor K as a ratio of the absolute permeability of the porous medium k (in m^2 or D) and the viscosity of the fluid μ (in N.s/m^2). Therefore, Darcy's law can be expressed generically for linear and single-phase flows by equation 3.9 [32].

$$Q = -\frac{k}{\mu}A\frac{dP}{dL} \tag{3.9}$$

3.1.4.1.1 Application of Darcy's law to radial flow

This thesis aims for a horizontal oil production well and a cylindrical tube can be used to represent a horizontal oil well. The reservoir can be represented by an outer annulus that shares the same axis as the well as shown in Figure 3.4. This means that the flow of oil from the reservoir into the well can be thought of as flowing in a radial direction (radial flow system).

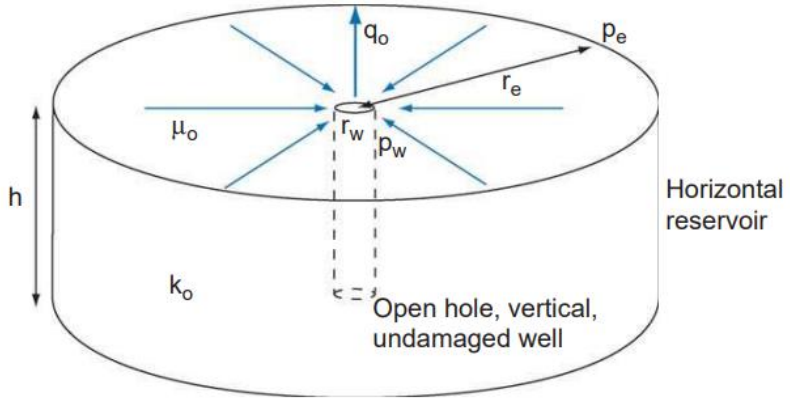

Figure 3.4: Flow system in radial direction [61].

Thus, Darcy's general equation 3.4, can be modified to equation 3.5, to mathematically express the radial flow [61]. As the fluid flow in radial direction, dL is substituted as dr.

$$Q = -\frac{k}{\mu} A \frac{dP}{dr} \tag{3.10}$$

The cross-sectional area normal to the radial flow A can be expressed as $2\pi rh$, where r is the radius of wellbore (m) and h is the length of wellbore (m).

3.1.4.2 Anisotropic permeability

The difference in pressure between the well and reservoir is the driving force for radial fluid flow from the reservoir to the wellbore. As stated in equation 3.10, the higher the absolute permeability of the reservoir the higher the flow rate. But the flow rate decreases with the higher fluid viscosity. This relationship, however, is only applicable to homogeneous reservoirs where permeability is constant. In actual reservoirs, reservoir rock has created with a sedimentation process, and this makes vertical permeability k_V is higher than horizontal permeability k_H, creating an ellipsoidal drainage pattern around the well, as illustrated in Figure 3.5. The term *anisotropy* refers to this directional dependency that can be quantified by the ratio of vertical permeability to horizontal permeability k_V/k_H [61].

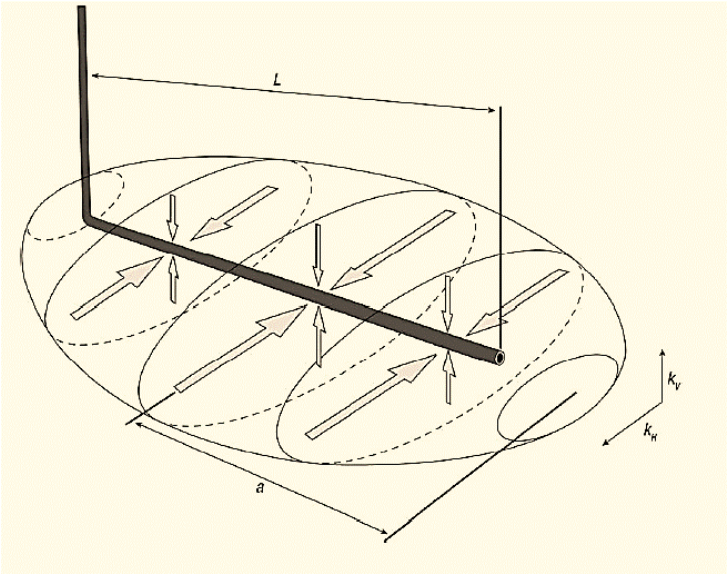

Figure 3.5: Drainage pattern of a horizontal well with a length, L [64].

Geometric average permeability k_{sp} can be calculated by on the permeabilities in x, y and, z directions k_x, k_y, k_z as shown in equation 3.11 [7], [65].

$$k_{sp} = \sqrt[3]{k_x k_y k_z} \tag{3.11}$$

3.1.4.3 Relative permeability

When reservoir rock pores are filled with multiple fluid phases (oil, water, gas), the phases share the same pore space and interact with each other. This requires introducing a new parameter called *effective permeability* instead of absolute permeability. Effective permeability depends on several factors like fluid saturation, pour shape, and wetting properties and it is

determined by lab tests. It is still valid to use effective permeability instead of absolute permeability in Darcy's equation.

The term *relative permeability* of each fluid is a measure of how effective it is at flowing through the rock compared to the other fluids present. [32]. As shown in equation 3.12, relative permeability of a fluid (fluid "i") k_{ri}, is determined by dividing the effective permeability of that fluid (fluid "i") k_{ei}, at a given saturation level by the absolute permeability of the same fluid at 100% saturation k. When the saturation level is 100%, the relative permeability is equivalent to the absolute permeability.

$$k_{ri} = \frac{k_{ei}}{k} \tag{3.12}$$

It is common to plot *relative permeability curves* to study how the relative permeability varies with saturation and wettability. Each phase's relative permeability (ex: oil and gas) is plotted as a function of saturation (typically the water saturation) [59]. Figure 3.6 shows the dependence of relative permeability on water saturation in a water-wetted system and oil-wetted system. When the system consists of only oil and water, the fluid saturation on the x-axis ranges from irreducible water saturation (S_{wc}) to residual oil saturation after water flooding (S_{orw}).

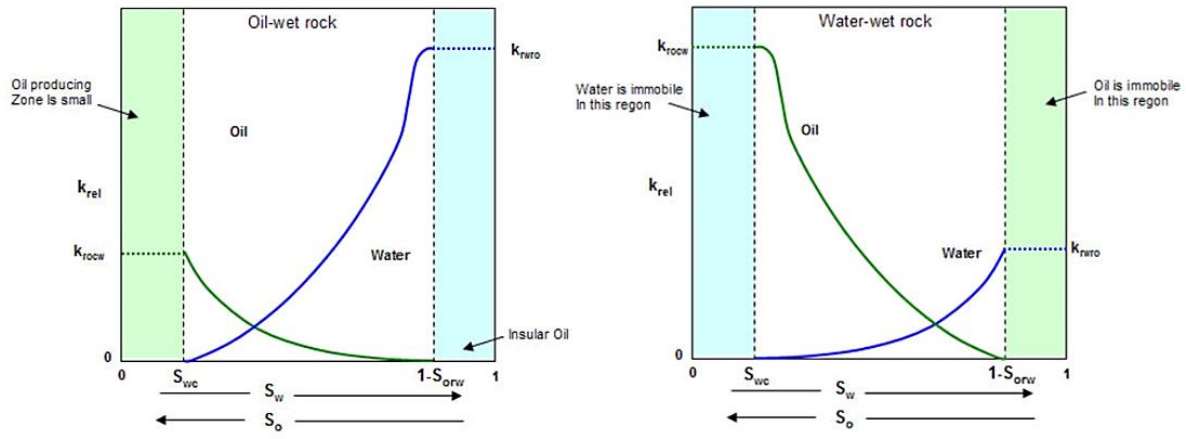

Figure 3.6: Relative permeability curves for strong water-wetted (a) and strong oil-wetted system (b) [66].

3.1.4.4 Capillary pressure

Capillary pressure is an important concept in reservoir engineering because it describes the pressure difference across the interface between two immiscible fluids, such as oil and water, in a reservoir rock. This is caused by the internal and external electrostatic forces acting on the fluids. Capillary pressure plays a critical role in the behavior of fluids in a reservoir and affects the ability to recover oil efficiently. Capillary pressure P_c can be defined as the difference in pressure of nonwetting phase P_{nwet} and pressure of wetting phase P_{wet}, as shown in equation 3.13. The difference in pressure is always nonzero [59], [67].

$$P_c = P_{nwet} - P_{wet} \geq 0 \tag{3.13}$$

When it comes to water-oil or water-gas systems or three-phase systems, water is always considered to be the wetting phase, whereas gas is always considered to be the nonwetting phase. Therefore capillary pressure for a water-oil system P_{cow} can be expressed by equation 3.14, where P_o is pressure in oil side and P_w is pressure in water side [67].

$$P_{cow} = P_o - P_w \geq 0 \tag{3.14}$$

Capillary forces are dependent on the interfacial forces, the wettability of the reservoir rock, and the pore size (capillary radius) [32]. Equation 3.15 can be used to calculate the oil-water capillary pressure, where δ_{ow} is oil-water interfacial tension, θ_{ow} is the oil-water contact angle, and r is the capillary radius.

$$P_{cow} = \frac{2\delta_{ow}\cos\theta_{ow}}{r} \tag{3.15}$$

In Figure 3.7, left side shows how the water rises above the Free Water Level (FWL) differently in capillary tubes with different radius, while the right side shows the same phenomenon occurs in porous mediums.

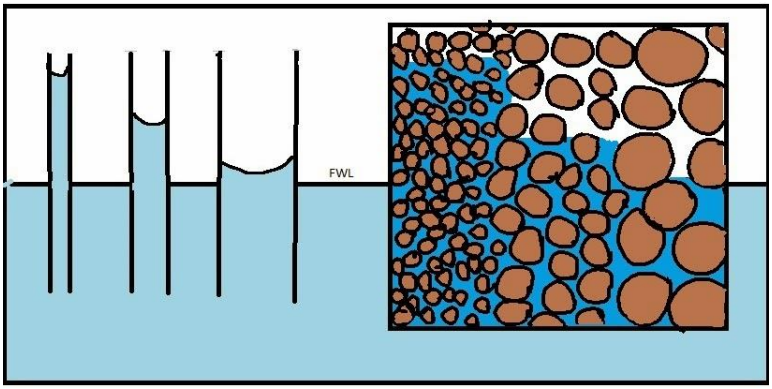

Figure 3.7: Capillary pressure changes with capillary radius [68].

3.2 Reservoir fluid properties

Typically, reservoir fluids consist of both hydrocarbons and non-hydrocarbons. During the breakdown of organic matter, hydrocarbons are formed, and then they migrate upward and trap in permeable rocks, by displacing water. An overview of some of the most important physical properties of reservoir fluids is provided in this subsection.

3.2.1 Types of reservoir fluids

According to the physical properties and phase behavior of petroleum reservoir fluids at different temperatures and pressures, there are five main categories as [61],

- Black oils
- Volatile oils
- Gas condensates

- Wet gases
- Dry gases

The following Figure 3.8 shows the basic characteristics of these 5 reservoir fluids.

Reservoir Fluid	API Gravity (°)	Viscosity (cP)	Color of Stock Tank Liquid[a]
Black oils	15–40	2 to 3–100 and up	Dark, often black
Volatile oils	45–55	0.25–2 to 3	Brown, orange, or green
Gas condensates	Greater than 50	In the range of 0.25	Light colored or water white
Wet gases	Greater than 60	In the range of 0.25	Water white
Dry gases	No liquid is formed, hence the name "dry"	0.02–0.05	—

Figure 3.8: Basic characteristics of five different reservoir fluids [61].

As shown in figure 3.9, an individual compound can only exist in a single phase of gas, liquid, or solid at a given pressure and temperature. But reservoir fluid is a mixture of different compounds. Therefore, petroleum reservoirs have distinct phase behaviors for each component of the mixture, which enables gas and liquid phases to coexist in vapor-liquid equilibrium over a wide range of temperature and pressure conditions [61], [69].

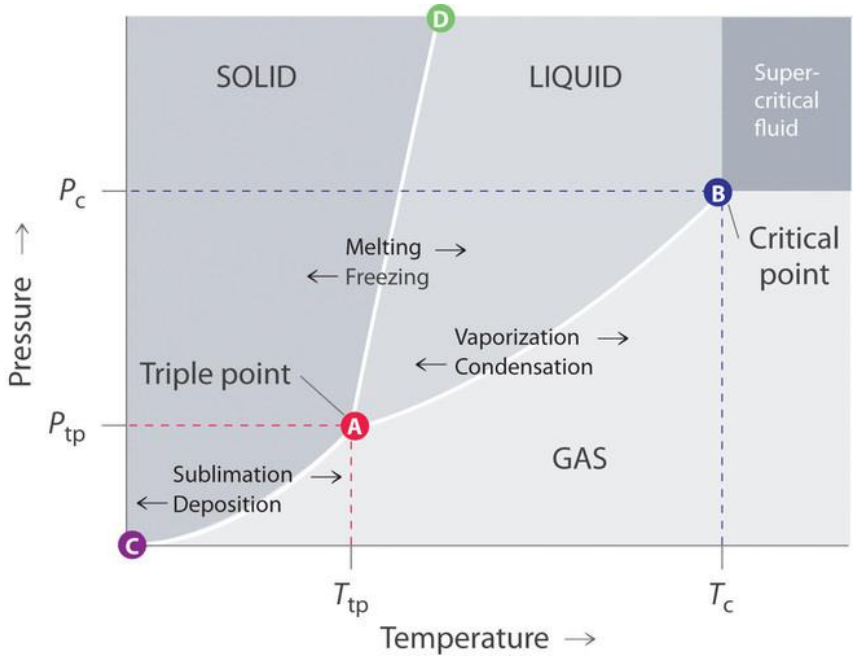

Figure 3.9; Temperature and pressure phase diagram for a single component [70].

To understand the phase behavior of multi-component systems, a phase envelope diagram can be constructed, as shown in Figure 3.9. In the critical point, all the properties of the liquid and gases are same. Separator conditions means the wellhead conditions. The liquid percentages of the mixtures are represented by dashed lines. This phase envelope diagram can be generated using either pressure-volume-temperature (PVT) data that have been obtained from laboratory experiments or using fluid models such as Equation Of State (EOS) [61], [69].

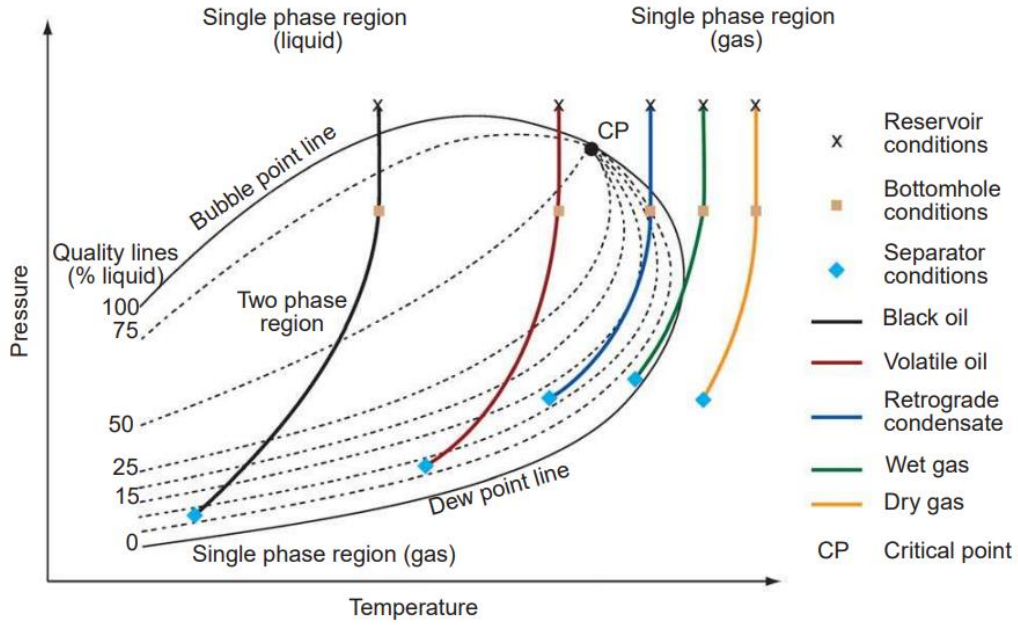

Figure 3.10: Phase envelope diagram for a hydrocarbon mixture [69].

According to Figure 3.10, each reservoir fluid has different phase behaviors at different temperatures and pressures. According to whether it produces liquid or not, gas in reservoirs is classified as either "dry" or "wet". Dry gas doesn't produce any liquid in the reservoir or completion, while wet gas doesn't produce liquid in the reservoir but does produce it in the completion due to the formation of condensate as the gas passes through the tubing. Under typical reservoir pressures and temperatures, black oils exist as liquids and are situated well below their critical point. During the extraction of black oils from the reservoir, the pressure will be reduced, and a small proportion of the fluid will vaporize. Likewise, phase envelope diagram can be used to compare the behavior of various types of reservoir fluids.

3.2.2 Properties of multiphase reservoir fluids

The specification of reservoir fluid is necessary for oil production simulation processes, which is accomplished by identifying reservoir fluid properties. It is an important step in the simulation process.

3.2.2.1 Oil and gas specific gravity

The dimensionless property, specific gravity of petroleum oil γ_o, is calculated by dividing the density of the oil ρ_o, by density of the water ρ_w, at standard conditions as $T_S = 288.71K$ and $P_S = 1$ atm, [61].

$$\gamma_o = \frac{\rho_o}{\rho_w} \tag{3.16}$$

Gas specific gravity is defined as γ_g, the ratio of density of the oil ρ_{gas}, by density of the air ρ_{air}, at standard conditions $T_S = 288.71K$ and $P_S = 1$ atm.

$$\gamma_g = \frac{\rho_g}{\rho_{air}} \tag{3.17}$$

3.2.2.2 Oil and gas viscosity

Oil viscosity μ refers to the measure of a fluid's resistance to flow in terms of its internal friction or resistance. Gas viscosity μ_g refers to the measure of a fluid's resistance to flow or deformation when it is in a gaseous state. Depending on the pressure applied, crude oil viscosity can be divided into three categories [32]:

- **Dead oil viscosity (μ_{od}):** viscosity of crude oil at atmospheric pressure (without gas in solution) and at a given system temperature.
- **Saturated (bubble point) oil viscosity (μ_{ob}):** viscosity at the bubble-point pressure and at the reservoir temperature.
- **Unsaturated oil viscosity (μ_o):** viscosity of the crude oil at a pressure above the bubble point and at the temperature of the reservoir.

The higher the viscosity, the thicker the fluid and it is more resistant to flow. If the friction between layers of the fluid is small, the fliud has low viscosity. All the calculations involving the any movement of fluids require the value of viscosity. Since viscosity is a strong function of the temperature, pressure, gravity and many more factors, empirical correlations are used to accurately determine viscosities.

3.2.2.3 Solution gas-oil ratio (R_s *or* GOR)

As shown in Figure 3.11, when oil is transported to surface, oil shrinks because gas evolves out of oil. This evolving gas is called *solution gas*. The solution gas ratio is ratio between produced volumetric gas flow $\dot{Q}_{gas}$, and produced volumetric oil flow $\dot{Q}_{oil}$ from the oil well, as equation 3.18, when both oil and gas are taken down to reservoir pressure *P* [71], [55], [61]. It is a measure of the amount of gas that will come out of solution as the pressure decreases during production. Empirical correlations are available to determine this ratio for a range of temperatures and pressures.

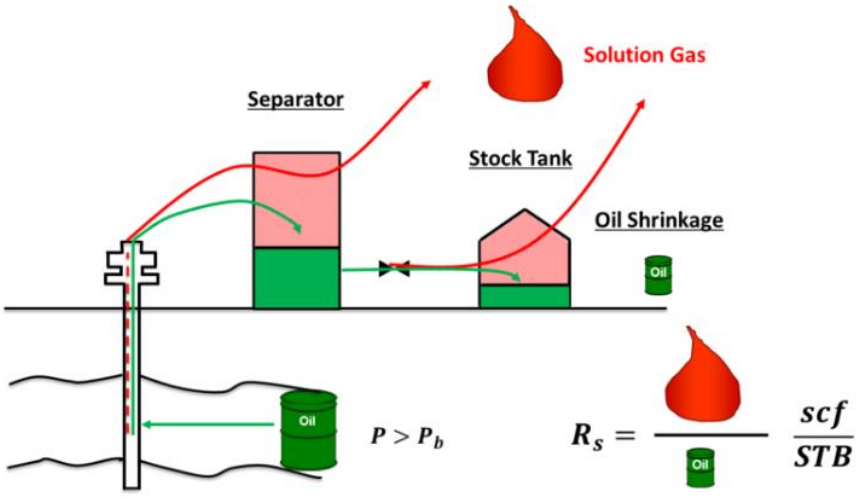

Figure 3.11:Oil shrinkage during the production, dur to gas evolves [71].

$$R_s = GOR = \frac{\dot{Q}_{gas}}{\dot{Q}_{oil}} \tag{3.18}$$

3.2.2.4 Oil and gas formation volume factors $(B_o \text{ and } B_g)$

Oil formation volume factor, B_o is defined as the ratio of oil volume produced at reservoir conditions (T_R and P_R) $\dot{Q}_{oil,R}$ to the ideal oil volume produced at standard conditions ($T_S = 288.71$K and $P_S = 1$ atm) $\dot{Q}_{oil,S}$ [72], [73]. Similarly, gas volume factor B_g is defined as the ratio of oil volume produced at reservoir conditions $\dot{Q}_{gas,R}$ to the ideal oil volume produced at standard conditions ($T_S = 288.71K$ and $P_S = 1$ atm) $\dot{Q}_{gas,S}$. Many empirical correlations are available to determine these ratios for a range of temperatures and pressures.

$$B_o = \frac{\dot{Q}_{oil,R}}{\dot{Q}_{oil,S}} \tag{3.19}$$

$$B_g = \frac{\dot{Q}_{gas,R}}{\dot{Q}_{gas,S}} \tag{3.20}$$

3.2.2.5 Gas-liquid ratio (GLR)

GLR refers to the ratio between volumetric gas flow $\dot{Q}_{gas}$, and volumetric liquid flow $\dot{Q}_{liquid}$. The liquid flow contains both water and oil. In total, this indicates how much gas is present in the flow from the well, as shown in equation 3.21 [7], [61].

$$GLR = \frac{\dot{Q}_{gas}}{\dot{Q}_{liquid}} = \frac{\dot{Q}_{gas}}{\dot{Q}_{oil} + \dot{Q}_{water}} \tag{3.21}$$

3.2.2.6 Water cut

A water cut (WC) is defined as the ratio of a volumetric water flow $\dot{Q}_{water}$, to a volumetric liquid flow $\dot{Q}_{liquid}$. This is a measure of how much water is associated with a produced liquid flow. Most commonly, it is expressed as a percentage by equation 3.22 [7], [61].

$$WC\% = \frac{\dot{Q}_{water}}{\dot{Q}_{liquid}} = \frac{\dot{Q}_{water}}{\dot{Q}_{oil} + \dot{Q}_{water}} \times 100\% \tag{3.22}$$

3.3 Black oil model

In most cases, oil reserves are composed of black oils, which are also known as ordinary oils. It is generally accepted that black oils contain more than 20% C7+, which indicates a high proportion of heavy hydrocarbons [61]. The typical phase envelope of ordinary black oil is shown in figure.

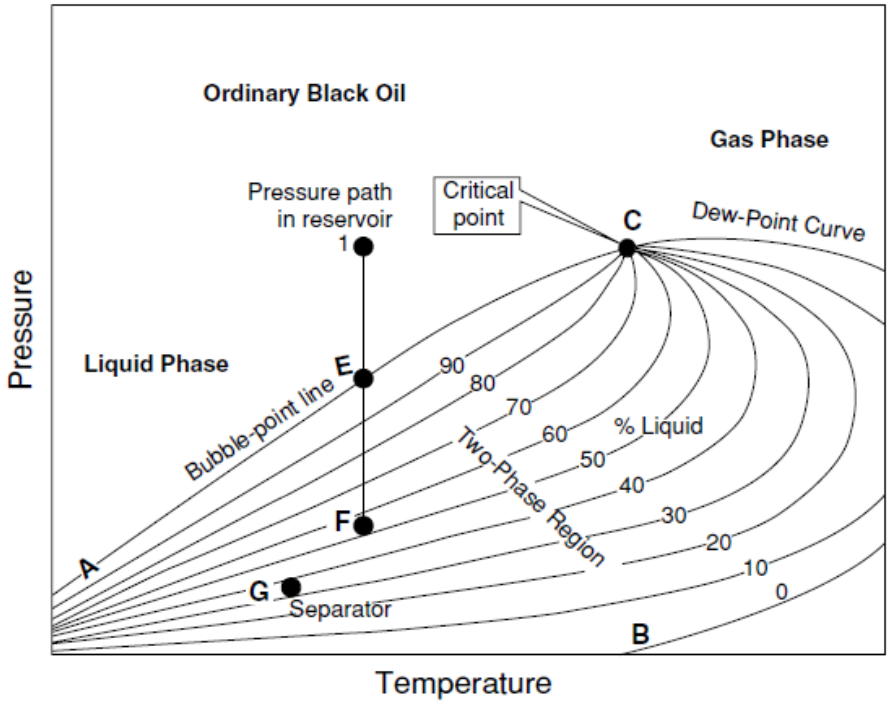

Figure 3.12: Phase envelope of ordinary black oil [32].

As shown in Figure 3.12, the vertical line 1EF indicates a pressure reduction in the reservoir at reservoir temperature. When the reservoir pressure is above the line AC (bubble-point line), the oil is a single-phase liquid or undersaturated, which implies that the oil can dissolve more gas if present. Once the reservoir pressure reaches point E, the oil becomes saturated at all pressures below the bubble point, and it is considered to be fully saturated with gas [32], [61]. F represents the conditions at separation point.

As black oil has a high critical temperature, reservoir conditions are usually on the left side of the critical point, as illustrated in Figure 3.12. As a result of this positioning, the bubble point pressure of black oil (pressure at E) is relatively low. The conditions during separation (F) are generally within the two-phase region of the phase envelope diagram, close to a high-quality liquid line (50%). As a result, a substantial amount of oil remains liquid phase and can be recovered at the surface.

Simulating the petroleum production from a reservoir requires a comprehensive knowledge of the physical properties of reservoir fluids as well as their phase behavior at various temperatures and pressures. Sometimes, experiments can be conducted to determine PVT data. And also, fluid models such as equations of state (EOS) can be employed, which use the reservoir fluid's temperature, pressure, chemistry, and composition, for the calculations. These EOS equations can be solved using software programs such as PVTsim and Multiflash. The process of obtaining PVT (pressure-volume-temperature) data through laboratory testing can be challenging and involves several complexities. And obtaining commercial software for analyzing PVT data may be limited and not easily accessible. As a response to these challenges, empirical correlations have been developed based on field data and laboratory results. These models assume that the reservoir fluids are black oils and can be utilized without knowledge

of the specific composition of reservoir fluid. Thus, these models are referred to as *black oil model*s [61].

3.3.1 Black oil correlations to determine reservoir rock and fluid properties

When the reservoir is modeled in ECLIPSE simulator, it is important to determine solution gas-oil ratio R_s, oil and gas formation factors (B_o, B_g), oil and gas viscosities (μ_o, μ_g) at reservoir temperature as a function of pressure [74]. Following black oil correlations are used to determine these important factors.

3.3.1.1 Correlation for solution gas-oil ratio

Standing's (1947) correlation in equation 3.23, is used to calculate the solution gas-oil ratio R_s [74].

$$R_s = \gamma_g \left[\left(\frac{p}{18.2} + 1.4\right) 10^{0.0125.\text{API} - 0.00091(T-460)}\right]^{1.2048} \tag{3.23}$$

Here, γ_g is the gas specific gravity, API is the stock tank oil gravity, T is the reservoir temperature and p is the reservoir pressure. It should be noted that the above correlation might result in big errors in the presence of nonhydrocarbon components [72].

3.3.1.2 Correlation for oil and gas formation factors

Standing (1947) correlation in equation 3.24 can be used to calculate oil formation factor B_o, as a function of R_s, oil specific gravity γ_o and gas specific gravity γ_g [74].

$$B_o = 0.9759 + 0.000120\left[R_s\left(\frac{\gamma_g}{\gamma_o}\right)^{0.5} + 1.25(T - 460)\right]^{1.2} \tag{3.24}$$

Gas formation factor B_g can be calculated by equation 3.25, where Z is the compressibility factor [74].

$$B_g = 0.02829\frac{ZT}{p} \tag{3.25}$$

3.3.1.3 Correlation for oil viscosity

As discussed in section 3.2.2.2, the crude oil viscosity varies according to the applied pressure. Three different oil viscosities, deal oil viscosity μ_{od}, unsaturated oil viscosity μ_o and saturated oil viscosity μ_{ob} can be calculated by using *Standing's (1981) correlations* shown in equations 3.26-2.28 [74].

$$\mu_{od} = 0.32 + \frac{18 \times 10^7}{API^{4.53}}\left(\frac{360}{T - 260}\right)^{10^{0.42} + \frac{8.332}{API}} \tag{3.26}$$

$$\mu_o = \mu_{ob} + 0.001(p - p_b)[0.0024 \cdot {\mu_{ob}}^{1.6} + 0.038 \cdot {\mu_{ob}}^{0.56}] \quad (3.27)$$

$$\mu_{ob} = 10^a \cdot {\mu_{od}}^b \quad (3.28)$$

Here, p and p_b are reservoir pressure and bubble point pressure respectively. And a, b can be calculated by equations 3.29-3.33.

$$a = R_s(2.2 \times 10^{-7} R_s - 7.4 \times 10^{-4}) \quad (3.29)$$

$$b = 0.68 \times 10^c + 0.25 \times 10^d + 0.062 \times 10^e \quad (3.30)$$

$$c = -0.0000862 \cdot R_s \quad (3.31)$$

$$d = -0.0011 \cdot R_s \quad (3.32)$$

$$e = -0.0037 \cdot R_s \quad (3.33)$$

3.3.1.4 Correlation for gas viscosity

Gas viscosity μ_g can be calculated by empirical correlation suggested by Lee et al. given in equation 3.34 [74].Here, ρ is the gas density.

$$\mu_g = 10^{-4} k_v \cdot \exp\left[x_v \left(\frac{\rho}{62.4}\right)^{y_v}\right] \quad (3.34)$$

Parameters x_v, y_v and k_v can be calculated by using molecular weight of gas, MW as follows:

$$x_v = 3.448 + 986.4 + 0.01009 \cdot \text{MW} \quad (3.35)$$

$$y_v = 2.4 - 0.2x_v \quad (3.36)$$

$$k_v = \frac{(0.379 + 0.0160 \cdot \text{MW})T^{1.5}}{209.2 + 19.26 \cdot \text{MW} + T} \quad (3.37)$$

3.3.1.5 Correlation for relative permeability

The generalized Corey model is one of the most accurate parametric models for estimating relative permeability for two-phase systems such as gas-oil, gas-water, and oil-water. According to the that model, the following functions can be used to estimate the relative permeabilities of oil and water (k_{ro} and k_{rw}) in an oil-water system [74].

$$k_{ro} = k_{rocw}\left[\frac{1 - S_w - S_{ro}}{1 - S_{wc} - S_{ro}}\right]^{n_{ow}} \quad (3.38)$$

$$k_{rw} = k_{rwro}\left[\frac{S_w - S_{wc}}{1 - S_{wc} - S_{ro}}\right]^{n_w} \quad (3.39)$$

Here, S_w is water saturation, S_{wc} is irreducible water saturation, S_{ro} is the residual oil saturation, k_{rocw} and k_{rwro} are the maximum relative permeability of oil and water respectively, whcih can be seen in Figure 3.6Figure 3.6. And n_{ow} and n_w are Coray exponents.

When solving these equations software uses, linear regression using the least-square method.

3.4 Pressure drops in horizontal wells

The pressure drop of fluid in horizontal wellbore, is composed of three individual components [75].

- **Frictional pressure drop** – caused by gas/liquid interactions with wellbore wall.
- **Acceleration pressure drop** – caused by radial flow and liquid holdup coming from perforations, which change the total flow rate (velocity).
- **Mixing pressure drop** – caused by the incoming flows coming through perforations to wellbore, which mixes the total fluid flow.

The following Figure 3.13 shows various types of pressure drops that act along horizontal wellbore.

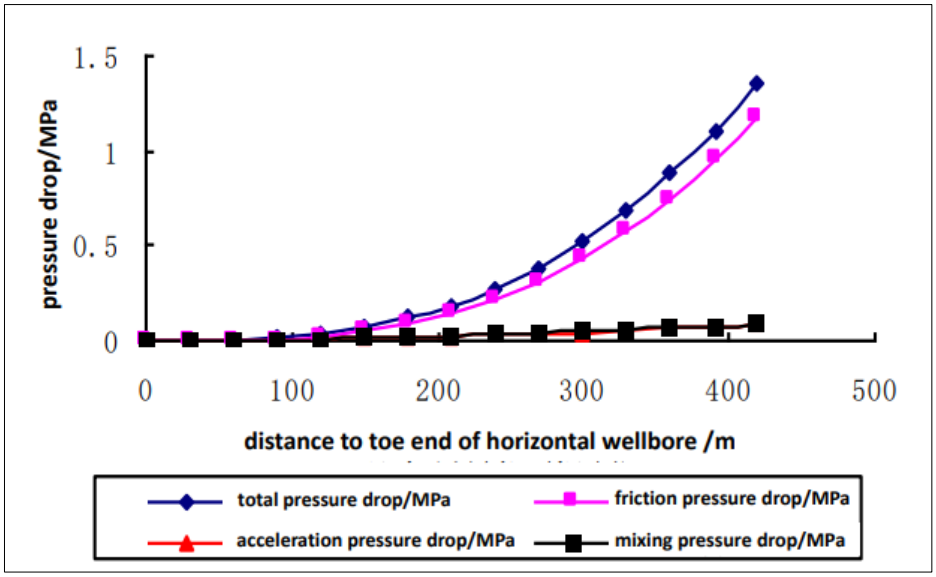

Figure 3.13: Various types of pressure drops along the horizontal wellbore [75].

According to Figure 3.13, *frictional pressure drop* makes the largest impact on total pressure drop along horizontal wellbore. To model and simulate the oil production from a horizontal well, it is important to accurately predict the frictional pressure drop. When fluid flows in the wellbore, it can be in a single-phase or multiphase state. In the case of multiphase flow, the pressure drop is a function of multiple parameters, and computer software is required to calculate it accurately. For single-phase flows, several straightforward equations have been proposed in recent years for calculating frictional pressure drops in pipes. The following equation 3.40 can be used to calculate single-phase frictional pressure drop ΔP_f [69]. L is the wellbore length, f is the Mody friction factor, ρ is the fluid density, v is the flow velocity, d is the diameter of wellbore pipe and g_c is a conversion factor [69].

$$\frac{\Delta P_f}{L} = \frac{f\rho v^2}{2g_c d} \tag{3.40}$$

The friction factor f varies depending on whether the flow is laminar or turbulent. A laminar flow does not depend on the roughness of the tubing ε, as there is no fluid movement adjacent to the pipe wall. Friction factor is calculated by equation 3.41, where Reynolds number Re is given by equation 3.42. Fluid viscosity is indicated by μ [69].

$$f = \frac{64\mu}{\rho v d} \tag{3.41}$$

$$Re = \frac{\rho v d}{\mu} \tag{3.42}$$

Usually in a pipe flow, turbulent flow is more common than laminar flow, and turbulent flow tends to cause greater pressure drops. When the Reynolds number is 2100-4000, laminar flow transforms into turbulent flow. The roughness of the pipe's inner surface ε becomes a factor in turbulent flow. There are various correlations to predict the single-phase friction factor in turbulent flow, and one of the most commonly used formulas in modern software is the Colebrook-White formula in equation 3.43 [69].

$$\frac{1}{\sqrt{f}} = 1.74 - 2\log\left(\frac{2\varepsilon}{d} + \frac{18.7}{Re\sqrt{f}}\right) \tag{3.43}$$

3.5 Mathematical models for ICDs

The operations of inflow control devices (ICDs) are defined by using specific mathematical models for each type of ICDs.

3.5.1 Passive inflow control devices (ICDs) - orifice type

As discussed in section 2.4.1, the working principle of ICDs is to delay the early water/gas breakthroughs by adding extra pressure drops to the well in order to balance the inflows along the well. This required pressure drop is achieved by passing the fluid through a restriction, which is schematically illustrated in Figure 3.14.

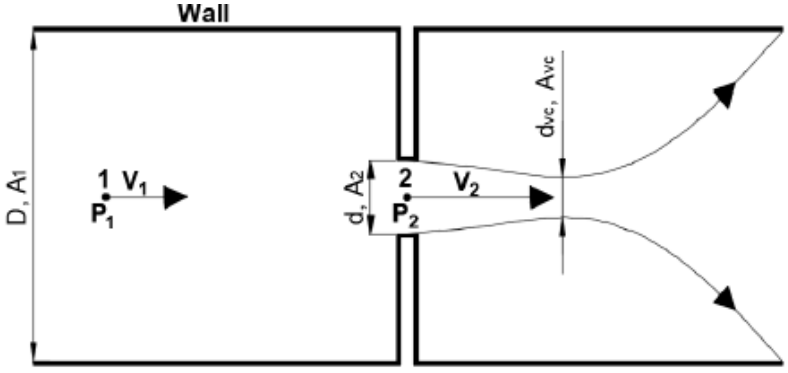

Figure 3.14: Schematic diagram for orifice plate [76].

It should be noted that, the design of nozzle/orifice type ICDs is typically focused mainly on creating a pressure drop across a series of nozzles, which helps to equalize the inflow rates, frictional pressure drop is not a primary consideration in this design.

Therefore, neglecting the frictional pressure drop and assuming the flow is incompressible and at steady state, applying the Bernoulli's equation to point 1 and 2, which are at same level,

$$P_1 + \frac{\rho v_1^2}{2} = P_1 + \frac{\rho v_1^2}{2} \tag{3.44}$$

Applying the Continuity equation,

$$\dot{Q} = v_1 A_1 = v_2 A_2 \tag{3.45}$$

Equation 3.44 and 3.45 can be simplified to determine the flow rate through the pipe $\dot{Q}$.

$$\dot{Q} = A_2 \sqrt{\frac{2(P_1 - P_2)/\rho}{1 - \left(\frac{A_2}{A_1}\right)^2}} \tag{3.46}$$

Discharge coefficient C_D is used to modify equation 3.46 to equation 3.47 for real cases where $C_D = A_2/A_{vc}$ and $\beta = d/D$. d is orifice diameter and D is production tubing diameter. A_{vc} is called Vena Contracta, which is the minimum jet area just downstream of the orifice.

$$\dot{Q} = C_D A_2 \sqrt{\frac{1}{1 - \beta^4}} \cdot \sqrt{\frac{2\Delta P}{\rho}} \tag{3.47}$$

Orifice type ICDs have very small orifice diameter ($d <<< D$). Therefore, $\beta = d/D \approx 0$. Valve opening and closing can be indicated by using a parameter a, which is $0 \leq a \geq 1$. Then the equation 3.47 can be modified to equation 3.38, which is the general equation to model the operation of orifice type ICDs [7], [74], [76].

$$\dot{Q} = a C_D A_2 \sqrt{\frac{2\Delta P}{\rho}} \tag{3.48}$$

3.5.2 Autonomous inflow control devices (AICDs) - RCP type

As discussed in section 2.4.2, AICDs are an improved version of ICDs that can operate autonomously, and RCP AICD is owned by Statoil. AICDs have a unique design that not only delays water or gas breakthrough, but also reduces the negative effects caused by such a breakthrough. This is achieved through a specialized valve that can limit the flow of low-viscosity fluids while favoring the flow of high-viscosity fluids, resulting in increased oil production compared to ICDs [52].

The working principle follows the Bernoulli equation. Since RCP AICDs are designed to actively control the inflow rate and respond to changes in the flow rate, it has been developed to consider frictional pressure drop $\Delta P_{Friction\ loss}$ [52].

$$P_1 + \frac{\rho v_1^2}{2} = P_1 + \frac{\rho v_1^2}{2} + \Delta P_{Friction\ loss} \tag{3.48}$$

Statoil developed the functionality of RCP based on the experimental data and they have implemented the RCP model in ECLIPSE simulation tool. According to the RCP model in equation 3.49, the differential pressure across the valve δP is a function of the fluid properties and volumetric flow across the valve q [52], [74].

$$\delta P = f(\rho, \mu) \cdot a_{AICD} \cdot q^x \tag{3.49}$$

Where, a_{AICD} and x are user input model constants, which depend on different RCP designs for different oil fields and their fluid properties.

The function $f(\rho, \mu)$ is an analytic function of fluid mixture density ρ and viscosity μ. It is expressed as [52], [74], [76].

$$f(\rho, \mu) = \left(\frac{\rho_{mix}^2}{\rho_{cal}}\right) \cdot \left(\frac{\mu_{cal}}{\mu_{mix}}\right)^y \tag{3.50}$$

Here, y is a user defined constant, ρ_{cal} is calibration density and μ_{cal} is calibration viscosity, and they can be defined as follows,

$$\rho_{mix} = \alpha_{oil}\, \rho_{oil} + \alpha_{water}\, \rho_{water} + \alpha_{gas}\, \rho_{gas} \tag{3.51}$$

$$\mu_{mix} = \alpha_{oil}\, \mu_{oil} + \alpha_{water}\, \mu_{water} + \alpha_{gas}\, \mu_{gas} \tag{3.52}$$

Here, α is the volume fraction of each phase.

RCP function was validated with many experiments conducted for various oils with different viscosities. The following Figure 3.15 shows some of validations results done by Statoil [52]. Dots represent the experimental data while lines represent the model function outputs, and this shows its specific working behaviors for different viscous fluids.

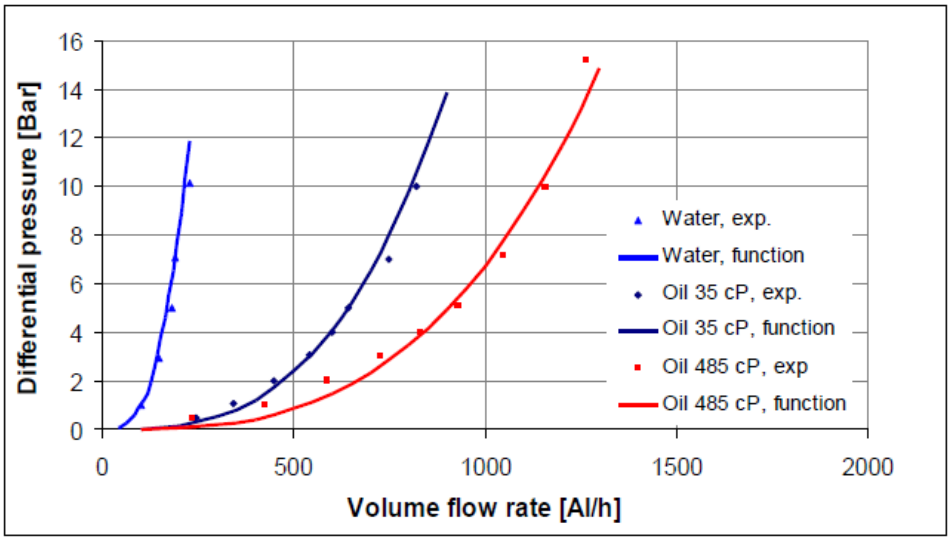

Figure 3.15: RCP model function validation with experimental data [52].

3.5.3 Autonomous inflow control valve (AICVs) - RCP type

Following the detailed discussion about AICV in section 2.4.3, when AICDs can partially close against unwanted fluids, AICVs can almost completely close when it is surrounded by a low-viscosity fluid compared to oil, such as water or gas. As shown in Figure 3.16, generally, AICVs are composed of a pipe-shaped laminar flow restrictor and a turbulent flow restrictor in series and AICVs function according to the difference between pressure drops across the two restrictors. The pressure drops across the laminar flow restrictor and turbulent flow restrictor were presented in equation 3.53 and 3.54, which can be reminded as follows [53], [74].

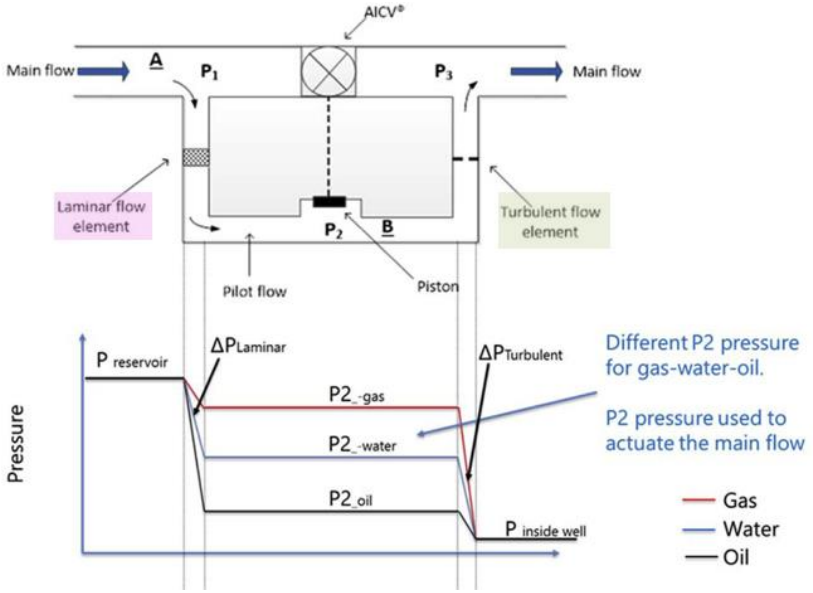

Figure 3.16: Simplified sketch of the flow paths on AICV and pressure changes inside for different fluids [54].

$$\Delta P_{Laminar} = \frac{32 \cdot \mu \cdot \rho \cdot \nu \cdot L}{D^2} \tag{3.53}$$

$$\Delta P_{Turbulent} = K \cdot \frac{1}{2} \cdot \rho \cdot \nu^2 \tag{3.54}$$

Here,

$\Delta P_{Laminar}$ - Pressure drop across the laminar flow restrictor

$\Delta P_{Turbulent}$ - Pressure drop across the turbulent flow restrictor

μ - Fluid viscosity

ν – Fluid velocity

ρ – Fluid density

D – Diameter of laminar flow restrictor

L – Length of laminar flow restrictor

K – Geometrical constant

According to equation 3.53, the $\Delta P_{Laminar}$ is determined by the ρ and μ of the fluid. As a result, viscous fluids like oil experience a greater pressure drop through a laminar flow restrictor than fluids with low viscosities like water and gas. As a result of this low pressure drop after the laminar flow restrictor, for low viscous fluids, the pressure in the chamber between the laminar and turbulent flow restrictors (P_2) becomes higher. In this manner, low-viscosity fluids can travel with greater velocity before passing through a turbulent flow restrictor.

The $\Delta P_{Turbulent}$ can be expressed as a function of ρ and v^2 based on equation 3.54. Due to the low viscosity, their pressure drops across turbulent flow restrictors are greater than those of oils.

Overall, P_2 is less for low high viscous fluids, while P_2 is higher for low viscous fluids as shown in the graph in Figure 3.16. As a result of these principles, AICVs are designed to remain open for oils, but close almost completely for unwanted fluids such as gas and water.

3.6 Advanced well completion

Horizontal wells completed with nozzle ICDs, RCP AICDs, and AICVs follow a similar process. The schematic of Figure 3.17 illustrates the advanced well completion using FCDs and AFI in a heterogeneous reservoir. Each production joint is around 12.4 m long and includes an FCD and a sand screen. A flow control device is usually installed per joint, but a maximum of four may be employed depending on the circumstances. The reservoir fluids enter the annulus, pass through the sand screen, and then flow into the inflow chamber, where the FCDs are located, before entering the production tubing. In areas with higher inflow, such as the heel section of the well or high-permeability zones, water or gas breakthrough can occur more quickly. By isolating these areas with Annular Flow Isolation (AFI), the annulus is prevented from filling with unwanted fluids. Furthermore, zonal isolation can improve oil recovery prior to water or gas breakthrough [74].

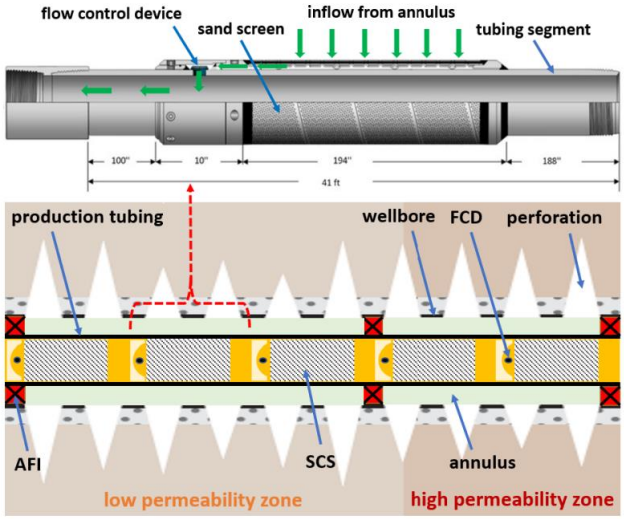

Figure 3.17: Schematic diagram of advanced well completion with the FCD and AFI for a heterogeneous reservoir [77].

3.7 Multi-Segmented well model (MSW)

The Multi-Segment Well model is a special extension available in both ECLIPSE 100 and ECLIPSE 300 that offers a comprehensive and accurate understanding of fluid behavior in the wellbore. The MSW is specially designed for horizontal and multilateral wells, but it can also be used for vertical wells [78].

It is complex to describe, the pressure gradient and changes in fluid composition induced by specific components of advanced wells. The MSW can be used to model this behavior. This model divides the production tubing into several one-dimensional segments as shown in Figure 3.18. In each segment, there is a node and a flow path, and each segment contains its own set of independent variables to describe the fluid conditions in that region. For each segment, the variables are evaluated by solving *material balance equations* for each phase or component, as well as a *pressure drop equation* that incorporates local hydrostatic, friction, and acceleration pressure gradients [77], [78].

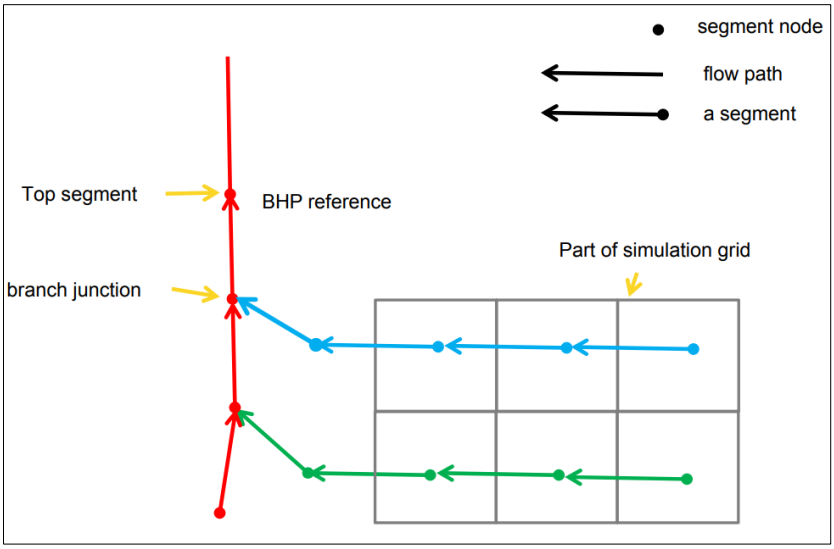

Figure 3.18: Simplified sketch for the representation of multi-segmented well with two parallel production tubing laterals [79].

Every segment within the wellbore is connected to one, or multiple grid blocks within the reservoir, or may be zero grids if there is no perforations in that segment [74], [78]. The way that segments connect to reservoir grid blocks is illustrated in Figure 3.19.

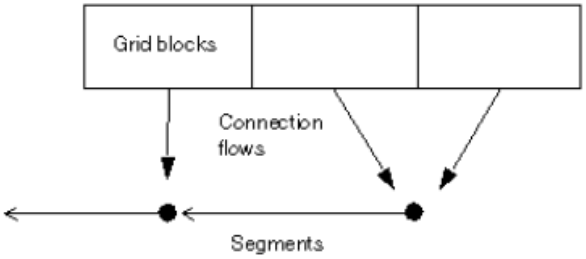

Figure 3.19: Possible connections of reservoir grid blocks with wellbore segments [78].

Figure shows a schematic illustration for MSW model for advanced horizontal well. According to MSW model, production tubing and wellbore are considered as two separate branches consisting of specific segments. Furthermore, certain segments can be configured to simulate Flow Control Devices (FCDs). The wellbore and production tubing are connected by these FCD segments (valve segments) as shown in Figure 3.20. Fluid enters the wellbore through the wellbore segments and then passes to the production tubing through FCD valve segments. Then the fluid flows to production outlet via production tubing segments [74], [78].

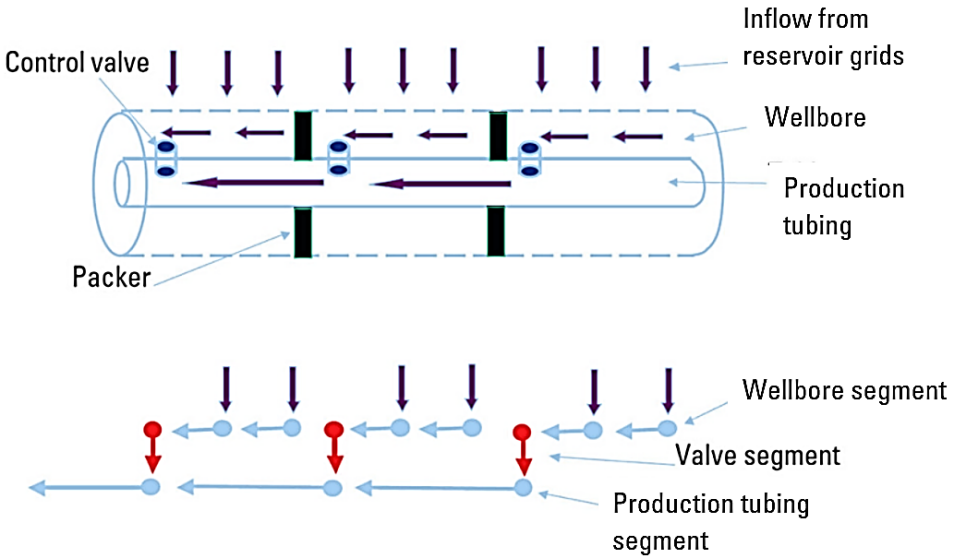

Figure 3.20: Schematic of a multi-segment well model [80].

4 Methods and calculation

The purpose of this chapter is to provide an overview of the necessary calculation methods for the development of models ECLIPSE and OLGA based on the theoretical background discussed in chapter 3.

4.1 Development of synthetic heterogeneous reservoir

The main objective of this study is to couple OLGA with ECLIPSE simulator tools to simulate improved oil recovery by water injection. Therefore, a rectangular heterogeneous reservoir is synthetically designed with specific reservoir characteristics. A petroleum reservoir is a porous medium filled with hydrocarbon mixture in all three phases. The properties of hydrocarbon mixture are specified for range of pressures and temperatures, later chapters. Porous medium specification method is discussed in this subchapter.

When designing the structure of a porous medium, the key parameters to consider are permeability and porosity. Porosity measures the percentage of void space in the medium relative to its total volume. Permeability refers to the porous medium's fundamental property that determines its ability to transmit a single fluid when the void space is entirely saturated with that fluid. As discussed in section 3.1.4.2, porosity has 2 components as horizontal (lateral) and vertical porosity. The permeability of a porous medium can exhibit a considerable contrast between its vertical and horizontal directions due to the gradual buildup of sediment over extended periods. However, there is typically no variation in permeability between the two horizontal directions [63]. Assuming a set of capillary tube is laminar, Carman and Kozeny developed a correlation between absolute permeability and porosity, names as *Carman-Kozeny correlation*, shown in equation 4.1 [63].

$$k = \frac{1}{8\tau A_v^2}\frac{\phi^3}{(1-\phi)^2} \tag{4.1}$$

Where the rock texture is defined by its tortuosity τ and specific surface area of pores A_v. Tortuosity is the ratio between the flow path length and distance between ends. Assuming that reservoir is made from spherical grains with diameter $d_p = 10$ µm, specific surface area $A_v = 9/d_p$, $\tau = 0.81$, Carman-Kozeny correlation simplifies to, equation 4.2 [63].

$$k = \frac{1}{72 \times 0.81}\frac{\phi^3 {d_p}^2}{(1-\phi)^2} \tag{4.2}$$

MATLAB programming tool has a free open-source software for reservoir modelling and simulation, called MATLAB Reservoir Simulation Toolbox (MRST), which can be used to design the reservoir. First the reservoir geometry is given as an input for the program. Assuming the porosity of the reservoir ranges 0.15-0.27 (mean porosity is 0.21), porosity ϕ is generated as a Gaussian porosity field using a build-in random values generating function. Using the generated porosity as an input for Carman-Kozeny correlation (equation 4.2), corresponding permeability k is generated. The data generated in MRST is imported into ECLIPSE in order to create the heterogeneous reservoir with provided dimensions.

4.2 Development of mathematical model for ICD, RCP AICD and AICV valves

The ICD behaves similarly to the fully open stage of the AICD, and thus can be modeled easily in ECLIPSE. However, to model the AICD completion, a mathematical model expressing its autonomous behavior (as shown in equation 4.3) must be derived first using linear regression. For AICV modelling, the same approach is used to model the Autonomous Inflow Control Valve (AICV), as ECLIPSE does not have specific keywords for this completion design. A mathematical model for autonomous behavior of the AICV is expressed in the format of equation 4.3, and the same method of AICD is employed [74].

As discussed in section 3.5.2, autonomous function of AICD can be expressed by equation 4.3.

$$\Delta P_{AICD} = a_{AICD} \cdot \left(\frac{\rho_{mix}^2}{\rho_{cal}}\right) \cdot \left(\frac{\mu_{cal}}{\mu_{mix}}\right)^{y} \cdot q^{x} \tag{4.3}$$

when,

$$\rho_{mix} = \alpha_{oil}\,\rho_{oil} + \alpha_{water}\,\rho_{water} + \alpha_{gas}\,\rho_{gas} \tag{4.4}$$

$$\mu_{mix} = \alpha_{oil}\,\mu_{oil} + \alpha_{water}\,\mu_{water} + \alpha_{gas}\,\mu_{gas} \tag{4.5}$$

The unknowns $x, y, a_{AICD}, \mu_{cal}$ and ρ_{cal} for AICD and AIVC can be calculated separately by using the experimental data obtained by experiments conducted for AICD and AICV respectively. The experiment test results used for this study are shown in Figure 4.1[74].

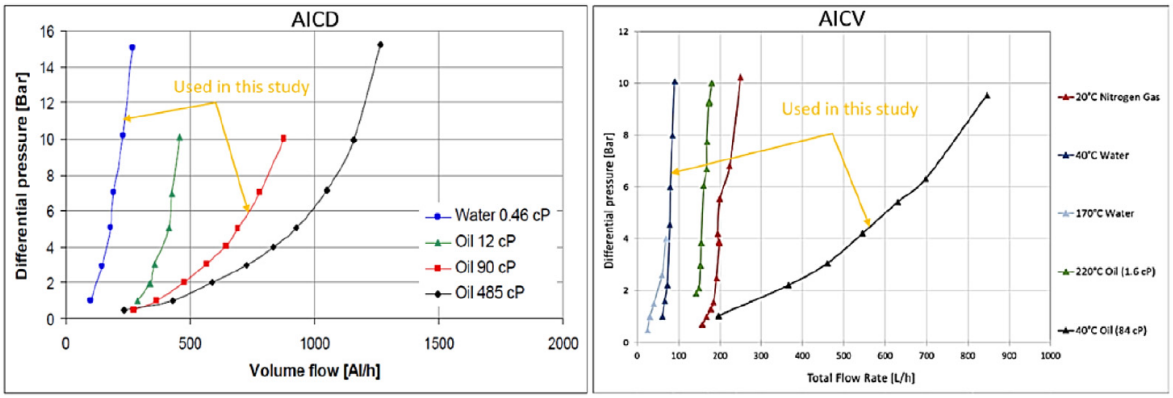

Figure 4.1: Experiment test results for the performance of AICD and AICV [74].

Using experimental data in figure 4.1, MATLAB can then be used to determine the unknowns through linear regression. And mathematical models for describing the performance of AICD and AICV (with their autonomous function) can be derived as equation 4.6 and 4.7 [74].

$$\Delta P_{AICD} = 0.2875 \cdot \left(\frac{\rho_{mix}^2}{1000}\right) \cdot \left(\frac{1}{\mu_{mix}}\right)^{0.6489} \cdot q_{AICD}^{2.6417} \tag{4.6}$$

$$\Delta P_{AICV} = 0.4127 \cdot \left(\frac{\rho_{mix}^2}{1000}\right) \cdot \left(\frac{1}{\mu_{mix}}\right)^{0.7532} \cdot q_{AICD}^{2.0115} \quad (4.7)$$

Following Figure 4.2 validates that developed mathematical models have a good agreement with test results.

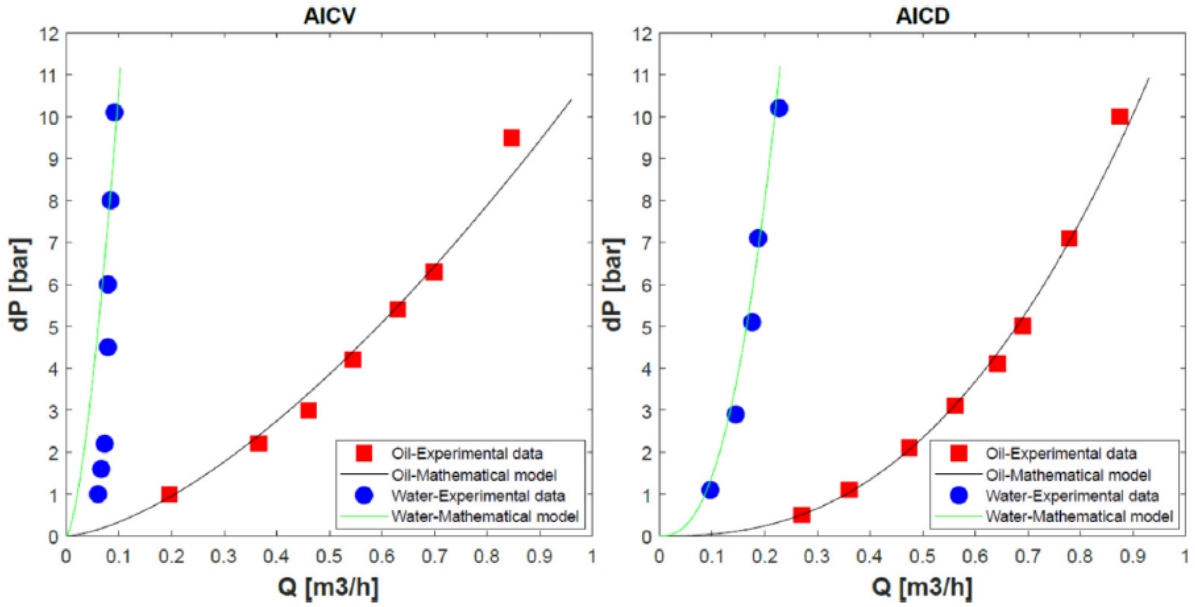

Figure 4.2: Comparison of derived mathematical model for AICD and AICV with experimental test results.

4.3 Control function in OLGA for the behavior of RCP AICD and AICV valves

ECLIPSE simulator is used to simulate the oil reservoir and production well is simulated by OLGA simulator. As the values are mounted in production well, valves should be modeled in the well model in OLGA. But OLGA does not provide any direct options for implementing valve behavior. Implementation of AICD and AICV in OLGA can be achieved by considering, vales are similar to a self-adjusting orifice ICD valve which has flexible flow area [74].

As discussed in section 3.5.1, mathematical equation governing the behavior of orifice ICD is,

$$\dot{Q} = aC_D A_{orifice} \sqrt{\frac{2\Delta P}{\rho}} \quad (4.8)$$

Combining equation 4.8 with equation 4.6 which described the model of AICD, valve opening for AICD (a_{AICD}),can be expressed by equation 4.9,

$$a_{AICD} = \frac{\left[\frac{\Delta P_{AICD}}{10^5 \times 0.2875 \cdot (\rho_{mix}^2/1000) \cdot (1/\mu_{mix})^{0.6489}}\right]^{\frac{1}{2.6417}}}{A_{orifice} \times 3600 \times C_D \cdot \sqrt{\frac{2 \cdot \Delta P_{AICD}}{\rho_{mix}}}} \quad (4.9)$$

Similarly for valve opening for AICV (a_{AICV}) can be expressed by equation 4.10,

$$a_{AICV} = \frac{\left[\frac{\Delta P_{AICV}}{10^5 \times 0.4127 \cdot (\rho_{mix}^2/1000) \cdot (1/\mu_{mix})^{0.7532}}\right]^{\frac{1}{2.0115}}}{A_{orifice} \times 3600 \times C_D \cdot \sqrt{\frac{2 \cdot \Delta P_{AICV}}{\rho_{mix}}}} \quad (4.10)$$

Where,

$$\rho_{mix} = \alpha_{oil}\,\rho_{oil} + \alpha_{water}\,\rho_{water} + \alpha_{gas}\,\rho_{gas} \quad (4.11)$$

$$\mu_{mix} = \alpha_{oil}\,\mu_{oil} + \alpha_{water}\,\mu_{water} + \alpha_{gas}\,\mu_{gas} \quad (4.12)$$

- ✓ Considering orifice diameter as 0.00265 m, the equivalent flow area of ICD $A_{orifice} = \pi \cdot \frac{0.00265^2}{4} = 5.515 \times 10^{-6} m^2$. When AICD and AICV are fully open, they behave like ICD.
- ✓ Pressure drops over AICD and AICV, $\Delta P_{AICD} = \Delta P_{AICV} = 10bar$
- ✓ Assuming, $C_D = 0.85$

Based on the equation 4.9 – 4.12, valve opening varies with water cut and valve opening can be calculated using water cut. When the valve is fully opened, $a = 1$ and oil is passing through the valve. Based on these relations, MATLAB code can be used to generate the valve opening data with respect to water cut. MATLAB generated data is plotted in Figure 4.3.

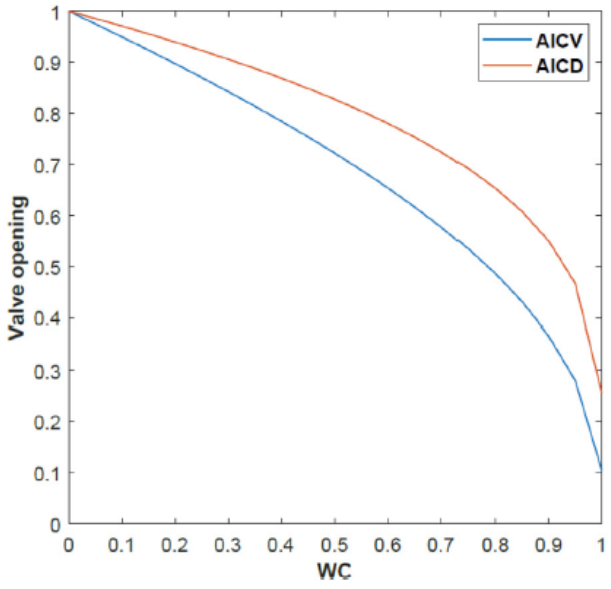

Figure 4.3: Valve opening versus water cut for AICD and AICV [74].

5 Development of the OLGA/ECLIPSE model

This study aims to model and simulate the process of improved oil recovery (IOR) in a synthetic heterogeneous reservoir with specific fluid and rock properties using an advanced horizontal well. The EOR process involves injecting water vertically from two points in the reservoir bed. To achieve this, a synthetic reservoir model is developed in the ECLIPSE simulation tool. The model incorporated the various heterogeneities present in the reservoir, such as variations in porosity and permeability, to accurately represent the reservoir's behavior. The advanced horizontal well is modeled using the OLGA simulation tool. The well was equipped with different types of inflow control valves to optimize its performance during the EOR process. To simulate the EOR process as a whole, two individual models are coupled and simulated for specific time periods, allowing them to interact and influence each other's behavior. This coupling enables us to investigate the impact of the advanced horizontal well and the water injections on the overall recovery of oil from the reservoir. A step-by-step approach to basic model development is discussed throughout this chapter, and at the end, further modified simulation models will be discussed.

5.1 Development of reservoir model in ECLIPSE

For ECLIPSE to run a simulation, one input file (script) must be created containing a complete description of the model. There are different parameters in the script which relate to the properties of the reservoir fluid and rock, as well as the recovery schedule. In ECLIPSE, input data is given using keywords. ECLIPSE simulation data files (scripts) consist of the following sections,

1. RUNSPEC section
2. GRID section
3. PROPS section
4. SOLUTION section
5. SUMMARY section
6. SCHEDULE section

Usually, ECLIPSE reads the data file section by section. At the end of the simulation, outputs can be visualized in postprocessors like Techplot software, which is used in this thesis. The same ECLIPSE file is used for all the different valve completions specified in the OLGA model. The ECLIPSE data file is given in Appendix B.

RUNSPEC section includes run specification information that specifies the simulation parameters and options for running the simulation, such as title, main dimensions, fluid model (with phases), simulation stating date, production, and injection well information, and simulation options, such as the time step size, the numerical method to be used, the convergence criteria, and any additional simulation options. Under the GRID section, the reservoir grid is explained in detail, and porosity and permeability data generated in MRST is imported to the GRID section. The PORPS section is used to specify the reservoir fluid properties, rock properties, and relative permeability data with respect to its saturation. In the SOLUTION section, the initial conditions (pressure, saturations, compositions) are defined. In the

SUMMARY section, output data is defined. Variables to be written to output summary files must be specified here (e.g., oil flow rate, water flow rate, accumulated oil and water flow rates.). In the absence of a SUMMARY section, ECLIPSE does not generate output results files. The SCHEDULE section is used to define production and injection wells and their operation, to describe operating schedules, boundary conditions, and control convergence [81].

5.1.1 Reservoir grid

Under the GRID section, the reservoir grid is described in detail. The main dimensions of the reservoir are given in table 5.1.

Table 5.1: Main dimensions of the reservoir.

Length of the reservoir (x)	1000 m
Width of the reservoir (y)	200 m
Height of the reservoir (z)	50 m

The reservoir geometry can be described using either Cartesian or cylindrical coordinates, but for horizontal wells, Cartesian coordinates are often used. The number of grids in (x, y, z) coordinates needs to be determined for discretizing the reservoir in OLGA/ECLIPSE. The grid resolution must be chosen carefully, as there is a trade-off between accuracy and calculation time. A suitable grid setting can be achieved by using finer mesh in areas with high variation in fluid properties and coarser mesh in other areas.

As discussed in section 3.6, each production joint has a length of 12.4 m. The horizontal well is positioned in the x-direction of the reservoir (length). Since the length is 1000 m, 80 ICDs can be placed along the well. But it is complex to simulate the real well with a huge number of ICDs as it requires a long simulation time. Therefore, one equivalent ICD is used to represent two real ICDs.

Thus, 40 cells are considered in the x direction, and 40 ICDs are used along the well. In the y and z directions, 16 and 5 cells are considered, respectively. The grid settings in ECLIPSE, including the number of cells and their sizes, are given in table 5.2.

Table 5.2: Number of cells and their sizes for the grid setting in ECLIPSE.

Direction	**Number of cells**	**Size of the cells (m)**
x	nx = 40	25 m (constant)
y	ny = 10	12.5 m (constant)
z	nz = 5	10 m (constant)

The horizontal well is positioned in the middle of the (x_i, 1, 1) cell row, as shown in figure 5.2. Initially, two vertical water injections are placed in the middle of (1,16, z_i) and (40,16, z_i) cell columns, as shown in figure 5.1. But the water is injected via the last three cells in the injections.

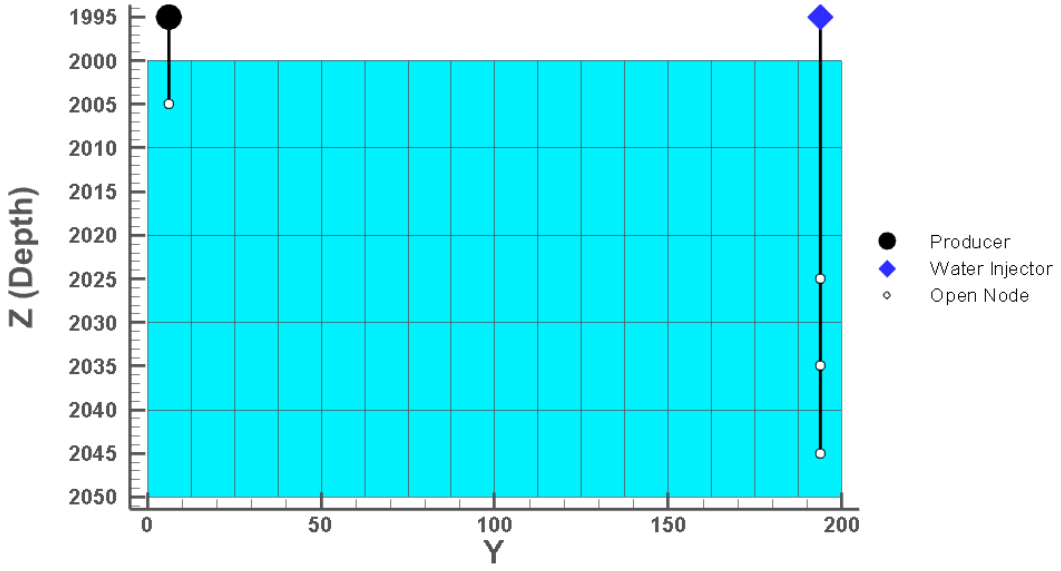

Figure 5.1: YZ plane of the reservoir through the 1st cell in x direction.

Reservoir geometry with horizontal well and two water injections is illustrated in figure 5.2.

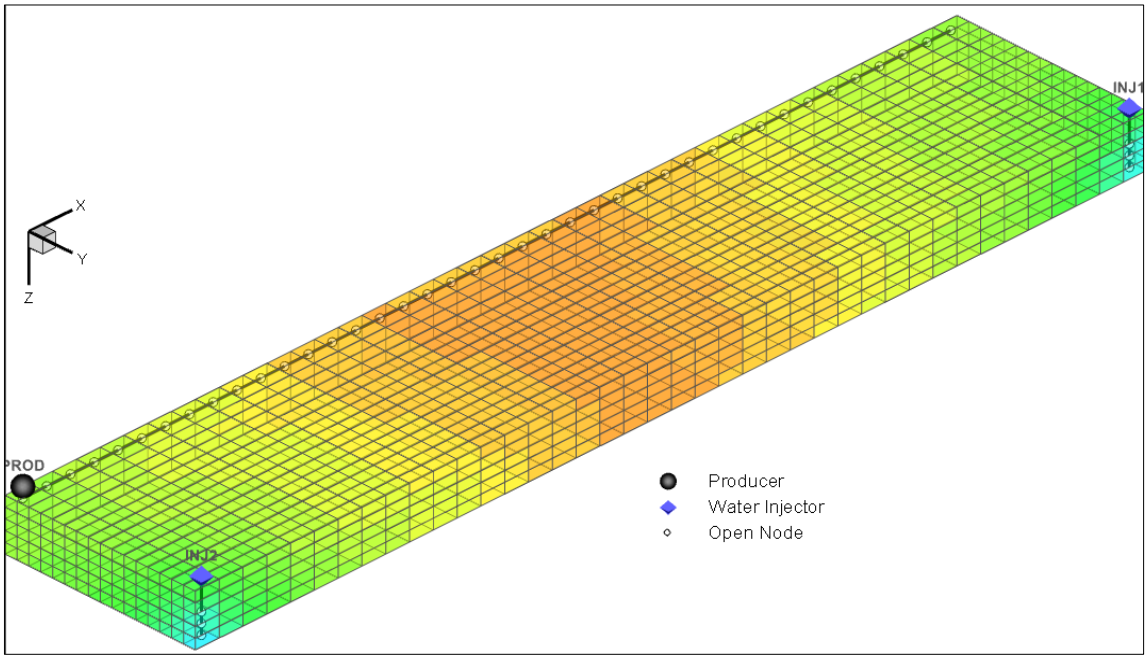

Figure 5.2: Reservoir geometry.

5.1.2 Reservoir fluid and rock properties

When the fluid properties are considered, there are two options for introducing reservoir fluid properties in ECLIPSE: the Black oil model and the PVT table. PVT tables are created through laboratory tests or commercially available software such as PVTsim or Multiflash that determines the phase behavior of reservoir fluids across a wide range of temperatures and pressures. Since these options can be difficult to access, the PVT table option is not feasible for this thesis.

According to figure 3.8, fluids in a reservoir can be categorized into five types. It is assumed that the designed reservoir contains a viscous oil with 90cP viscosity. Therefore, the reservoir fluid can be considered as a black oil type (viscosity is 2 to 3 – 100 and up). Thus, the Black oil model option in ECLIPSE can be used to introduce fluid properties. As mentioned in section **Error! Reference source not found.**, according to the application, there are various types of black oil correlations to solve the black oil model.

Reservoir fluid properties and some rock properties used for the OLGA/ECLIPSE model are listed in table 5.3 [74].

Table 5.3: Fluids properties in reservoir [74].

Parameter	**Valve**
Solution GOR	50 Sm^3/Sm^3
Oil density	990 kg/m^3
Water density	1050 kg/m^3
Gas density	0.67 kg/m^3
Oil Viscosity	90 cP
Water Viscosity	0.46 cP
Temperature	60℃
Mean porosity	0.21
Initial water saturation	0.12
Pressure	200 bara

In this study, oil is pushed towards the well by two water injections from the reservoir side, and because of this, oil is produced. The components of water drive feed and oil feed are listed in table 5.4.

Using the blck oil correlations discussed in section 3.3.1, solution gas-oil ratio R_s, oil and gas formation factors (B_o, B_g), oil and gas viscosities (μ_o, μ_g) at reservoir temperature as a function of pressure, are calculated and plotted in figure 5.3.

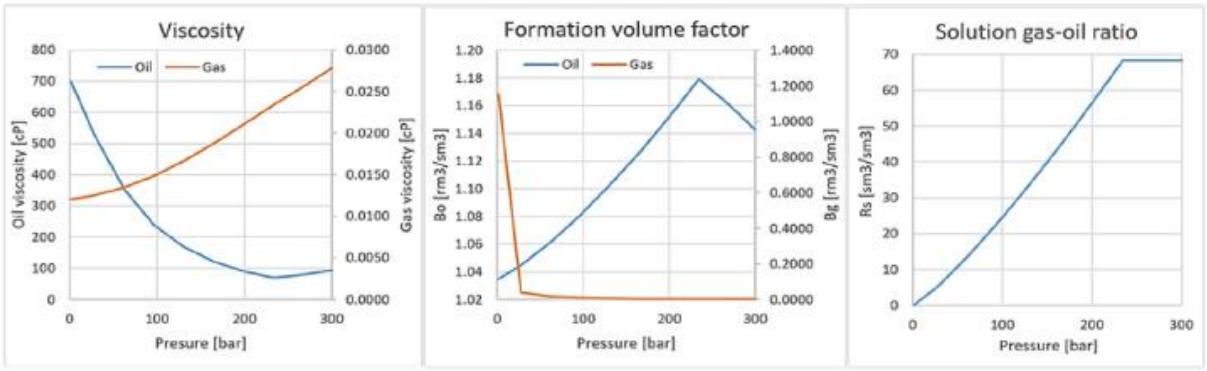

Figure 5.3: Physical properties of oil and gas at the reservoir temperature based on different pressures [74].

5.1.3 Reservoir permeability

The reservoir is considered a heterogeneous sandstone reservoir. As discussed in section 3.1.4, reservoir permeability is determined by three parameters: absolute permeability, permeability anisotropy, and relative permeability. Long-normal *absolute permeability* of the reservoir in this study is assumed in the range 100 - 800 mD millidarcies to account for uncertainty in the reservoir, which means that the actual permeability value is not known with certainty but is expected to fall within this range. As discussed in section 3.3.1.5, *the generalized Corey model* can be used to calculate the *relative permeabilities* of oil and gas (k_{ro} and k_{rw}), with the use of ECLIPSE software. Likewise, generated values plotted in figure 5.4 are inputs for the ECLIPSE model. Here, S_{wc} is irreducible water saturation is 0.12 and S_{ro} is the residual oil saturation is 0.05.

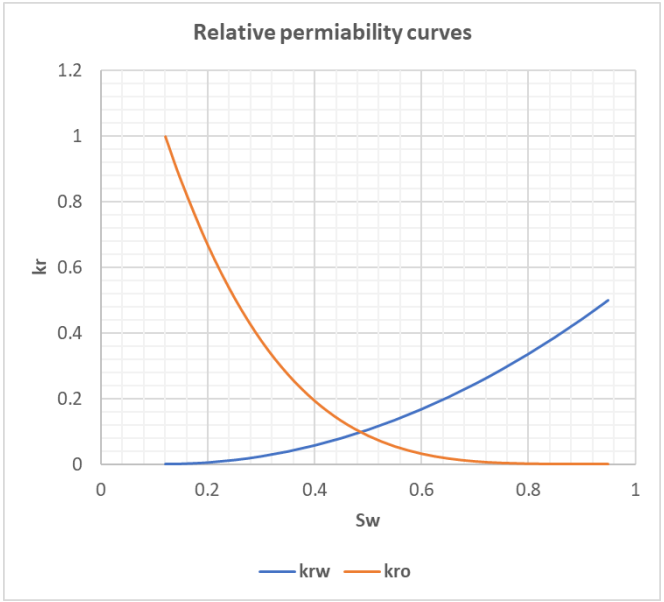

Figure 5.4: Generated relative permeability values.

It is assumed that the reservoir is a heterogeneous sandstone reservoir with a Gaussian distribution of porosity in the range of 0.15 and 0.27, with a mean value of 0.21 throughout the reservoir. As discussed in section 4.1, permeability has a great relation to porosity, and the Carman—Kozeny relation in equation 4.2, is used to calculate the permeability variation based on the porosity distribution. As discussed in section 4.1, using the Carman-Kozeny relation, MRST can be used to design synthetic heterogeneous reservoirs based on the normal porosity range (0.15-0.27) and long normal permeability range (100-800 mD). Figure 5.5 illustrates the resulting porosity and permeability reservoir model. Then the generated data by MRST is imported to ECLIPSE to create a heterogenous reservoir in ECLIPSE. Porosity values and permeability values are imported to the ECLIPSE by *poro.INC* and *perm.INC* files, respectively, under the GRID section.

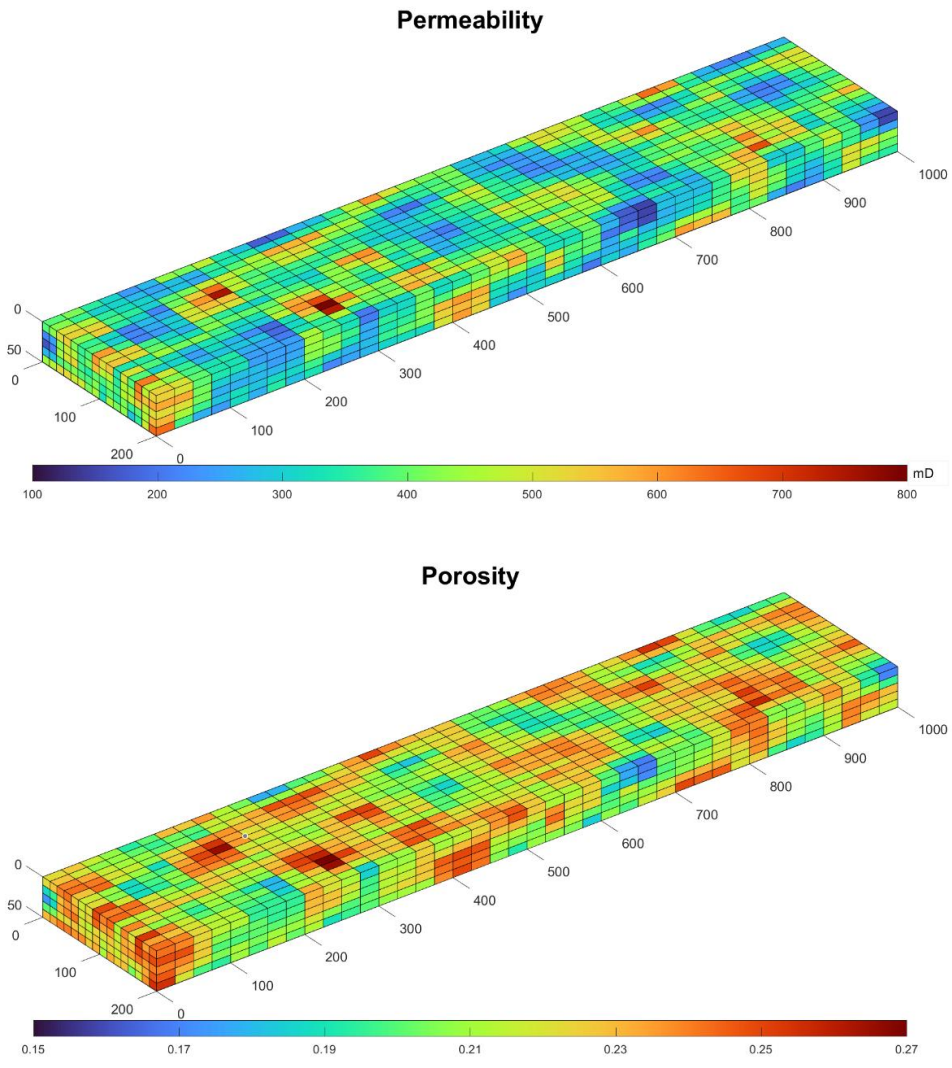

Figure 5.5: Porosity and permeability variations throughout the reservoir.

5.1.4 Initial conditions

For the development of the reservoir model in ECLIPSE, it is assumed that initially, the reservoir is filled with oil with a saturation of 0.88 but with a water saturation of 0.12. Initial gas saturation is considered as 0. Meaning that $S_o, S_w \; and \; S_g$ are 0.88, 0.12, and 0, respectively. Initial temperature and pressure are 60°C and 190 bar, respectively. Figure 5.7 shows the initial saturations of the reservoir and initial pressure.

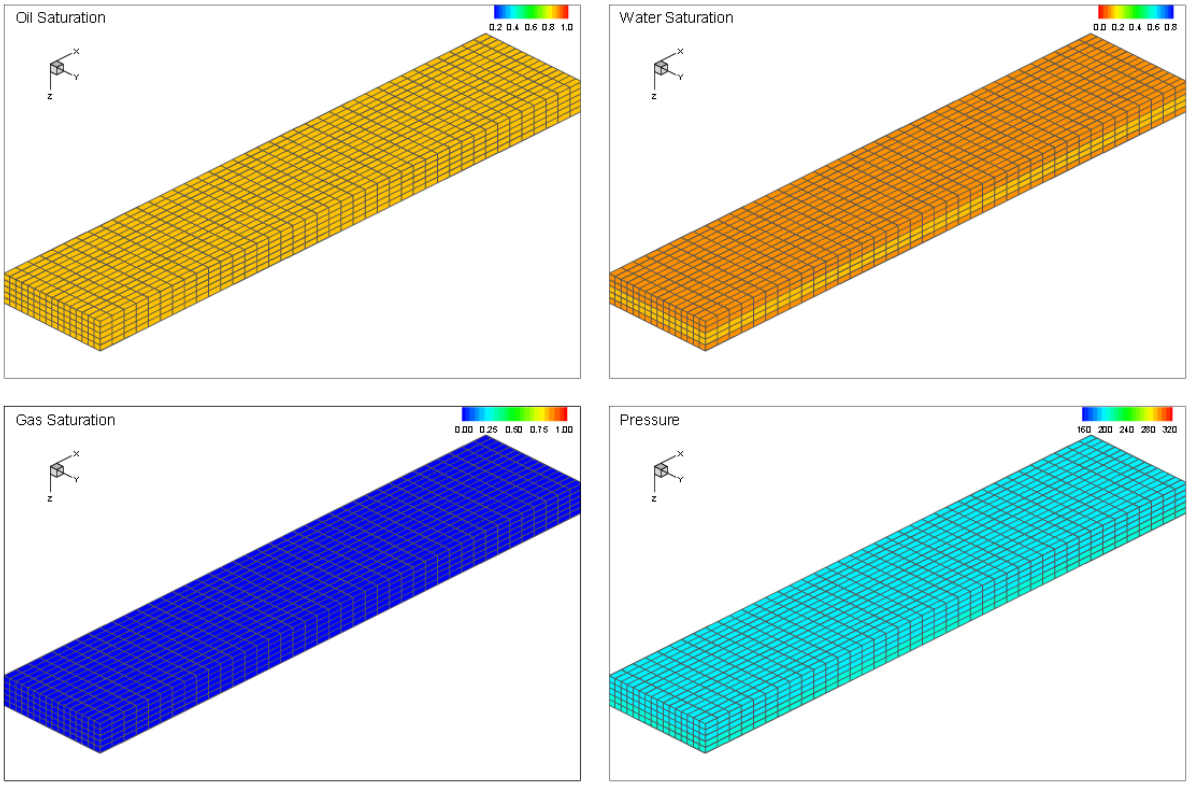

Figure 5.6: Initial oil, water, and gas saturation and initial pressure profiles.

5.1.5 Boundary conditions

As explained in figure 5.1, the horizontal well is placed in the x direction, 6.25m distance in y direction, and 5m depth (z direction) from the surface. It is assumed that the production well is controlled by a constant 190 bar Bottom Hole Pressure (BHP).

As the mean porosity of the reservoir is 0.21, the total void volume can be calculated as, $1000\text{m} \times 200\text{m} \times 50\text{m} \times 0.21 = 2100000\ \text{m}^3$. Assuming, the $^1/_3$ of the reservoir liquid is produced over 1000days, the required water injection flow rate by one injection can be calculated as, $\frac{2100000\ \text{m}^3}{3\times1000\ \text{days}} = 700\ \text{m}^3/\text{day}$. This water injection flow rate is impossible because of the limitation for maximum pressure allowed for the injection, which is 300 bar according to practical injection rates in the industry. Therefore, it is decided to inject water through two similar injections where, each one with a water flow rate of $350\ \text{m}^3/\text{day}$. This means the injection well is controlled by an injection rate of 350 m^3/day, limited by the maximum allowed injection pressure of 300 bar.

Initially, water injections are placed in the middle of (1,16, zi) and (40,16, zi) cell columns, as shown in figure 5.1. And the water is injected via the last three cells in both injections. The optimum water injection location is found as (29,16, zi) and (13,16, zi) by sensitivity analysis, and it will be explained in detail in section 5.1.7.1.

5.1.6 Simulation setting

The ECLIPSE model is run with one day as the time step for 1000 days (1000*1).

5.1.7 Water injections

Figure 5.7 shows the x-z plane in the 16th cell in the y direction, where the water injections are initially placed in the 1st and 40th cells in the x direction.

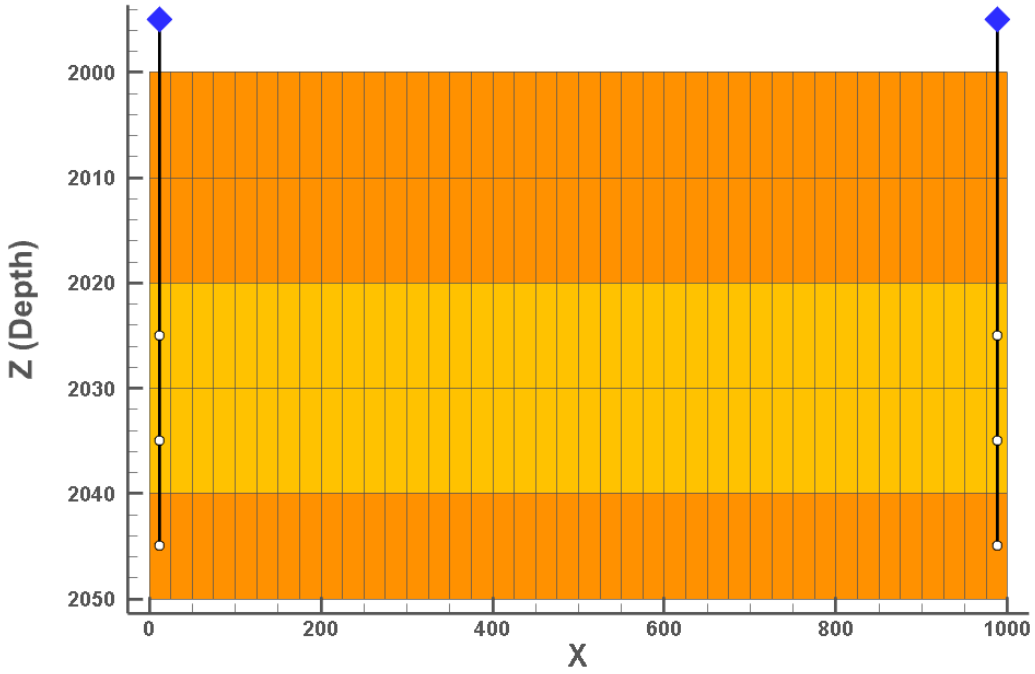

Figure 5.7: x-y plane in 16th cell in y direction to show the water injections.

5.1.7.1 Injection location optimization

In order to find the optimum locations for two water injections that produce maximum oil amount and minimum water amount, a sensitivity analysis is conducted for 7 water injection locations in x directions, where the considered x direction cell locations are 1, 5, 13, 21, 29, 36, 40 as shown in figure 5.8.

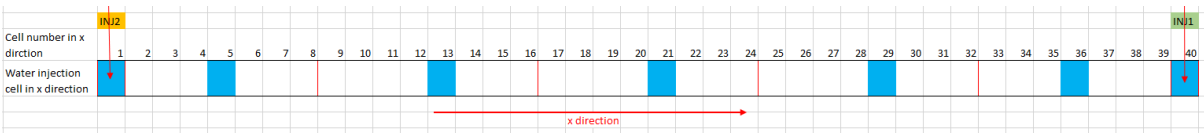

Figure 5.8: Water injection cell location in X direction for location optimization.

When there are possible 7 locations for 2 similar injections, 21 distinct combinations can be generated. These combinations are listed in Appendix C. For each combination, an ECLIPSE simulation was run. Assuming that the whole reservoir liquid is produced over 2000 days (5 years), the required water injection flow rate by one injection can be calculated as, $\frac{2100000\ \mathrm{m}^3}{2000\ \mathrm{days}} = 1050\ \mathrm{m}^3/\mathrm{day}$. Since two similar injections are used, each one with a water flow rate of $525\ \mathrm{m}^3/\mathrm{day}$ was applied for location optimization simulations. Figure 5.9 visually illustrates the oil production rates for each case, and it proves that optimum oil production can be obtained when water injections are placed in the 29th cell and 13th cell in the x direction.

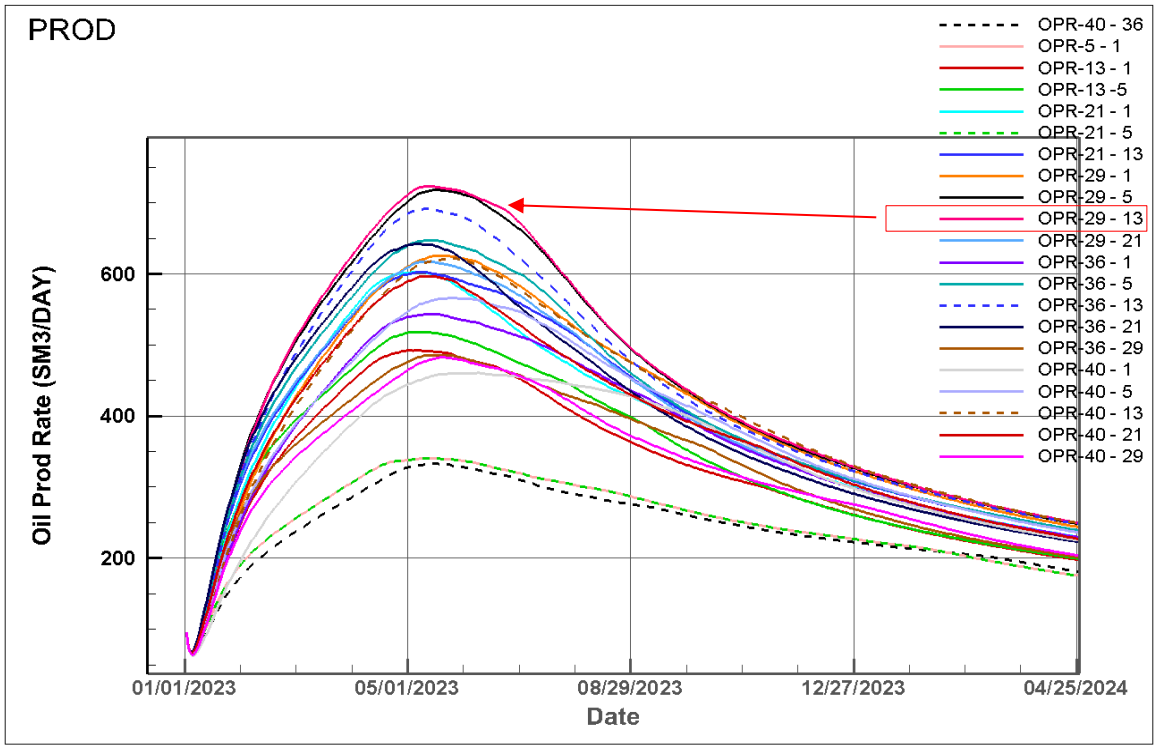

Figure 5.9: Oil production rates for 21 combinations of water injection locations.

But water is an unwanted byproduct produced in oil production, and water separation takes a cost in addition to the income of produced oil. Considering the oil price is 504 $/Sm^3 and the water separation cost is 11$/Sm^3, the discount rate is 7.5%, the Net Present Value (NPV) of each oil production case was estimated for five years, based on the total oil production rate and total water production rate. However, NPV calculation also proves that optimum oil production can be obtained when water injections are placed in the 29th cell and 13th cell in the x direction, and the rest of the simulations conducted for the OLGA/ECLIPSE model, water is injected from the determined optimum locations. The NPV calculation is given in Appendix D.

5.2 Development of well model in OLGA

Production well is modeled in OLGA software, and it is coupled with ECLIPSE software to simulate total oil production. The setup in OLGA has a production pipeline, inflow control devices, packers, and annulus, as shown in figure 5.10.

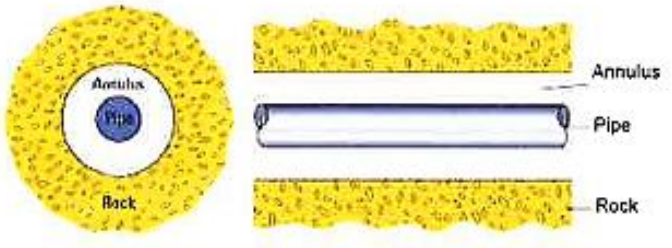

Figure 5.10: illustration of pipe in horizontal annulus [9].

Since OLGA does not have a method to simulate the flow through the annulus and then inflow control devices, the OLGA model is developed using two separate pipelines called production tubing and wellbore [9]. Under this subchapter, the main steps involving developing the OLGA model are described.

5.2.1 Structure

In OLGA, wellbore and production tubing are specified as both pipes have made with the same material combination, where internal pipe has made of 9mm thickness of API 5L Grade B carbon steel and other layers consist of two 2 cm concrete layers as shown in figure 5.11. The standard properties of these two materials are used for OLGA model development.

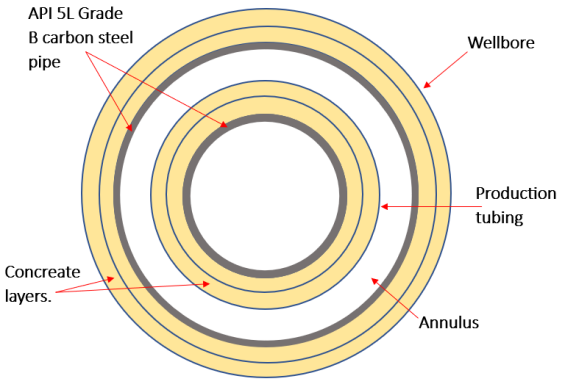

Figure 5.11: Material structure of wellbore and production tubing.

5.2.2 Table and curves

Autonomous functions of AICD and AICV are implemented in the OLGA model with a table controller and transmitter. The table controller controls the valve opening based on the WC set point. According to equation 4.9 – 4.12, the corresponding valve opening values with respect to WCs were generated and plotted in the Figure 5.4.

5.2.3 Case definition

Under the case definition, it is set to run the basic model for 1000 days. A minimum time step of 0.00001 seconds and a maximum time step of 1000 seconds have been specified. To develop the model, a three-phase system with the black oil model is considered. To solve the mass equations, a first-order discretization scheme is selected.

5.2.4 Compositional

It is necessary to define three Black oil components for oil, water, and gas in this setting in order to run the simulation for all three components. This can be defined the same as it is defined in ECLIPSE. Also, the water drive and oil drive are defined in table 5.4.

Table 5.4: Water and oil feed components.

Feed	Gas fraction	Water cut
Oil	50 Sm^3/Sm^3 (GOR)	0.0001
Water	0.0001 Sm^3/Sm^3 (GLR)	0.99

5.2.5 Flow component

To develop the well model in OLGA, it is assumed that the wellbore and production pipe are made of API 5L Grade B carbon steel and internal absolute roughness is considered as 4.572 x 10^{-5} m for both pipes [82]. The diameter of the production tubing and wellbore are assumed as 0.1397m and 0.2159m, respectively. The production well has 40 valves. Since one valve is equivalent to 2 real valves, the diameter of one valve (AICD/AICV) is 0.00265 m, considering CD as 0.85.

It is assumed that oil is produced from 40 zones in the well, each of which contains two hypothetical sections. As a result, the production tubing and wellbore are divided into 80 hypothetical sections of 12.5 m each. Figure 5.12 shows a simplified sketch of one oil production zone.

Production zones are separated by packers shown in figure 5.12, which are used to prevent reservoir fluid from flowing in between adjacent zones through annulus. Near-well source in the OLGA model is used to connect the OLGA with ECLIPSE, where ECLIPSE cell is connected to the OLGA wellbore section accordingly. Then the fluid enters the wellbore through section I after passing through the inflow control device (ICD/AICD/AICV) in figure 5.12. The fluid that entered the wellbore passes to the production tubing via the leak in section II. This setup was proposed by Haarvard Aakre in 2012 and this method has been used for many researches [7], [9].

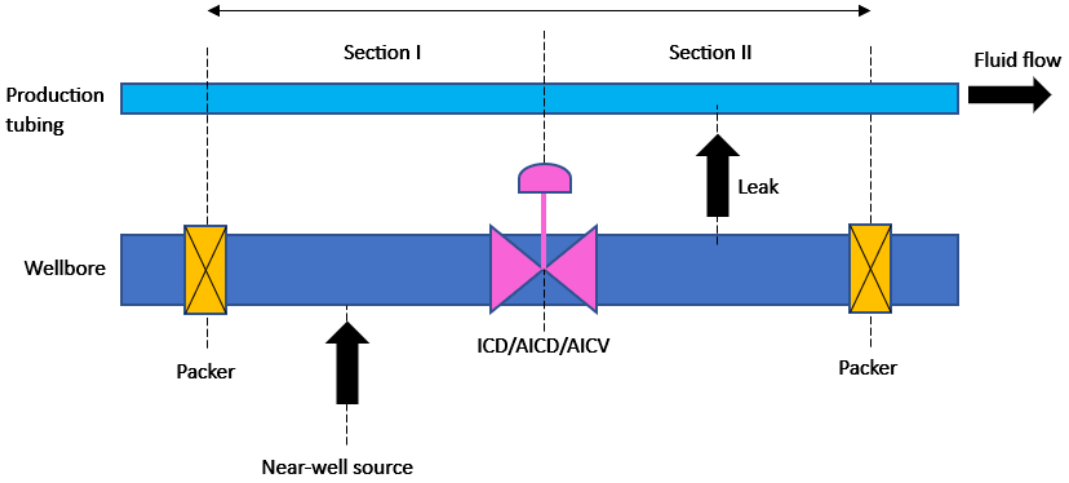

Figure 5.12: Simplified sketch for one oil production zone.

If the oil production simulation does not use any inflow control devices, it is called the OPENHOLE case. Wellbore OLGA model for one production section for OPENHOLE, ICD, AICD and AICV are given in figure 5.13. The full models are illustrated in Appendix E.

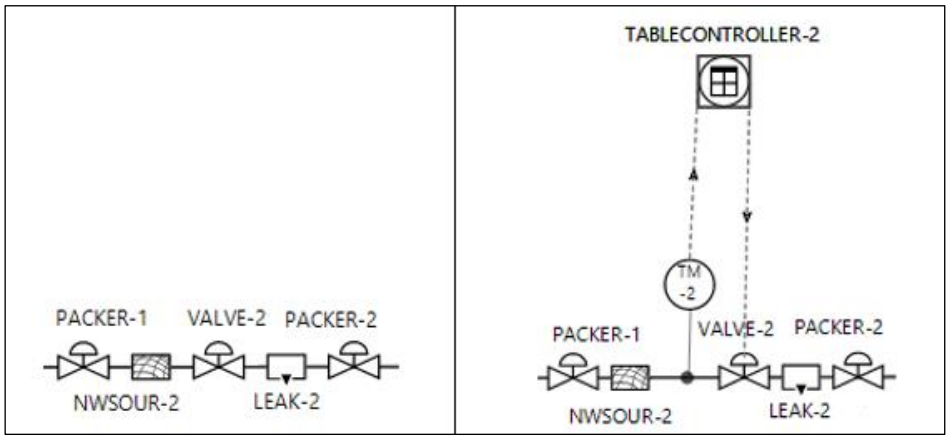

Figure 5.13: OLGA models for one production section for OPENHOLE/ICD (left) and for AICD/AICV (right).

OLGA does not offer specific options for modeling the autonomous function of AICV and AICD; therefore, it is modeled as a VALVE with a table controller and transmitter [9]. The water cut (WC) of fluid is the set point for the table controller, which controls valve opening. When the WC varies, the valve opening percentage changes. The WC values and corresponding valve opening percentages are given through a control table, which is generated based on the control functions described in section 4.3. AICD and AICV have 2 different control tables as they have different valve opening behaviors for WC. The base case specifications for each component for OPENHOLE, ICD, AICD, and AICV models are listed in Table 5.5.

Table 5.5: Components specifications for OPENHOLE, ICD, AICD and AICV base case OLGA models.

Component name		**OLGA Module**	**Description**			
Near-well source		Near-well	Coupled with the correspond ECLIPSE model file			
			Diameter (m)	**CD**	**Opening control**	**Connected pipe**
Leak		Leak	0.12	1	-	Wellbore
Valve	OPENHOLE	Valve/Table Controller	0.12	0.85	Opening = 1 (fully open)	Wellbore
	ICD	Valve/Table Controller	0.00265	0.85	Opening = 1 (fully open)	Wellbore
	AICD	Valve/Table Controller	0.00265	0.85	AICD is controlled by a Table Control	Wellbore
Packer		Valve (closed)	0.12	-	Opening = 0 (fully closed)	Wellbore

As discussed in section 5.1.5, production is controlled by 190 bar BHP, which is the boundary condition for the production tubing outlet. The boundary conditions of the flow paths are defined as the pressure boundary. The other end of the production tubing and two ends of the wellbore are considered closed ends. Boundary conditions for production tubing and wellbore are listed in table 5.6.

Table 5.6: Boundary conditions for flow paths.

Flow path name	**Boundary Name**	**Boundary Type in OLGA**
Wellbore	Inlet	Closed node
	Outlet	Closed node
Production tubing	Inlet	Closed node
	Outlet	Pressure node, Pressure =190 bar, Temp. = 60˚C

5.3 Simulation cases

The thesis primarily focuses on the simulation of 2 OLGA/ECLIPSE combination models. The first combination is referred to as the "Base case", while the second combination is a modified version of the base case and is named as "Case 2" throughout the report. Up to section 5.3, the report explains the development method of the "Base case". The base case was conducted for a heavy oil reservoir with the viscosity of 90 cP, while case 2 was conducted for a light oil reservoir with an oil viscosity of 2.7 cP. The modifications made to the base case to create case 2 are described in Appendix F and G. A summary of all simulated cases is listed in table 5.7.

Table 5.7: Summary for all the simulated cases.

Case	Valve				Number of valves	Pressure drawdown (bar)	BHP (bar)	Initial conditions of the reservoir		Simulation duration (days)
	Valve type	Diameter	CD	Opening control				T (^{0}C)	P (bar)	
Base case	OPENHOLE	0.12	0.85	Opening = 1 (fully open)	40	10	190	60	200	1000
	ICD	0.00265	0.85	Opening = 1 (fully open)	40	10	190	60	200	1000
	AICD	0.00265	0.85	AICD is controlled by a Table Control	40	10	190	60	200	1000
Case 2	OPENHOLE	0.12	0.85	Opening = 1 (fully open)	30	15	115	68	130	1500
	ICD	0.0042	0.85	Opening = 1 (fully open)	30	15	115	68	130	1500
	AICD	0.0042	0.85	AICD is controlled by a Table Control	30	15	115	68	130	1500
	AICV	0.0042	0.85	AICD is controlled by a Table Control	30	15	115	68	130	1500

6 Results and discussion

This thesis discusses improved oil production using water injection from synthetically designed heterogeneous reservoirs. The results of the simulations generated by the OLGA/ECLIPSE model developed in the previous chapters are presented and discussed in this chapter. Furthermore, the effectiveness of ICD, AICD, and AICV valves in enhancing oil recovery from this well is evaluated as compared to the OPENHOLE case. A total of 7 sub-cases have been simulated under two main cases, as shown in Table 5.7.

6.1 Oil production over water breakthrough

When oil is produced from a horizontal well, the phenomenon of water coning can cause a decrease in productivity. Over time, this can lead to an early water breakthrough and a significant reduction in oil production. Typically, overall oil production gradually increases until a breakthrough occurs. However, once the breakthrough happens, more and more water is pushed toward the well, which in turn suppresses and reduces oil production. The observed results from this study for base case AICD completion can be used to represent this phenomenon by using Figure 6.1. The process of separating water from oil requires specialized equipment and processes, which can add significant costs to the overall production process. Moreover, the disposal of produced water can be a challenge, as it may need to be treated to meet environmental regulations. Consequently, it is essential to minimize the amount of water produced and to delay the breakthrough of water for optimal production efficiency and cost reduction.

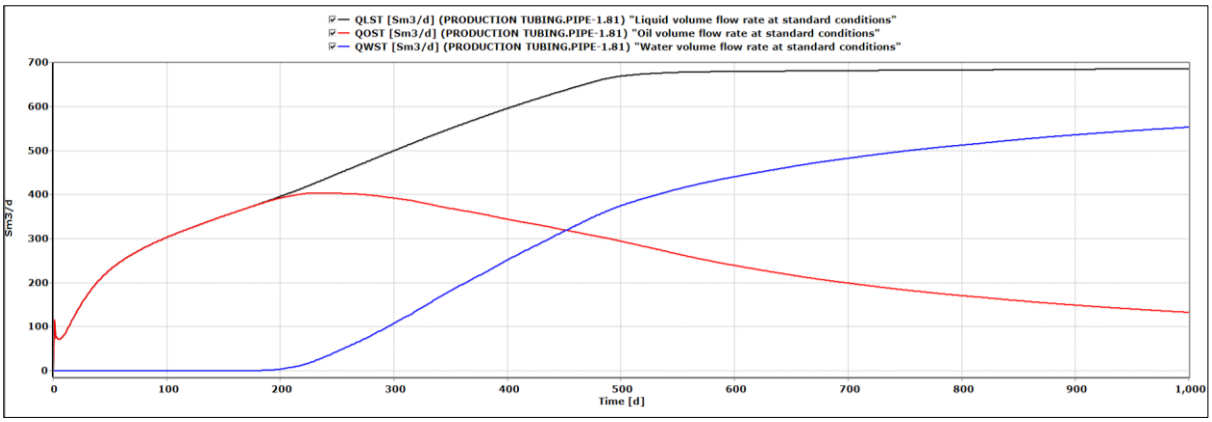

Figure 6.1: The development of oil production for base case AICD completion.

According to the observed results shown in Figure 6.2 and Figure 6.3, Table 6.1 lists the breakthrough occurring times for base case and case 2. The installation of FCDs in the well resulted in delayed breakthroughs of 10 days for the base case and 180 days for case 2. However, it appears that case 2 has a more significant delay in water production compared to the base case. This may be due to the impact of the water flooding method employed, as the base case utilized two vertical injections while case 2 employed a horizontal water injection. Results show that in vertical flooding (base case), water breakthrough occurs earlier, unlike

horizontal flooding (case 2), where water breakthrough occurs later. This has been experienced in the study [58] also. However, the FCDs have effectively reduced the total water produced from the well, which is beneficial for hydrocarbon recovery with a minimum cost.

Table 6.1: Breakthrough times for base case and case 2.

Case name	Breakthrough for OPENHOLE case	Breakthrough for FCD completion
Base case	150th day	160th day
Case 2	620th day	800th day

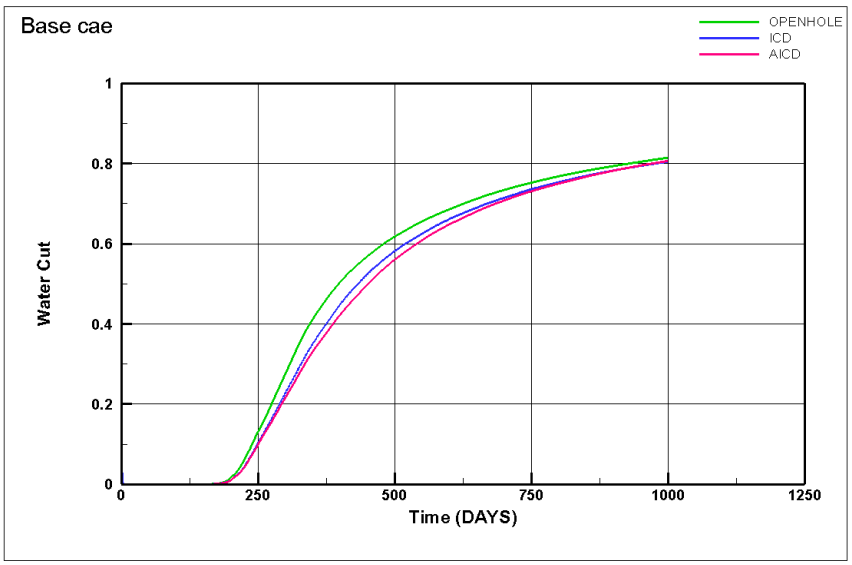

Figure 6.2: Water cut for base case (vertical water flooding) for different FCD completions.

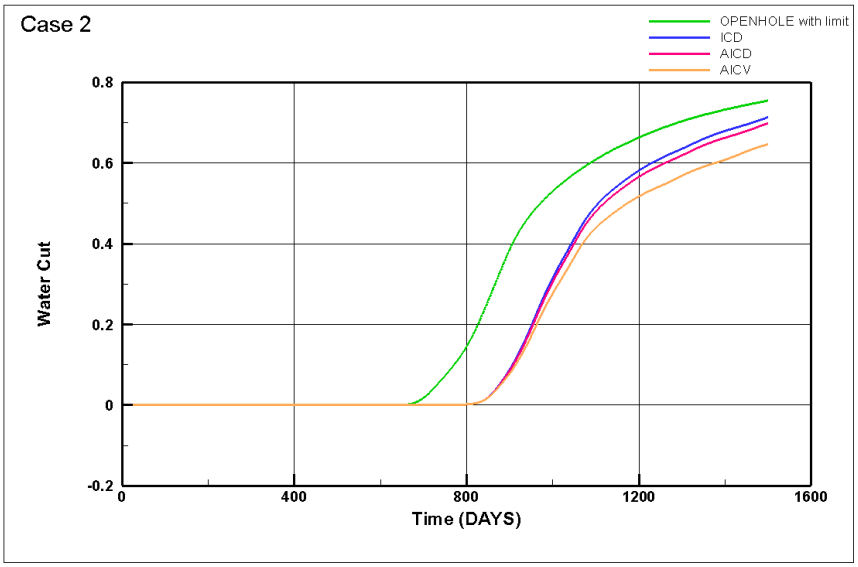

Figure 6.3: Water cut for case 2 (horizontal water flooding) for different FCD completions.

The fluid flow movement around a well is influenced by three major forces: capillary, gravity, and viscous forces. At any given time, the balance between these forces determines how the fluid is distributed around the well. When the pressure force from the reservoir to the well is strong enough, it creates enough viscous force to overcome gravity and capillary forces. This causes water to move towards the well, creating water conning.

Several factors contribute to early water breakthrough and water conning, but the heel-to-toe effect and heterogeneity of the reservoir play the most significant roles. The heel-to-toe effect means the pressure in the heel becomes higher than the pressure in the toe as a result of frictional pressure drop. In this study, the fixed BHP was the production controlling method in both cases, where BHPs of base case and case to were kept at 190 bar and 115 bar, respectively. As shown in Figure 6.4 for the OPENHOLE base case, the frictional pressure drop just before the water breakthrough was 0.057 bar which is a very low value. Liquid flow velocity is proportional to frictional pressure drop, as discussed in sectionPressure drops in horizontal wells 3.4. Therefore, a low liquid flow rate before the breakthrough may be the cause for the low frictional pressure drop before the breakthrough. This implies that reservoir heterogeneity has more impact on water breakthrough than the heel-to-toe effect.

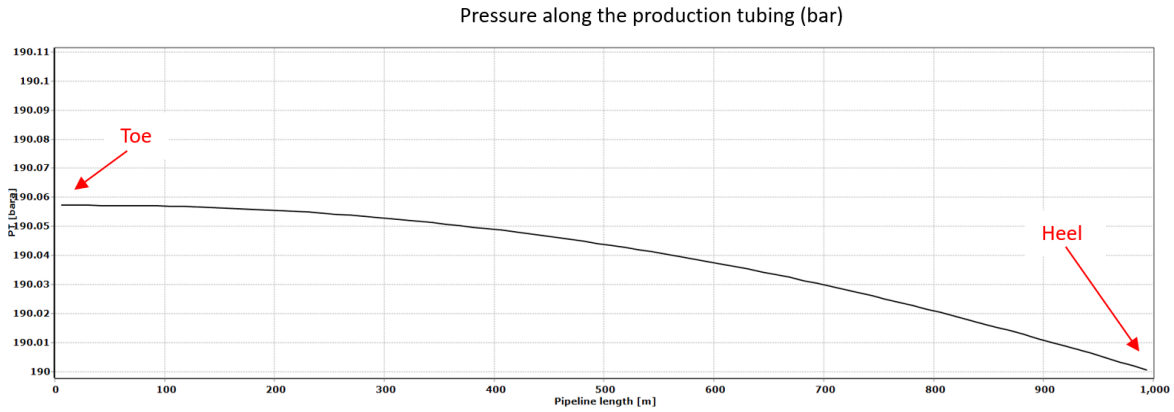

Figure 6.4: OPENHOLE pressure along the production tubing on 146th day (just before the breakthrough).

As discussed in section 5.1.7.1, the optimum oil production can be obtained when water injections are placed in 29th cell and 13th cell locations in X direction. Since the heel-to-toe effect causes less effect on water conning and breakthrough, water conning occurs through the near well cells parallel to two water injection locations which can be proved by Figure 6.5 and Figure 6.6. And, because open-hole wells provide a greater open surface area to produce reservoir fluids, their water production levels are higher than those of advanced wells. Therefore, open-hole completions have resulted in a greater water cut than AICD.

Showing similar behavior, appendix H illustrates the water cut development for case 2 and the oil saturation profile just after the water breakthrough. Similarly, the OPENHOLE case has a higher water cut than FCD completions. AICD and AICV have lesser water cuts compared to ICD because of their self-adjusting ability for low viscous fluid like water. AICVs have more capability for getting closed compared to AICDs.

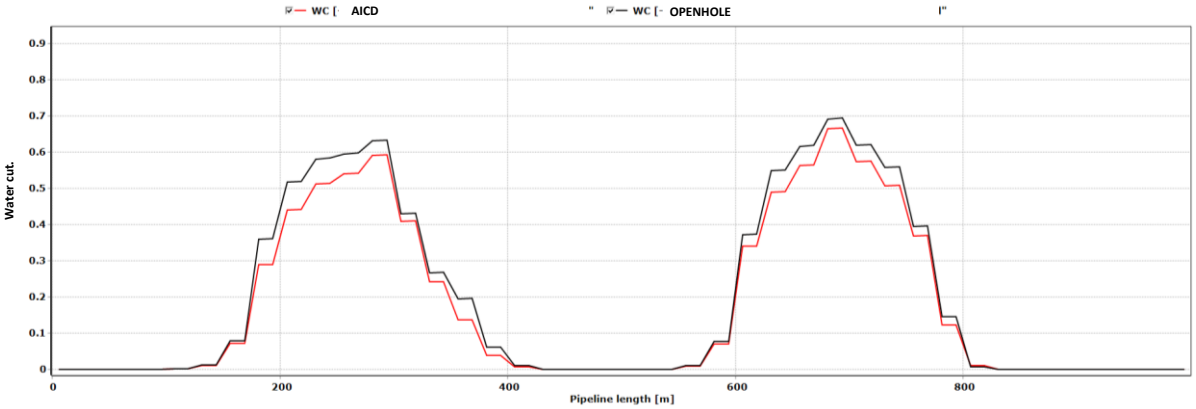

Figure 6.5: Water cut development for AICD and OPENHOLE completions in base case.

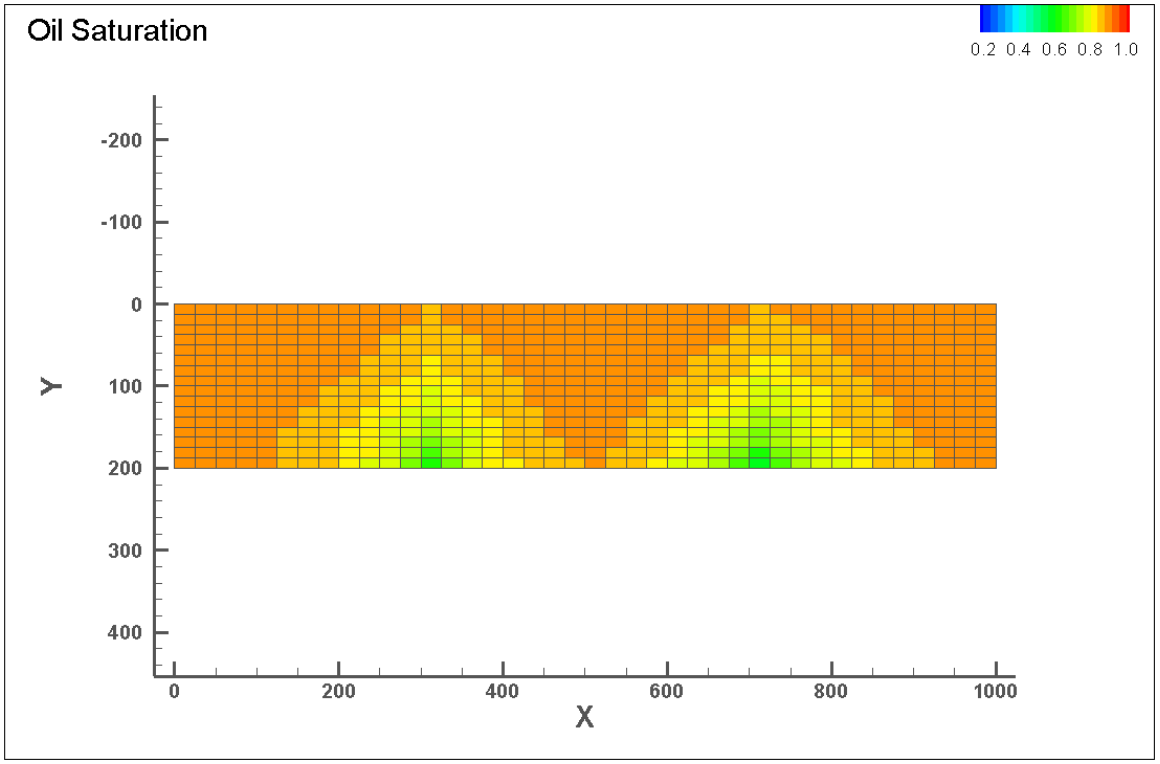

Figure 6.6: Base case oil saturation just after the water breakthrough.

6.2 Results validation with multi-segment well (MSW) model

As discussed in section 3.7, the Multi-Segment Well (MSW) model is a special extension available in ECLIPSE 300 that offers a comprehensive and accurate approach to wellbore simulation. When the MSW model is used, the valve control function can be modeled in ECLIPSE by using the valve segments in the MSW model. Likewise, the MSW model allows for the modeling of both the reservoir and wellbore in a single simulation framework. In this study, base case simulations for OPENHOLE, ICD, and AICD are conducted in ECLIPSE 300 using MSW model. Coupling ECLIPSE with OLGA is a new approach tested in this thesis for

overall oil production simulation and standard well model (SWM) was used for the base cases. The results obtained by MSW model simulations can be used to validate the results obtained by OLGA/ECLIPSE coupled model.

Figure 6.7 shows the comparison between the results. By comparing the results, obtaining the same results for oil and water production from both methods proves that coupling of the OLGA with ECLIPSE has been successful in this thesis study.

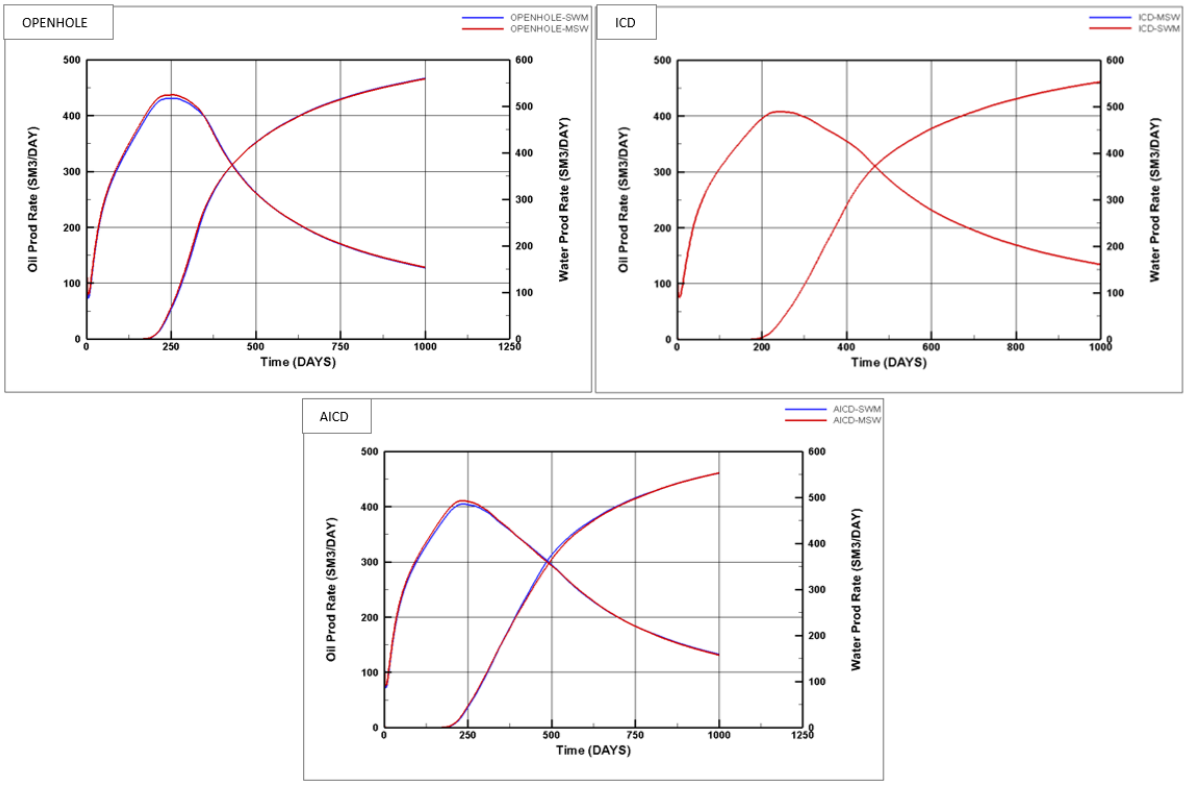

Figure 6.7: Validation of OLGA/ECLIPSE SWM with results of ECLIPSE MSW model for OPENHOLE, ICD and AICD well completions.

6.3 Comparison of the functionality of the FCDs in a heavy oil reservoir

In the base case, a heavy oil reservoir with an oil viscosity of 90 cP was considered to simulate oil production. The study compares the production results of advanced well completions that utilized ICDs and AICDs with the production results of an OPENHOLE completion.

6.3.1 Accumulated oil and water production

To assess oil production and compare the performance of different inflow control devices, it is essential to consider two factors: accumulated oil and water. Figure 6.8 displays the accumulated oil and water produced from the base case well using ICD and AICD completions

and for the OPENHOLE completion. The results indicate that there is not much difference in the accumulated oil production for all completion methods after 1000 days of production. However, when the well is equipped with ICDs and AICDs, accumulated water production has significantly reduced.

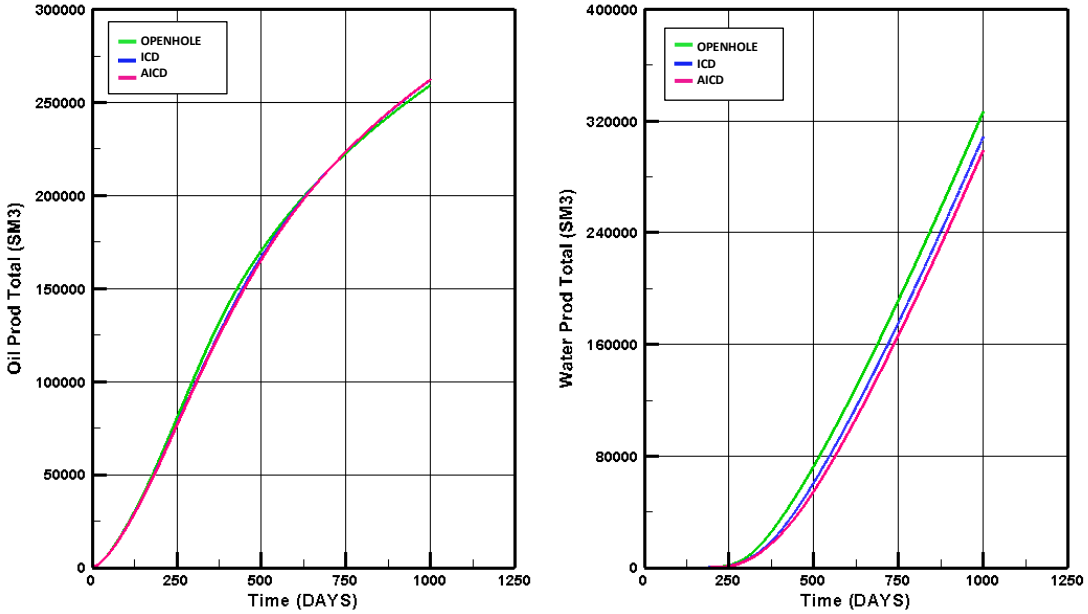

Figure 6.8: Base case accumulated oil and water production for open hole and different FCD completions.

Table 6.2: Accumulated oil and water production rates at the end of 1000days of operation.

	Accumulated oil (Sm^3)	Accumulated water (Sm^3)
For OPENHOLE completion	259128	326453
For ICD completion	262111	308439
For AICD completion	262202	298660
% change (from OPENHOLE to ICD)	1.15 %	-5.52 %
% change (from OPENHOLE to AICD)	1.19 %	-8.51 %

The readings of Figure 6.8 are listed and sorted in Table 6.2. According to the results, compared to the OPENHOLE case, cumulative oil productions from ICD and AICD completions have relatively increased by 1.15% and 1.19%, respectively, after 1000 days of operation. Moreover, cumulative water production has reduced by 5.52% and 8.51%, respectively. Therefore, the

use of advanced wells equipped with FCD completions results mainly in a significant decrease in the production of undesirable fluids.

6.3.2 Oil and water production

Oil and water production rates for the base case with a heavy oil reservoir are presented in figure 6.8. According to the figure, in all cases, oil flow rates initially rise to their maximum values after production starts, but this changes once the water breakthrough occurs. In this study, as discussed with Figure 5.4: Generated relative permeability values., irreducible water saturation is 0.12, and irreducible water saturation is 0.05. As oil is extracted from the well, the oil saturation near the well gradually decreases while the water saturation rises. Whenever the water saturation near the wellbore exceeds the irreducible water saturation, water enters the well, causing the reservoir to yield more water than oil. This is called the water breakthrough. As a result, oil production drops significantly, and water production increases after the water breakthrough. Oil can be produced until the oil saturation near the well drops to residual oil saturation.

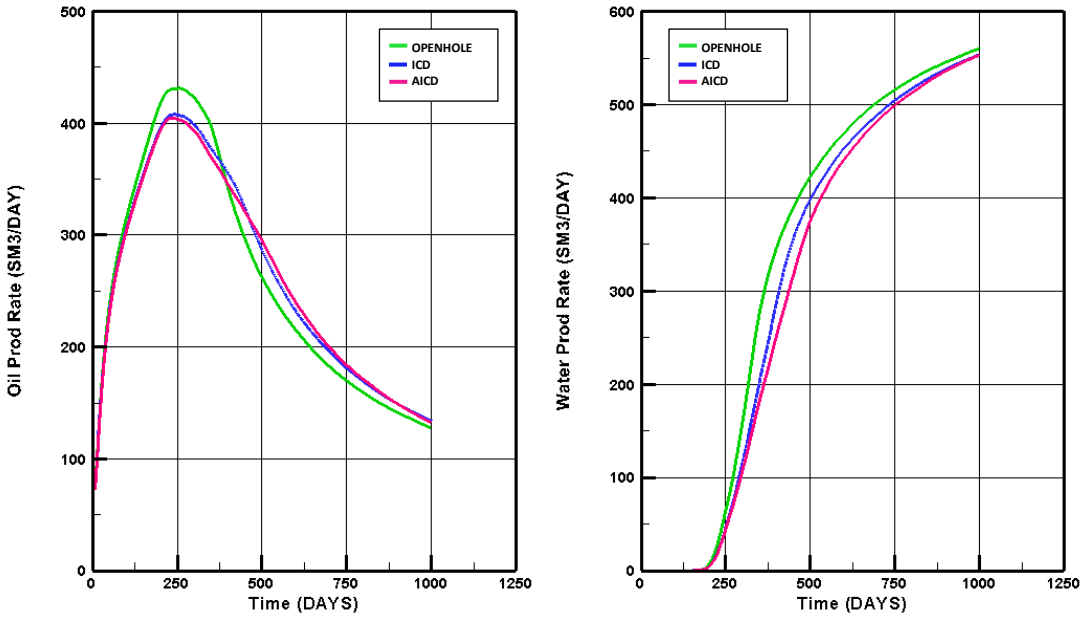

Figure 6.9: Case 2 volumetric oil production rates for open hole and advanced wells with different FCD completions.

The values obtained from Figure 6.9, for the comparison of FCD cases with OPENHOLE are listed in Table 6.3. Results show that the maximum oil production rate obtained by OPENHOLE case is higher than both ICD and AICD cases, but it significantly drops to a lesser rate compared to FCD cases at the end of 1000 days. And also, the water production rate of OPENHOLE case is higher than FCD cases throughout the operation period. Thus, it can be concluded that, although the OPENHOLE case suddenly produced much more oil at the beginning, the implementation of FCDs has reduced the additional cost related to the unwanted water production. Comparing ICD with AICD, the maximum oil production rate is 0.74 %

higher for the AICD case and final water production rate is 0.13% lesser for AICD compared to ICD case. Moreover, according to Figure 6.2, WCs have reached to around a maximum of 0.8 for all cases. According to Figure 4.3, when the WC is more than 0.9, AICD valve closure is significantly higher. Since this study has been conducted for 1000 days of operation, it is suggested to conduct the simulation for more time to see the impact of AICD valve on water and oil production.

Table 6.3: Volumetric oil production rates for the operation of 100 days.

	Volumetric oil flow rate		Volumetric water flow rate after 1000days (Sm^3/d)
	Maximum (Sm^3/d)	After 1000days (Sm^3/d)	
For OPENHOLE completion	431.3	127.60	560.26
For ICD completion	408.1	134.04	553.84
For AICD completion	404.9	132.81	553.10
% change (from OPENHOLE to ICD)	-5.39 %	5.04 %	-1.15 %
% change (from OPENHOLE to AICD)	-6.13 %	4.08 %	-1.28 %

6.4 Comparison of functionality of the FCDs in a light oil reservoir

In case 2, a light oil reservoir with an oil viscosity of 2.7 cP was considered to produce oil. The study compares the production results of advanced well completions that utilized ICDs, AICDs and AICVs with the production results of an OPENHOLE completion.

In practical oil and gas production, the total liquid production from a well can be limited by the maximum capacity of the surface facilities. This means that even if the well has the potential to produce more liquid, it may not be possible to do so due to limitations in processing and storage capacity. It is important to understand the maximum production capacity of surface facilities to optimize production and avoid potential production bottlenecks. In the case 2 OPENHOLE simulation, the maximum liquid production rate is set as 2400 m^3/day.

6.4.1 Accumulated oil and water production

The accumulated oil and water production from case 2 are given in Figure 6.10. The simulations have been conducted for 4 well completions, OPENHOLE, ICD, AICD and AICV. The simulation results show that the OPENHOLE case initially has higher oil production compared to the other FCD cases. As a result of the early OPENHOLE breakthrough, oil production has significantly decreased in comparison with advanced wells. As a result of that,

after 1500 days of operation, advanced wells have produced more oil compared to the OPENHOLE case. Additionally, the OPENHOLE case produces a larger amount of water compared to the advanced wells throughout the operation. With the same pressure drawdown, open-hole wells provide a larger surface area for reservoir fluid production, which explains why liquid production from such wells is higher than from advanced wells. Accordingly, the open-hole completion results in higher liquid production. Values and deviations obtained by figure 6.10 are listed in Table 6.4.

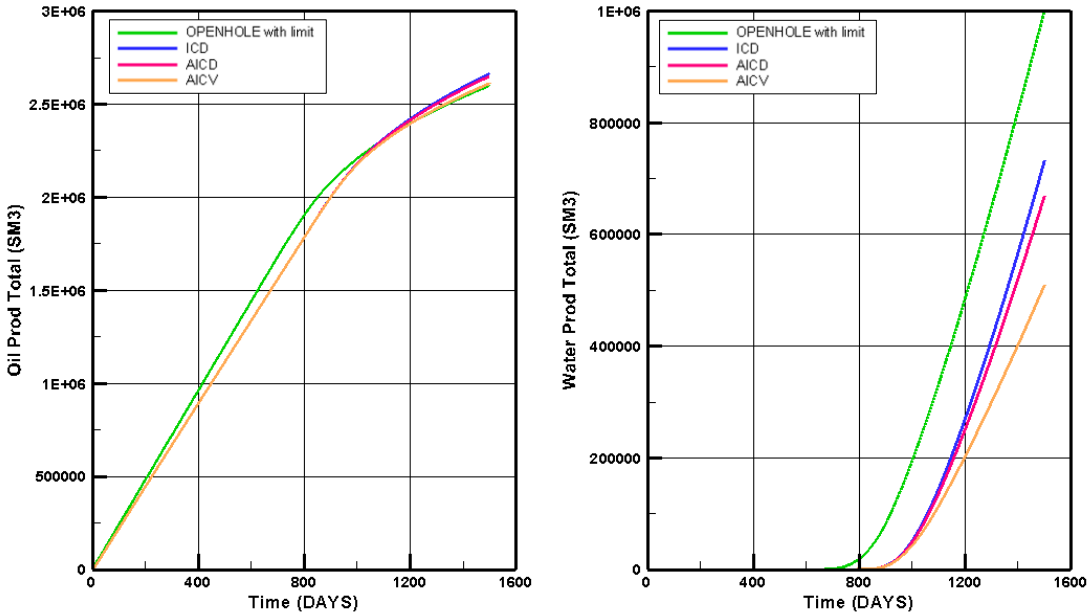

Figure 6.10: Case 2 accumulated oil and water production for open hole and different FCD completions.

Table 6.4: Accumulated oil and water production rates at the end of 1500days of operation.

	Accumulated oil (Sm^3)	Accumulated water (Sm^3)
For OPENHOLE completion	2600321	999679
For ICD completion	2658192	731664
For AICD completion	2644424	668424
For AICV completion	2605369	508766
% change (from OPENHOLE to ICD)	2.22 %	-26.8 %
% change (from OPENHOLE to AICD)	1.7 %	-33.1 %
% change (from OPENHOLE to AICV)	0.2 %	-49.1 %

Results in Figure 6.10 show that AICDs and AICVs function in a similar manner to ICDs before the water breakthrough, as they are fully open prior to the breakthrough. But figure 1 in Appendix G indicates that after a breakthrough, valves become partially closed when the WC increases. As a result of these choking effects, less oil and water are produced from AICD and AICV completions compared to ICD completion after breakthrough. Since AICVs have more choking capabilities for low viscous fluids, they have more tendency to close the values compared to AICDs. As a result of this, AICV completion has less liquid production than AICD completion.

According to the results in Table 6.4, compared to the OPENHOLE case, cumulative oil productions from ICD, AICD, and AICV completions have relatively increased by 2.22%, 1.7%, and 0.2%, respectively, after 1500 days of operation. Moreover, cumulative water production ICD, AICD, and AICV have considerably reduced by 26.8%, 33.1%, and 49.1%, respectively, compared to the OPENHOLE case. It is evident that although ICDs have the highest oil production rate, they also have the highest water production rate, which is undesirable. Interestingly, the completion of AICV has reduced water production by almost half (49.1%). However, according to the water production variations of advanced well completions, the oil production variations are comparatively low. Therefore, AICV completion offers the best performance for the oil production from the light oil reservoir considered in this study. However, the type of FCD completions for specific reservoirs is determined based on many different factors. But this study shows that advanced wells completed with FCD completions can considerably reduce the production of unwanted fluid.

6.4.2 Oil and water production

The simulation results observed for oil and water production rates for case 2 with a light oil reservoir are plotted in Figure 6.11. The flow rate values and deviations of maximum flow rates and flow rate at the end of 1500 days of production are listed in Table 6.5.

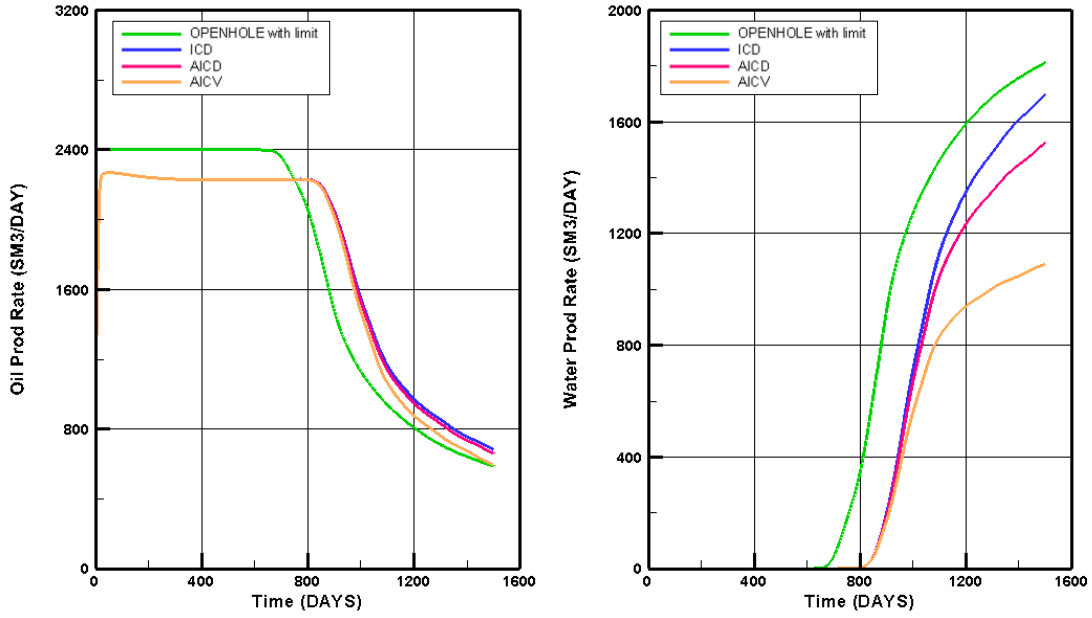

Figure 6.11: Case 2 volumetric oil production rates for open hole and advanced wells with different FCD completions.

Initially, the OPENHOLE case has the maximum oil production rate compared to other advanced wells, and the production rate lasts until the water breakthrough. Although advanced well completions have a 5.61% lower oil production rate, it lasts longer period since the water breakthrough is delayed in advanced wells. After the breakthrough, as more water enters to the wellbore, water production rates have continuously increased in all cases, but the OPENHOLE case has the highest water production rate throughout the production duration.

Table 6.5: Volumetric oil production rates for the operation of 100 days.

	Volumetric oil flow rate		Volumetric water flow rate after 1500days (Sm^3/d)
	Maximum (Sm^3/d)	After 1500days (Sm^3/d)	
For OPENHOLE completion	2400	587.9	1812
For ICD completion	2265.3	681.4	1699.2
For AICD completion	2265.2	658.9	1526.0
For AICV completion	2265.5	595.8	1090.3
% change (from OPENHOLE to ICD)	-5.61 %	16 %	-6.2 %
% change (from OPENHOLE to AICD)	-5.62 %	12.1 %	-15.8 %
% change (from OPENHOLE to AICV)	-5.61 %	1.3 %	-39.8 %

Since both AICD and AICV behaved similarly to ICD function before the water breakthrough, all advanced well completions with ICD, AICD, and AICV have almost the same maximum oil production rate (~2265 Sm^3/d) at the beginning. But at the end of 1500 days of operation, the OPENHOLE case has achieved the lowest oil production rate as it doesn't have control over the water production after the breakthrough. And ICD, AICD, and AICV completions have achieved 16%, 12.1%, and 1.3% increments in oil production compared to the OPENHOLE case. But end water production rates of ICD, AICD, and AICV completions have reduced by 6.2%, 15%, and 39.8% compared to the OPENHOLE case. The autonomous valve closing mechanisms in AICDs and AICVs have been highly effective in reducing water production rates, but they also have a slight impact on reducing oil production rates. As AICV technology is more prone to choke the fluids, it was the lowest water production rate of all. It appears that despite advanced well completions having a small impact on oil production rates,

they can significantly reduce water production by improving the oil production process in a cost-effective manner.

Figure 6.3 explains that at the end of 1500 days of operation, WC reached around 0.7 and 0.65 for AICD and AICV cases, respectively. According to figure 1 in appendix G, AICD and AICV valves close more and more when the WC increases, and this implies that the impact of the autonomous function of AICD and AICV can be clearly seen if the WC exceeds around 0.9. But the oil production should last longer than 1500 days in order to achieve a higher WC. Therefore, it is recommended to extend the simulation period to observe the true impact of utilizing advanced well technologies for achieving more efficient oil production processes.

6.5 Discussion

The following sections discuss the significant outcomes derived from the simulation results.

6.5.1 Impact of early water breakthrough on oil production

Early water breakthroughs are a major problem in oil production and delaying the water breakthrough and reducing the total water production is a major concern in the oil industry. For improved oil recovery, the base case was based on a heavy oil reservoir with two similar vertical water injection wells, while case 2 was based on a light oil reservoir with a horizontal water injection. As discussed in section 6.1, the water flooding method and the type of reservoir fluid has made a major impact on delaying early water breakthrough. According to the results, it can be argued that using separate vertical injections for a heavy oil reservoir has encouraged the water-fingering effect through the heterogeneity of the reservoir, which results in the early water breakthrough. Because in base case, even with the advanced well completions, water breakthrough occurs comparatively early. Advanced well completions in the light oil case with horizontal water injection show a good improvement in delaying the water breakthrough. As explained in section 2.1.2.3, for heavy oil reservoirs, polymer flooding is more recommended because by using a polymer, the viscosity of the injected fluid can be increased, by minimizing the fingering effect, the early breakthrough can be delayed. This proves that different water flooding mechanisms will make huge differences for reservoirs with different oil viscosities. Moreover, for the heavy oil reservoir case, it can be recommended to use horizontal water injections to see the impact for the water breakthrough time.

The advanced well technologies used in light oil reservoir have considerably delayed the water breakthrough and reduced the water production. As advanced well completions function the same as ICD before the breakthrough, there are no variations in breakthrough delays between advanced well completions.

The heel-to-toe effect and heterogeneity of the reservoir are the main two factors that affect the early water breakthrough. According to the results of heterogeneous reservoirs of base case and case 2, breakthroughs do not occur in the heel side, and this implies heel-to-toe effect has less impact and the heterogeneity of the reservoir has more impact on water breakthroughs. In both cases, the water breakthrough occurs in well locations parallel to water injection locations.

6.5.2 Functionality of ICD, AICD, and AICV in enhanced oil recovery

The use of advanced well technologies for both heavy and light oil reservoirs shows a good improvement in the oil production process. When a production well is completed with FCDs, the oil production has a little increment, but the water production has considerably reduced after the breakthrough. Prior to the water breakthrough, all ICD, AICD and AICV well completions resulted in the same oil productions as AICD and AICV are in fully open stage and function like ICD. After the breakthrough, these valves get partially closed with increasing water cut. As a result of that, less oil and water are produced from AICD and AICV compared to ICD. Since AICVs have more capability to choke low viscous fluids compared to AICD, liquid production from AICV is lower than AICD case.

Management of water content during oil production is essential in order to reduce the costs associated with handling and disposing of excess fluids. Therefore, the effectiveness of FCDs is determined by their ability to maximize profits by reducing the production of unwanted fluids per barrel of produced oil. The results of this thesis show the potential of different types of flow control devices, and it proves that advanced technologies can improve the performance of the cost-effective oil production process.

6.5.3 Challenges in water injection

Water injection well is a common method used to enhance oil recovery in heavy oil reservoirs. However, water injection in oil reservoirs can present unique challenges. In heavy oil reservoirs, oil has a high viscosity, which makes it challenging to displace with injected water. The injected water tends to make a fingering effect through the heavy oil, resulting in low sweep efficiency and reduced oil recovery. To overcome this issue, a polymer flooding technique is used, which is water mixed with a polymer to increase the viscosity of water. It can be argued that the water injection technique also affects the efficiency of the oil recovery. Rather than using single vertical injections, horizontal injections may be more effective. Considering different factors, selecting the proper injection technique may be a challenge.

In heavy oil reservoirs, the oil is highly viscous and does not flow easily through the reservoir rock. Therefore, a significant amount of water is injected into the reservoir to displace and mobilize the oil towards the production wells. This means that a high water-oil ratio is often required to achieve optimal oil recovery. Therefore, a high water-oil ratio in heavy oil reservoirs can result in increased costs associated with water treatment, handling, and disposal, which can affect the overall profitability of the project. If the objective is to achieve optimum oil recovery, alternative improved oil recovery methods are better for heavy oil reservoirs. Therefore, achieving a cost-effective oil recovery through normal water flooding is challenging.

Moreover, water injection may cause the formation of water-oil emulsions, which can reduce the effectiveness of the water flooding process and increase the difficulty of separating oil from water during production.

In practice, when water is injected into a heavy oil reservoir, it can cause damage to the formation in various ways. One way is the mobilization of fine particles, also known as fines, in the reservoir rock. Fines can be released from the rock matrix and transported by the injected water, leading to clogging of the pore space and reduced permeability. This can result in a decrease in the flow of oil and water through the formation, leading to reduced oil recovery.

This fine migration can be minimized by pre-flush of low salinity water, using polymer or by using an additive to reduce fines migration.

6.5.4 Suggestions for further works

Based on the findings of this thesis study, several areas for future research can be suggested.

Multi-lateral wells: As discussed in section 2.3.4, the use of multi-lateral wells is a proven advanced technology in the oil industry. Multilateral wells can increase the contact area between the wellbore and the reservoir, which can enhance production rates by accessing more oil or gas. Rather than drilling several horizontal wells, drilling multiple branches from a single wellbore may achieve the optimum recovery in a cost-effective manner. It can be suggested to conduct research for OLGA/ECLIPSE oil production simulations with multi-lateral wells for the base case and case 2.

An initial model with two laterals in the x and y directions has been developed by the author. The initially developed OLGA model has been included in Appendix I for further reference.

7 Conclusion

The main objective of this thesis is to investigate the performance of advanced well technologies for oil production from reservoirs with different oil viscosities by coupling the ECLIPSE simulator for reservoir simulation and the OLGA simulator for oil production well simulation. The coupling of these software tools is a novel approach in this field of research.

The oil industry has been a dominant force in the energy sector for many decades, providing a significant portion of the world's energy supply. But according to 2022 reports, over 50% of oil in existing fields in NCS cannot be produced with the available oil recovery technologies. Therefore, in an energy transition period, improving the efficiency of oil recovery methods is very important. Based on the literature study, different oil recovery technologies and enhanced recovery methods have been used over the years to improve the efficiency of the oil production process. In industry, long horizontal wells are used to maximize oil production and recovery, but they can lead to early gas or water breakthrough due to the water conning effect towards the heel. This issue is mainly caused by the heel-toe effect and heterogeneity along the horizontal well. To prevent negative effects of early breakthroughs, various inflow control devices such as ICDs, AICVs, and AICDs are commonly used in oil well completion. ICDs can balance the drawdown pressure and fluid flow along the horizontal well, thus delaying the early water breakthrough, but they cannot choke the water once it eventually enters the well. AICD delays the water breakthrough more and can locally and autonomously choke low viscous fluids after the breakthrough. AICV has both delaying and choking abilities, but it has more choking abilities than AICD. Thus, the self-adjusting functions of these devices allow for an increase in oil production while reducing total water production, enabling the well to produce oil for a longer period.

This study evaluated the performance of these advanced well technologies in horizontal oil production wells in heterogeneous heavy oil reservoirs (case 1) and light oil reservoirs (case 2). These reservoirs were synthetically designed using the MRST tool in MATLAB based on assumed permeability and porosity ranges. According to the literature study water flooding EOR method has more potential to recover oil from fields in NCS. Therefore, water flooding was used to enhance oil production, and two vertical water injections were used for the heavy oil reservoir, while a single horizontal injection well was used for the light oil reservoir. The optimum locations for two water injections in the heavy oil case were determined by conducting a sensitivity analysis of 21 possibilities in ECLIPSE and calculating NPV. The optimal locations were determined as the 13^{th} and 29^{th} cells in the x-direction, and the study proceeded to evaluate the performance of advanced wells using these optimal injection locations.

Reservoirs were modeled in ECLIPSE simulator, and production wells with advanced well technologies were modeled in OLGA simulator, and the total production was simulated by combining these two software. The autonomous function of AICD and AICV were developed in OLGA using a table controller that opens the valve area based on the varying WC. For the base case, the models were developed for OPENHOLE, ICD, and AICD well completions. The simulations for each case were carried out for 1000 days of operation. For case 2, the models were developed for OPENHOLE, ICD, AICD, and AICV well completions, and the simulations were done for 1500 days of operation for each case. To obtain more realistic

outputs, a total production limit of 2400m^3/day was set for case 2 OPENHOLE production, considering the usual total liquid production limit used in the industry.

Based on the results, water breakthrough in both cases has been encouraged by the water injection method and heterogeneity of the reservoir. However, in the heavy oil reservoir of the base case, the use of advanced well technologies resulted in a delay of water breakthrough by only 10 days, which can be considered relatively small compared to the 180days delay achieved in the light oil case. It can be argued that this may be because the applied separate vertical water injection method for heavy oil reservoirs has encouraged the water conning effect and has resulted in early water breakthroughs even for advanced wells. Moreover, the literature study recommends polymer injections for heavy oil reservoirs since polymers increase viscosity and thereby the sweep efficiency. This minimizes the coning effect and increases the water breakthrough.

Before water breakthrough, AICDs and AICVs are fully open and act like ICDs. However, after the breakthrough valves get partially closed by increasing water cut. From the results of heavy oil reservoir simulations, compared to the OPENHOLE case, cumulative oil productions from ICD and AICD completions have relatively increased by 1.15% and 1.19%, respectively, after 1000days of operation. Moreover, cumulative water production is reduced by 5.52% and 8.51%, respectively. In light oil reservoir simulations, compared to the OPENHOLE case, cumulative oil productions from ICD, AICD and AICV completions have relatively increased by 2.22%, 1.7%, and 0.2%, respectively, after 1500days of operation. Moreover, cumulative water productions in ICD, AICD and AICV have considerably reduced by 26.8%, 33.1%, and 49.1%, respectively, compared to OPENHOLE case. And also, it was observed that when the horizontal water injection method is used, maximum oil production rates last a long period. Overall, it was observed that the use of advanced well technologies like ICD, AICD, and AICV have delayed the water breakthroughs, and they have significantly reduced the cumulative water production while increasing oil production slightly. Water production during oil production is a significant challenge in the industry. The production of unwanted water results in additional costs associated with separation and handling. Furthermore, due to the environmental impact of produced water disposal, companies should adhere to regulations and guidelines that govern the disposal of produced water. Therefore, reducing water production during oil production is a priority for the industry for a cost-effective and productive oil recovery process. AICV completion has shown the best performance in light oil reservoirs by reducing large amounts of water, and it can be suggested to conduct further studies on AICV technology.

In addition to that, the challenges related to water injection are discussed. The impact of different oil viscosities to select the most appropriate water injection technology, the water-oil ratio in the reservoir, formation damages caused by water flooding, and the formation of oil-water emulsions are some challenges in waterflooding.

At the end of the study, recommendations for future research are provided based on the findings. It is suggested to conduct further research for advanced multi-lateral wells (AMW) for optimum oil recovery and to see its benefits and limitations. Because use of multi-lateral wells instead of drilling multiple horizontal wells may be a favorable option. The attempts made by the author are also attached for further reference in this study. Furthermore, it can be concluded that the main objective of the thesis, which was to couple OLGA and ECLIPSE software to simulate total oil production, has been successfully achieved. It is suggested that further studies be conducted on this new combination to explore its advantages and limitations.

8 References

[1] 'How Ancients Used Oil'. http://www.dnr.louisiana.gov/assets/TAD/education/BGBB/2/ancient_use.html (accessed Feb. 21, 2023).

[2] J. Sherman, *Drake Well Museum and Park: Pennsylvania Trail of History Guide*. Stackpole Books, 2002.

[3] DNV, *DNV Energy Transition Outlook 2022: A Global and Regional Forecast to 2050*. 2022.

[4] 'Exports of Norwegian oil and gas', *Norwegianpetroleum.no*. https://www.norskpetroleum.no/en/production-and-exports/exports-of-oil-and-gas/ (accessed Feb. 22, 2023).

[5] Ø. Fevang and G. H. Lille, 'OG21 – The national technology strategy for the petroleum industry', Force seminar, Feb. 2016. [Online]. Available: https://www.npd.no/globalassets/2-force/2019/documents/archive-2010-2018/joining-forces-2016/og21--the-national-technology-strategy-for-the-petroleum-industry.pdf

[6] '2 – Remaining petroleum resources'. Accessed: Feb. 22, 2023. [Online]. Available: https://www.npd.no/en/facts/publications/reports/resource-report/resource-report-2022/2-remaining-petroleum-resources/

[7] A. Moradi, 'Cost-effective and safe oil production from existing and near-future oil fields', Thesis, University of South-Eastern Norway (USN), Norway, 2020.

[8] S. Sund *et al.*, *Simulation of Oil Production from Homogenous North Sea Reservoirs with Inflow Control using OLGA/Rocx*. 2017, p. 195. doi: 10.3384/ecp17138188.

[9] Haavard Aakre, 'The impact of autonomous inflow control valve on increased oil production and recovery: Vol. no. 32', University College of Southeast Norway, Faculty of Technology, Natural Sciences and Maritime Sciences, 2017.

[10] O. Bhujange, A. Moradi, A. Kumara, and B. Moldestad, 'Modeling and analysis of secondary oil recovery with water flooding from a heterogeneous reservoir through advanced wells.', *Scand. Simul. Soc.*, pp. 285–290, Oct. 2022, doi: 10.3384/ecp192040.

[11] *The FUNCTION of inflow control; ICD, AICD & AICV*, (Jun. 21, 2021). Accessed: Feb. 23, 2023. [Online Video]. Available: https://www.youtube.com/watch?v=TIl8R752Sio

[12] D. Zhambrovskii, 'Application of Multilateral Wells as an alternative solution for costs optimization', Master thesis, University of Stavanger, Norway, 2018. Accessed: Feb. 22, 2023. [Online]. Available: https://uis.brage.unit.no/uis-xmlui/handle/11250/2569342

[13] D. Yergin, *The Prize: The Epic Quest for Oil, Money & Power*. Simon and Schuster, 2011.

[14] C. Bittner, 'Impact of Innovations on Future Energy Supply – Chemical Enhanced Oil Recovery (CEOR)', *CHIMIA*, vol. 67, no. 10, p. 724, Oct. 2013, doi: 10.2533/chimia.2013.724.

[15] K. Lie, 'Introduction to Flow Simulation as Used in Reservoir Engineering'.

[16] A. Yethiraj and A. Striolo, 'Fracking: What Can Physical Chemistry Offer?', *J. Phys. Chem. Lett.*, vol. 4, no. 4, pp. 687–690, Feb. 2013, doi: 10.1021/jz400141e.

[17] G. E. King, 'Hydraulic Fracturing 101: What Every Representative, Environmentalist, Regulator, Reporter, Investor, University Researcher, Neighbor and Engineer Should Know About Estimating Frac Risk and Improving Frac Performance in Unconventional Gas and Oil Wells.', in *All Days*, The Woodlands, Texas, USA: SPE, Feb. 2012, p. SPE-152596-MS. doi: 10.2118/152596-MS.

[18] '1.4: Improved Oil Recovery and Enhanced Oil Recovery Methods | PNG 301: Introduction to Petroleum and Natural Gas Engineering'. https://www.e-education.psu.edu/png301/node/642 (accessed Feb. 24, 2023).

[19] L. Romero-Zern, Ed., *Introduction to Enhanced Oil Recovery (EOR) Processes and Bioremediation of Oil-Contaminated Sites*. InTech, 2012. doi: 10.5772/2053.

[20] J. G. Speight, *Enhanced Recovery Methods for Heavy Oil and Tar Sands: A Guide to Heavy Oil*. Austin, UNITED STATES: Gulf Publishing Company, 2009. Accessed: Feb. 24, 2023. [Online]. Available: http://ebookcentral.proquest.com/lib/ucsn-ebooks/detail.action?docID=1457957

[21] G. J. Stosur, J. R. Hite, N. F. Carnahan, and K. Miller, 'The Alphabet Soup of IOR, EOR and AOR: Effective Communication Requires a Definition of Terms', presented at the SPE International Improved Oil Recovery Conference in Asia Pacific, OnePetro, Oct. 2003. doi: 10.2118/84908-MS.

[22] J.-L. Salager, 'Physico-chemical properties of surfactant-water-oil mixtures [microform] : phase behavior, micro-emulsion formation and interfacial tension /', Feb. 2023.

[23] A. Hamid and S. Anuar, 'Computational investigations of viscous fingering in enhanced oil recovery', Feb. 2019, doi: 10.25560/78801.

[24] 'thermal_recovery'. https://glossary.slb.com/en/terms/t/thermal_recovery (accessed Feb. 27, 2023).

[25] 'in-situ_combustion'. https://glossary.slb.com/en/terms/i/in-situ_combustion (accessed Feb. 27, 2023).

[26] L. Xue, P. Liu, and Y. Zhang, 'Development and Research Status of Heavy Oil Enhanced Oil Recovery', *Geofluids*, vol. 2022, pp. 1–13, Feb. 2022, doi: 10.1155/2022/5015045.

[27] 'miscible_displacement'. https://glossary.slb.com/en/terms/m/miscible_displacement (accessed Feb. 27, 2023).

[28] 'Low shear polymer injection - Typhonix'. https://www.typhonix.com/learn-more-about-low-shear/technology-principles/low-shear-polymer-injection (accessed Feb. 27, 2023).

[29] 'A brief description of EOR methods'. https://www.npd.no/en/facts/publications/reports/resource-report/resource-report-2017/technical-potential/avanserte-utvinningsmetoder-eor/a-brief-description-of-eor-methods/ (accessed Feb. 28, 2023).

[30] J. T. Smith and W. M. Cobb, *Waterflooding*. Midwest Office of the Petroleum Technology Transfer COuncil, 1997.

[31] 'Water injection'. https://www.npd.no/en/facts/production/improved-oil-recovery-ior/water/ (accessed Feb. 28, 2023).

[32] T. Ahmed, *Reservoir Engineering Handbook*. Gulf Professional Publishing, 2018.

[33] S. Rellegadla *et al.*, 'An Effective Approach for Enhanced Oil Recovery Using Nickel Nanoparticles Assisted Polymer Flooding', *Energy Fuels*, vol. 32, no. 11, pp. 11212–11221, Nov. 2018, doi: 10.1021/acs.energyfuels.8b02356.

[34] S. D. Joshi, 'Cost/Benefits of Horizontal Wells', in *All Days*, Long Beach, California: SPE, May 2003, p. SPE-83621-MS. doi: 10.2118/83621-MS.

[35] 'Horizontal Drilling & Directional Drilling: Natural Gas Wells'. https://geology.com/articles/horizontal-drilling/ (accessed Mar. 07, 2023).

[36] 'Horizontal wells', *PetroWiki*, Jan. 15, 2018. https://petrowiki.spe.org/Horizontal_wells (accessed Mar. 07, 2023).

[37] 'Advantages, limitations, and classification of horizontal wells', *petroblogweb*, Aug. 14, 2016. https://petroblogweb.wordpress.com/2016/08/14/advantages-limitations-and-classification-of-horizontal-wells/ (accessed Mar. 07, 2023).

[38] M. Hossain, 'Production Technology Horizontal Well Technology', Curtin University of Technology, 2009.

[39] S. D. Joshi, *Horizontal Well Technology*. PennWell Publishing Company, 1991.

[40] A. Almajidi, *Applications of Horizontal Well*. 2021.

[41] *Coning lecture/part 1/Production petroleum Engineering*, (Mar. 30, 2020). Accessed: Mar. 08, 2023. [Online Video]. Available: https://www.youtube.com/watch?v=az94JosC8JE

[42] Z. Li, P. Fernandes, and D. . Zhu, 'Understanding the Roles of Inflow-Control Devices in Optimizing Horizontal-Well Performance', *SPE Drill. Complet.*, vol. 26, no. 03, pp. 376–385, Sep. 2011, doi: 10.2118/124677-PA.

[43] R. Shaibu, I. Klewiah, C. Cobbah, M. A. Mahamah, I. E. Acquah, and S. W. Asiedu, 'An Intelligent Well Approach to Controlling Water Coning Problems in Horizontal Production Wells', *Int. J. Eng. Res. Technol.*, vol. 6, no. 1, Jan. 2017, doi: 10.17577/IJERTV6IS010265.

[44] T. Jokela *et al.*, 'Inflow Control Devices — Raising Profiles', 2010. Accessed: Mar. 09, 2023. [Online]. Available: https://www.semanticscholar.org/paper/Inflow-Control-Devices-%E2%80%94-Raising-Profiles-Jokela-Kvernstuen/4529dd2db69cc15818e285d63d2cc61f8242933b

[45] 'Defining Multilateral Wells'. https://www.slb.com/resource-library/oilfield-review/defining-series/defining-multilateral-wells (accessed Feb. 22, 2023).

[46] Bosworth, Steve *et al.*, 'Key Issues in Multilateral Technology', *Oilfield review*, vol. 10, no. 4, pp. 14–28, 1998.

[47] F. Farsi Madan, 'Application of autonomous inflow control valve for enhanced bitumen recovery by steam assisted gravity drainage', Master thesis, University of South-

Eastern Norway, 2022. Accessed: Mar. 10, 2023. [Online]. Available: https://openarchive.usn.no/usn-xmlui/handle/11250/3011945

[48] V. M. Birchenko, K. M. Muradov, and D. R. Davies, 'Reduction of the horizontal well's heel-toe effect with inflow control devices', *J. Pet. Sci. Eng.*, vol. 75, no. 1–2, pp. 244–250, Dec. 2010, doi: 10.1016/j.petrol.2010.11.013.

[49] E. M. K. Eltaher, M. H. Sefat, K. Muradov, and D. Davies, 'Performance of Autonomous Inflow Control Completion in Heavy Oil Reservoirs', presented at the International Petroleum Technology Conference, OnePetro, Dec. 2014. doi: 10.2523/IPTC-17977-MS.

[50] 'EquiFlow_AICD_Data_Sheet_-_H08364.pdf'. Accessed: Mar. 14, 2023. [Online]. Available: https://cdn.brandfolder.io/OUSGG99Q/as/k8k7sjgcvjsqts7v6kb28kz/EquiFlow_AICD_Data_Sheet_-_H08364.pdf

[51] M. Mgimba, 'Numerical Study on Autonomous Inflow Control Devices: Their Performance and Effects on the Production from Horizontal Oil Wells with an Underlying Aquifer', Master thesis, NTNU, 2018. Accessed: Mar. 14, 2023. [Online]. Available: https://ntnuopen.ntnu.no/ntnu-xmlui/handle/11250/2559475

[52] V. Mathiesen, H. Aakre, B. Werswick, G. Elseth, and S. Asa, 'The Autonomous RCP Valve-New Technology for Inflow Control In Horizontal Wells', 2011. Accessed: Mar. 14, 2023. [Online]. Available: https://www.semanticscholar.org/paper/The-Autonomous-RCP-Valve-New-Technology-for-Inflow-Mathiesen-Aakre/7a5ff3cb9df0673f1b411c7fc635c09ed173570c

[53] H. Aakre, B. Halvorsen, B. Werswick, and V. Mathiesen, 'Smart Well With Autonomous Inflow Control Valve Technology', presented at the SPE Middle East Oil and Gas Show and Conference, OnePetro, Mar. 2013. doi: 10.2118/164348-MS.

[54] H. Aakre, V. Mathiesen, and B. Moldestad, 'Performance of CO2 flooding in a heterogeneous oil reservoir using autonomous inflow control', *J. Pet. Sci. Eng.*, vol. 167, pp. 654–663, Aug. 2018, doi: 10.1016/j.petrol.2018.04.008.

[55] A. Malagalage and B. Halvorsen, *Near Well Simulation and Modelling of Oil Production from Heavy Oil Reservoirs*. 2015, p. 298. doi: 10.3384/ecp15119289.

[56] R. Aryal, 'Near well simulation of oil production from heavy oil reservoirs', Master thesis, Høgskolen i Telemark, 2015. Accessed: Mar. 22, 2023. [Online]. Available: https://openarchive.usn.no/usn-xmlui/handle/11250/2439070

[57] 'ECLIPSE Blackoil Reservoir Simulation. Training and Exercise Guide Version PDF Free Download'. https://docplayer.net/62152871-Eclipse-blackoil-reservoir-simulation-training-and-exercise-guide-version-2-0.html (accessed Mar. 22, 2023).

[58] A. Ugwu and B. Moldestad, *Simulation of Horizontal and Vertical Waterflooding in a Homogeneous Reservoir using ECLIPSE*. 2018, p. 741. doi: 10.3384/ecp17142735.

[59] E. R. Jomark, 'Simulation Studies of Hybrid EOR', Master thesis, The University of Bergen, 2019. Accessed: Mar. 22, 2023. [Online]. Available: https://bora.uib.no/bora-xmlui/handle/1956/20354

[60] Schlumberger, 'OLGA - Dynamic multiphase flow simulator, User manual 2016.2', 2017.

[61] A. Y. Dandekar, *Petroleum Reservoir Rock and Fluid Properties*, Second edition. Taylor & Francis Group, LLC, 2013.

[62] O. Tors and M. Abtahi, 'EXPERIMENTAL RESERVOIR ENGINEERING LABORATORY WORK BOOK'.

[63] K.-A. Lie, *An Introduction to Reservoir Simulation Using MATLAB/GNU Octave: User Guide for the MATLAB Reservoir Simulation Toolbox (MRST)*. Cambridge: Cambridge University Press, 2019. doi: 10.1017/9781108591416.

[64] M. J. Economides, A. D. Hill, and C. Ehlig-Economides, *Petroleum production systems*. Prentice-Hall/Neodata, Des Moines, IA (United States), 1994.

[65] K. Moncada *et al.*, 'Determination of Vertical anD Horizontal Permeabilities for Vertical oil anD Gas Wells WitH Partial comPletion anD Partial Penetration usinG Pressure anD Pressure DeriV atiVe Plots WitHout tyPe-cur Ve matcHinG', *CTF - Cienc. Tecnol. Futuro*, vol. 3, Dec. 2005.

[66] 'Relative Permeability'. https://www.ihsenergy.ca/support/documentation_ca/Harmony/content/html_files/reference_material/general_concepts/relative_permeability.htm (accessed May 04, 2023).

[67] F. Kamyabi, 'Multiphase Flow in Porous Media', Master thesis, Institutt for petroleumsteknologi og anvendt geofysikk, 2014. Accessed: Apr. 04, 2023. [Online]. Available: https://ntnuopen.ntnu.no/ntnu-xmlui/handle/11250/240503

[68] 'Reservoir Engineering Online: Capillary Pressure', *Reservoir Engineering Online*, Aug. 03, 2014. http://reservoironline.blogspot.com/2014/08/capillary-pressure.html (accessed Apr. 04, 2023).

[69] L. Hand, *Well Completion Design - Jonathan Bellarby*. Accessed: Apr. 17, 2023. [Online]. Available: https://www.academia.edu/8361169/Well_Completion_Design_Jonathan_Bellarby

[70] '12.4: Phase Diagrams', *Chemistry LibreTexts*, Jan. 18, 2015. https://chem.libretexts.org/Bookshelves/General_Chemistry/Map%3A_General_Chemistry_(Petrucci_et_al.)/12%3A_Intermolecular_Forces%3A_Liquids_And_Solids/12.4%3A_Phase_Diagrams (accessed Apr. 17, 2023).

[71] B. Tolbert, 'Solution Gas Oil Ratio (Rs) - Top Dog Engineer', Mar. 01, 2019. https://topdogengineer.com/test-post/ (accessed Apr. 30, 2023).

[72] *Fluid Phase Behavior for Conventional and Unconventional Oil and Gas Reservoirs*. Accessed: Apr. 30, 2023. [Online]. Available: https://learning.oreilly.com/library/view/fluid-phase-behavior/9780128034460/XHTML/B9780128034378000075/sec-s0095_split_a.xhtml

[73] 'Gas formation volume factor and density', *PetroWiki*, Jul. 09, 2015. https://petrowiki.spe.org/Gas_formation_volume_factor_and_density (accessed Apr. 30, 2023).

[74] A. Moradi, N. A. Samani, A. S. Kumara, and B. M. E. Moldestad, 'Evaluating the performance of advanced wells in heavy oil reservoirs under uncertainty in permeability parameters', *Energy Rep.*, vol. 8, pp. 8605–8617, Nov. 2022, doi: 10.1016/j.egyr.2022.06.077.

[75] L. Hua, L. Yan, P. Xiaodong, L. Xindong, W. Laichao, and G. Hongqi, 'Pressure drop calculation models of the wellbore fluid in perforated completion horizontal wells', *Int. J. Heat Technol.*, vol. 20, pp. 11665–11679, Jan. 2015, doi: 10.18280/ijht.340110.

[76] A. Moradi and B. M. E. Moldestad, 'A Proposed Method for Simulation of Rate-Controlled Production Valves for Reduced Water Cut', *SPE Prod. Oper.*, vol. 36, no. 03, pp. 669–684, Aug. 2021, doi: 10.2118/205377-PA.

[77] A. Moradi, B. M. E. Moldestad, and A. S. Kumara, 'Simulation of Waterflooding Oil Recovery With Advanced Multilateral Wells Under Uncertainty by Using MRST', presented at the SPE Reservoir Characterisation and Simulation Conference and Exhibition, OnePetro, Jan. 2023. doi: 10.2118/212700-MS.

[78] 'Eclipse Technical Description | PDF', *Scribd*. https://www.scribd.com/doc/280504868/Eclipse-Technical-Description (accessed May 04, 2023).

[79] K. Bao, 'Multi-segment wells and well modeling', Department of Applied Mathematics, SINTEF, Jun. 01, 2016. [Online]. Available: https://opm-project.org/wp-content/uploads/2016/06/opm2016-bao-multi-segment-wells.pdf

[80] A. Moradi, J. Tavakolifaradonbe, and B. M. E. Moldestad, 'Data-Driven Proxy Models for Improving Advanced Well Completion Design under Uncertainty', *Energies*, vol. 15, no. 20, Art. no. 20, Jan. 2022, doi: 10.3390/en15207484.

[81] 'Eclipse Input Data - petrofaq'. http://petrofaq.org/wiki/Eclipse_Input_Data#SOLUTION (accessed May 01, 2023).

[82] 'API 5L Grade B Pipe, CS Gr. B Seamless and ERW Pipe in PSL1 and PSL2'. https://www.neelconsteel.com/api-5l-grb-carbon-steel-pipes.html#roughness (accessed May 03, 2023).

Appendices

Appendix A: Task Description

University of South-Eastern Norway

Faculty of Technology, Natural Sciences and Maritime Sciences, Campus Porsgrunn

FMH606 Master's Thesis

Title: Simulation and analysis of waterflooding oil recovery through advanced multilateral wells

USN supervisor: Prof. Britt M. E. Moldestad, Prof. Amaranath S. Kumara, and Ali Moradi

External partner: Equinor and SINTEF

Task background:
Norway has great potential to supply petroleum to the global market, and the Norwegian Continental Shelf (NCS) is one of the most technologically advanced petroleum regions in the world. To secure the competitiveness of the NCS in the international market and to ensure that NCS is at the forefront of adopting the latest technological innovations, OG21 (Oil and gas for the 21st century) has developed a national technology strategy for guiding research efforts in the field of petroleum technology. The main strategic objective of OG21 is to obtain efficient, secure, and environmentally friendly value creation from the Norwegian oil and gas resources for several generations.

In line with the OG21 strategy, in collaboration with Equinor and SINTEF, there is an ongoing research project called *DigiWell* (*digital wells for optimal production and drainage*) at USN. The project aims at developing new methods, algorithms, and tools for the prediction of oil production under uncertain conditions in order to maximize profit margins by minimizing production costs. As part of this project, it is of great interest to model and evaluate the performance of advanced wells with the goal of improving oil recovery.

A hydrocarbon reservoir can be considered as a rigid sponge that is confined inside an insulating material and has all its pores filled with hydrocarbons, which may appear in the form of a liquid oleic and a gaseous phase. Extraction of oil from a reservoir starts by drilling a well into the oil zone. If the initial pressure inside the reservoir is sufficiently high, it will push oil up to the surface which is referred as primary production (see Figure 1 for further details). As the oleic phase is produced, the pressure inside the reservoir will decline. Therefore, other mechanisms like gas and/or water injection are used for maintaining pressure and producing more oil from the reservoir. This production system is called secondary production (see Figure 2 for further details).

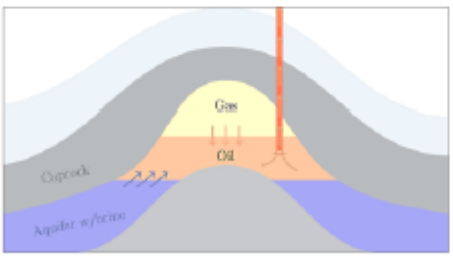

Figure 1. Primary oil production

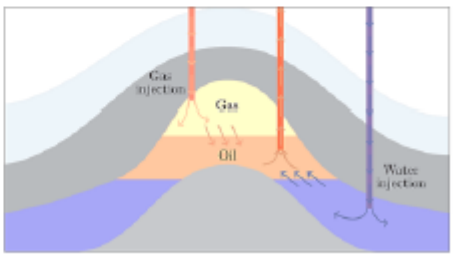

Figure 2. Secondary oil production

One of the main principles to achieve cost-effective and efficient oil recovery is maximizing the well-reservoir contact by using long horizontal wells. One of the main challenges of using such wells is early gas and/or water breakthrough due to the heel-toe effect and heterogeneity along the horizontal wells. To tackle this problem, Advanced (smart or intelligent) Multilateral Wells (AMWs) are widely applied today. The term "*advanced*" refers to horizontal wells completed with downhole Flow Control Devices (FCDs), Sand Control Screens (SCSs), Annular Flow Isolation (AFI), as well as other equipment such as sensors, downhole pumps and separators, etc. Figure 3 illustrates the schematic of Advanced Well Completions (AWCs).

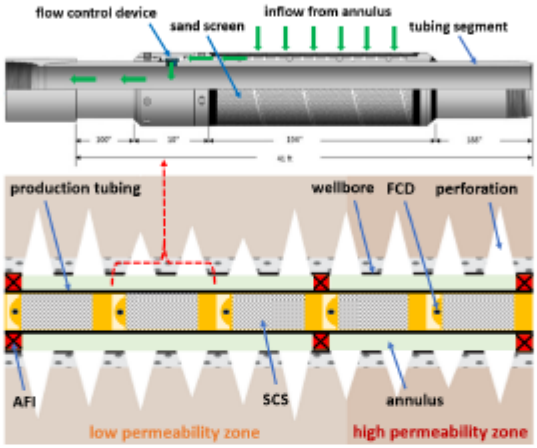

Figure 3. Schematic of advanced well completions.

AMWs are capable of contacting a larger portion of the formation, as well as multiple discrete oil-bearing zones. Besides, the production of unwanted fluids (water or gas) can be considerably reduced by applying such wells. However, the drilling and completion costs of AMWs are much higher compared to those of conventional wells. As a result, a significant improvement in economic recovery is required to justify their utilization. The results of reservoir simulations are crucial to making this judgment. The simulation model needs to reliably predict the performance of AMWs across the lifespan of the reservoir in order to deliver meaningful results. To provide such a high level of functionality, an appropriate model for AMWs must be developed and employed. The aim of this project is to generate more insight into the long-term performance of AMWs in waterflooding oil recovery by developing suitable simulation models.

Task description:

The objective of this research project can be achieved by completing the following tasks:

1. Literature study
   - Improved oil recovery by water flooding
   - Advanced multilateral wells
2. Developing suitable models for the simulation of oil recovery through AMWs
   - OLGA which is a dynamic multiphase flow simulator in combination with ECLIPSE which is a reservoir simulator should be used for this purpose.
3. Evaluating the performance of AMWs in secondary oil recovery
   - The performance of AMWs completed with different types of FCDs as well as AFI in a heterogeneous reservoir with water flooding should be analyzed.

4. If time permits, preparing a paper based on the results for the next SIMS conference is highly appreciated.

Student category: EET and PT students

The task is suitable for online students (not present at the campus): No

Practical arrangements: Necessary software will be provided by USN.

Supervision:
As a general rule, the student is entitled to 15-20 hours of supervision. This includes necessary time for the supervisor to prepare for supervision meetings (reading material to be discussed, etc).

Signatures:

Supervisor (date and signature):

Student (write clearly in all capitalized letters):

Student (date and signature):

Appendix B: ECLIPSE data file for reservoir model for base case

```
-- ================================================================
-- ALI MORADI
-- SIMS/2023 - RESERVOIR MODEL
-- "Simulation of waterflooding oil recovery through advanced wells"
-- ================================================================

RUNSPEC  ================================================================

TITLE
    BASE CASE - 1000 DAYS

DIMENS
--  NX  NY  NZ
    40   16  5 /

BLACKOIL

OIL
WATER
GAS
DISGAS

METRIC

ENDSCALE
    DIRECT IRREVERS /

HWELLS

START
--  DAY  MONTH  YEAR
    01   JAN    2023 /

MESSAGES
    3* 100 5* 100 /

EQLDIMS
--  NETQUL  #DEPTH NODE  NDRXVD  NTTRVD  NSTRVD
    1*      1*           1*      1*      1* /

TABDIMS
--  #SATURATION-  #PVT-     #MAX LINES IN-    #MAX LINES IN-  #MAX FIP-  #MAX RS-
--  TABLE         FAMILIES  REL.PERM. TABLES  PVT TABLES      REGIONS    NODES
    1*            1*        25                1*              1*         1* /

```

```
WELLDIMS
--  #MAX-    #MAX CELL-     #MAX-     #MAX WELLS-
--  WELLS    CONNECTIONS    GROUPS    IN GROUPS
    3        50             2         2 /

WSEGDIMS
--  #MAX MULTISEG. #MAX SEG.-    #MAX BRANCHES  NCRDMAX
--  WELLS          PER WELLS
    1              30            20             20 /

NUPCOL
--  #NEWTON ITRATION IN EACH TIME STEP
    10 /

NSTACK
    100 /

--NOSIM

UNIFIN

UNIFOUT

GRID     ============================================================

INIT

--BOX
----------------BOX-------------
--  IX1  IX2  JY1  JY2  KZ1  KZ2
--  1    40   1    16   1    5
/

INCLUDE
poro.INC
/

INCLUDE
perm.INC
/
NOECHO

DX
--  [m]
    3200*25 /

DY
--  [m]
    3200*12.5 /

DZ
--  [m]
    3200*10 /

TOPS
    640*2000 /

GRIDFILE
    0 1 /
```

```
PROPS    ================================================================

SWFN
--  SWAT  KRW      PCOW
--  [-]   [-]      [bar]
    0.12  0        5
    0.15  0.00065  1*
    0.2   0.00464  1*
    0.25  0.01226  1*
    0.3   0.02351  1*
    0.35  0.03839  1*
    0.4   0.0569   1*
    0.45  0.07903  1*
    0.5   0.10480  1*
    0.55  0.13419  1*
    0.6   0.16722  1*
    0.65  0.20387  1*
    0.7   0.24415  1*
    0.75  0.28806  1*
    0.8   0.3356   1*
    0.85  0.38677  1*
    0.9   0.44157  1*
    0.95  0.5      1*
    1     1        0 /

SGFN
--  SGAS  KRG      PCOG
--  [-]   [-]      [bar]
    0     0        0
    0.05  0.00277  1*
    0.1   0.01108  1*
    0.15  0.02493  1*
    0.2   0.04432  1*
    0.25  0.06925  1*
    0.3   0.09972  1*
    0.35  0.13573  1*
    0.4   0.17728  1*
    0.45  0.22437  1*
    0.5   0.277    1*
    0.55  0.33518  1*
    0.6   0.39889  1*
    0.65  0.46814  1*
    0.7   0.54293  1*
    0.75  0.62326  1*
    0.8   0.70914  1*
    0.85  0.80055  1*
    0.88  1        1 /
```

```
SOF3
--  SOIL   KRO       KRG
--  [-]    [-]       [-]
    0.05   0         0
    0.1    1.3E-05   1*
    0.15   0.00021   1*
    0.2    0.00106   1*
    0.25   0.00337   1*
    0.3    0.00823   1*
    0.35   0.01706   1*
    0.4    0.03161   1*
    0.45   0.05394   1*
    0.5    0.0864    1*
    0.55   0.13169   1*
    0.6    0.19281   1*
    0.65   0.27308   1*
    0.7    0.37613   1*
    0.75   0.50591   1*
    0.8    0.6667    1*
    0.85   0.86307   1*
    0.88   1         1 /

PVTW
--  REF. PR.  REF. FVF   COMP.    REF. VISCO.  VISCOSIBILITY
--  [bar]     [rm3/sm3]  [1/bar]  [cP]         [1/bar]
    200       1.01       1.0E-5   0.55         0 /

ROCK
--  REF. PR.  COMP.
--  [bar]     [1/bar]
    1         1.0E-5 /

DENSITY
--  OIL    WATER  GAS
--  [kg/m3]
    990    1050   0.67 /

--  PVT PROPERTIES OF DRY GAS (NO VAPOURISED OIL)
--  WE WOULD USE PVTG TO SPECIFY THE PROPERTIES OF WET GAS
```

```
SWATINIT
    3200*0.1 /

PVDG
--  PGAS    BGAS       VISGAS
--  [bar]   [rm3/sm3]  [cp]
    1       1.1532     0.012
    28      0.0406     0.012
    62      0.0170     0.013
    97      0.0104     0.015
    131     0.0074     0.017
    165     0.0057     0.019
    200     0.0048     0.021
    234     0.0042     0.023
    269     0.0038     0.026
    303     0.0035     0.028 /

PVTO
--  RS          POIL   FVFO       VISCO.
--  [sm3/sm3]   [bar]  [rm3/sm3]  [cP]
    0.097       1      1.035       699.9 /
    5.185       28     1.045       530.1 /
    13.773      62     1.062       352.9 /
    23.454      97     1.081       239.5 /
    33.885      131    1.103       167.7 /
    44.899      165    1.127       121.1 /
    56.397      200    1.153       90.0  /
    68.310      234    1.180       68.5
                269    1.175       80.9
                303    1.170       93.3  /
/

ECHO
SOLUTION ================================================================


EQUIL

--  DATUM-  DATUM-  OWC-   OWC-  GOC-   GOC-  RSVD-  RVVD-  SOLN-
--  DEPTH   PR.     DEPTH  PCOW  DEPTH  PCOG  TABLE  TABLE  METH
--  [m]     [bar]   [m]    []    []     []    []     []     []
    2025    200     2050   0     2000   0     1      0      0 /

RSVD

--  DEPTH  RS
--  [m]    [-]
    2000   50
    2050   50 /

RPTRST
    PRE SWAT SGAS SOIL /

RPTSOL
    PRE SWAT SGAS SOIL /
```

```
SUMMARY  =====================================================================

FOPT
FGPT
FWPT

WBHP
   INJ1
   INJ2
   PROD /
WOPR
   PROD /
WWPR
   PROD /
WGPR
   PROD /
WWCT
   PROD /
WOPT
   PROD /
WWPT
   PROD /
WGPT
   PROD /
WLPR
   PROD /
WLPT
   PROD /
WGOR
   PROD /
WWIR
   INJ1
   INJ2   /
WWIT
   INJ1
   INJ2   /

RUNSUM
SEPARATE
```

```
SCHEDULE ============================================================



RPTSCHED
  'PRES'  'SWAT'  'SGAS'  'RESTART=1'  'RS'  'WELLS=2'  'SUMMARY=2'
  'CPU=2' 'WELSPECS'   'NEWTON=2' /

TUNING
   1 1 /
   /
   2* 100 1* 16 /
/

WELSPECS
--  WELL-      GROUP-  WELLHEAD(HEEL)   REF. DEPTH-  PREFFERED-   DRAINAGE-  FLAG  INSTRUCTION-  CROSS FLOW-    PR. TAB.-  TYPE OF DEN.-
--  NAME       NAME    I LOC.  J LOC.   FOR BHP      PHASE WELL   REDIUS           FOR SHUT IN   ABILITY FLAG   NUMBER     CALCULATION
    PROD       G1      1       1        2005       OIL          1*         1*    STOP          1*             1* /
    INJ1       G2      29      16       2045       WAT /
    INJ2       G2      13      16       2045       WAT /
/
```

```
COMPDAT
    PROD  1 1 1 1   OPEN  2*  0.216   3*   X  /
    PROD  2 1 1 1   OPEN  2*  0.216   3*   X  /
    PROD  3 1 1 1   OPEN  2*  0.216   3*   X  /
    PROD  4 1 1 1   OPEN  2*  0.216   3*   X  /
    PROD  5 1 1 1   OPEN  2*  0.216   3*   X  /
    PROD  6 1 1 1   OPEN  2*  0.216   3*   X  /
    PROD  7 1 1 1   OPEN  2*  0.216   3*   X  /
    PROD  8 1 1 1   OPEN  2*  0.216   3*   X  /
    PROD  9 1 1 1   OPEN  2*  0.216   3*   X  /
    PROD  10 1 1 1  OPEN  2*  0.216   3*   X  /
    PROD  11 1 1 1  OPEN  2*  0.216   3*   X  /
    PROD  12 1 1 1  OPEN  2*  0.216   3*   X  /
    PROD  13 1 1 1  OPEN  2*  0.216   3*   X  /
    PROD  14 1 1 1  OPEN  2*  0.216   3*   X  /
    PROD  15 1 1 1  OPEN  2*  0.216   3*   X  /
    PROD  16 1 1 1  OPEN  2*  0.216   3*   X  /
    PROD  17 1 1 1  OPEN  2*  0.216   3*   X  /
    PROD  18 1 1 1  OPEN  2*  0.216   3*   X  /
    PROD  19 1 1 1  OPEN  2*  0.216   3*   X  /
    PROD  20 1 1 1  OPEN  2*  0.216   3*   X  /
    PROD  21 1 1 1  OPEN  2*  0.216   3*   X  /
    PROD  22 1 1 1  OPEN  2*  0.216   3*   X  /
    PROD  23 1 1 1  OPEN  2*  0.216   3*   X  /
    PROD  24 1 1 1  OPEN  2*  0.216   3*   X  /
    PROD  25 1 1 1  OPEN  2*  0.216   3*   X  /
    PROD  26 1 1 1  OPEN  2*  0.216   3*   X  /
    PROD  27 1 1 1  OPEN  2*  0.216   3*   X  /
    PROD  28 1 1 1  OPEN  2*  0.216   3*   X  /
    PROD  29 1 1 1  OPEN  2*  0.216   3*   X  /
    PROD  30 1 1 1  OPEN  2*  0.216   3*   X  /
    PROD  31 1 1 1  OPEN  2*  0.216   3*   X  /
    PROD  32 1 1 1  OPEN  2*  0.216   3*   X  /
    PROD  33 1 1 1  OPEN  2*  0.216   3*   X  /
    PROD  34 1 1 1  OPEN  2*  0.216   3*   X  /
    PROD  35 1 1 1  OPEN  2*  0.216   3*   X  /
    PROD  36 1 1 1  OPEN  2*  0.216   3*   X  /
    PROD  37 1 1 1  OPEN  2*  0.216   3*   X  /
    PROD  38 1 1 1  OPEN  2*  0.216   3*   X  /
    PROD  39 1 1 1  OPEN  2*  0.216   3*   X  /
    PROD  40 1 1 1  OPEN  2*  0.216   3*   X  /
    INJ1  29 16 1 5 OPEN  2*  0.216   3*   Z  /
    INJ2  13 16 1 5  OPEN  2*  0.216   3*   Z  /
/
WCONPROD
--  WELL-     OPEN-      CONTROL-  OIL RATE-  WAT. RATE-  GAS RATE-  LIQ. RATE-  N/A   BHP-
--  NAME      SHUT FLAG  MODE      TARGET     TARGET      TARGET     TARGET            TARGET
    PROD      OPEN       BHP       1*         1*          1*         1000        1*     190 /
/

WCONINJE
    INJ1        WAT     OPEN    RATE   350   1*   300 /
    INJ2        WAT     OPEN    RATE   350   1*   300 /
/

WECON
--  WELL-     MAX OIL-  MIN GAS-  MAX WAT.-  MAX-  MAX-  WORKOVER-  END RUN-
--  NAME      RATE      RATE      CUT        GOR   WGR   PROCEDURE  FLAG
    PROD      1*        1*        0.95       1*    1*    WELL       YES /
/

WSEGITER
25 5 0.1 3.0 /


TSTEP
    1000*1 /

END
```

Appendix C: Possible water injection combination for location optimization

X direction cell number for INJ1	X direction cell number for INJ2
5	1
13	1
21	1
29	1
36	1
40	1
13	5
21	5
29	5
36	5
40	5
21	13
29	13
36	13
40	13
29	21
36	21
40	21
36	29
40	29
40	36

Appendix D: NPV calculation for water injection location optimization

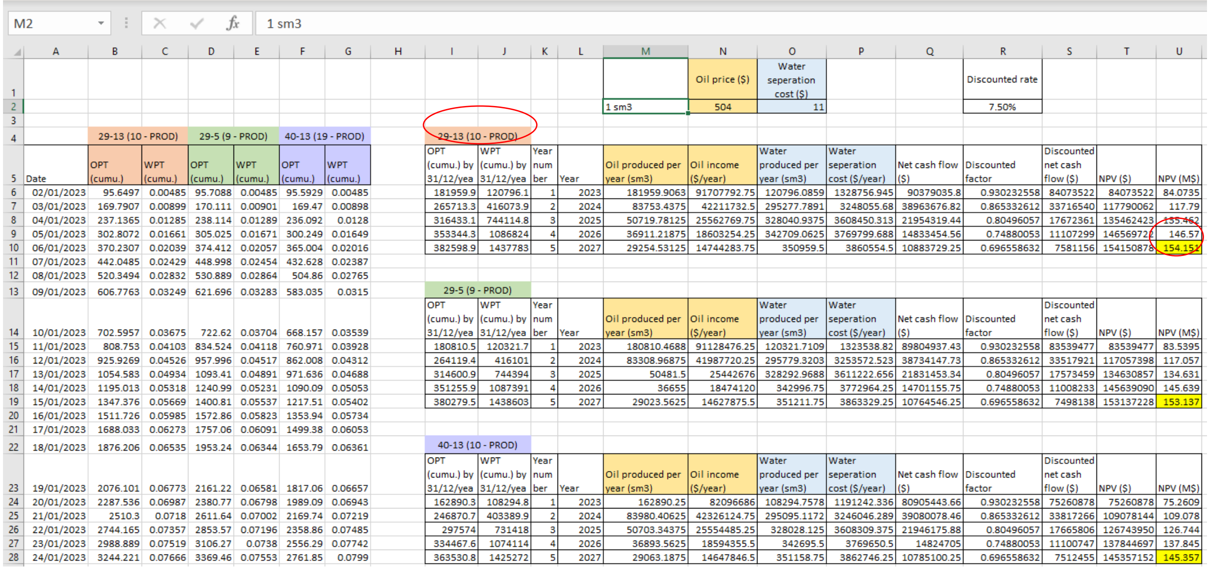

M2 | 1 sm3

	Oil price ($)	Water seperation cost ($)	Discounted rate
1 sm3	504	11	7.50%

Date	29-13 (10 - PROD) OPT (cumu.)	29-13 (10 - PROD) WPT (cumu.)	29-5 (9 - PROD) OPT (cumu.)	29-5 (9 - PROD) WPT (cumu.)	40-13 (19 - PROD) OPT (cumu.)	40-13 (19 - PROD) WPT (cumu.)
02/01/2023	95.6497	0.00485	95.7088	0.00485	95.5929	0.00485
03/01/2023	169.7907	0.00899	170.111	0.00901	169.47	0.00898
04/01/2023	237.1365	0.01285	238.114	0.01289	236.092	0.0128
05/01/2023	302.8072	0.01661	305.025	0.01671	300.249	0.01649
06/01/2023	370.2307	0.02039	374.412	0.02057	365.004	0.02016
07/01/2023	442.0485	0.02429	448.998	0.02454	432.628	0.02387
08/01/2023	520.3494	0.02832	530.889	0.02864	504.86	0.02765
09/01/2023	606.7763	0.03249	621.696	0.03283	583.035	0.0315
10/01/2023	702.5957	0.03675	722.62	0.03704	668.157	0.03539
11/01/2023	808.753	0.04103	834.524	0.04118	760.971	0.03928
12/01/2023	925.9269	0.04526	957.996	0.04517	862.008	0.04312
13/01/2023	1054.583	0.04934	1093.41	0.04891	971.636	0.04688
14/01/2023	1195.013	0.05318	1240.99	0.05231	1090.09	0.05053
15/01/2023	1347.376	0.05669	1400.81	0.05537	1217.51	0.05402
16/01/2023	1511.726	0.05985	1572.86	0.05823	1353.94	0.05734
17/01/2023	1688.033	0.06273	1757.06	0.06091	1499.38	0.06053
18/01/2023	1876.206	0.06535	1953.24	0.06344	1653.79	0.06361
19/01/2023	2076.101	0.06773	2161.22	0.06581	1817.06	0.06657
20/01/2023	2287.536	0.06987	2380.77	0.06798	1989.09	0.06943
21/01/2023	2510.3	0.0718	2611.64	0.07002	2169.74	0.07219
22/01/2023	2744.165	0.07357	2853.57	0.07196	2358.86	0.07485
23/01/2023	2988.889	0.07519	3106.27	0.0738	2556.29	0.07742
24/01/2023	3244.221	0.07666	3369.46	0.07553	2761.85	0.0799

29-13 (10 - PROD)

OPT (cumu.) by 31/12/yea	WPT (cumu.) by 31/12/yea	Year number	Year	Oil produced per year (sm3)	Oil income ($/year)	Water produced per year (sm3)	Water seperation cost ($/year)	Net cash flow ($)	Discounted factor	Discounted net cash flow ($)	NPV ($)	NPV (M$)
181959.9	120796.1	1	2023	181959.9063	91707792.75	120796.0859	1328756.945	90379035.8	0.930232558	84073522	84073522	84.0735
265713.3	416073.9	2	2024	83753.4375	42211732.5	295277.7891	3248055.68	38963676.82	0.865332612	33716540	117790062	117.79
316433.1	744114.8	3	2025	50719.78125	25562769.75	328040.9375	3608450.313	21954319.44	0.80496057	17672361	135462423	135.462
353344.3	1086824	4	2026	36911.21875	18603254.25	342709.0625	3769799.688	14833454.56	0.74880053	11107299	146569722	146.57
382598.9	1437783	5	2027	29254.53125	14744283.75	350959.5	3860554.5	10883729.25	0.696558632	7581156	154150878	154.151

29-5 (9 - PROD)

OPT (cumu.) by 31/12/yea	WPT (cumu.) by 31/12/yea	Year number	Year	Oil produced per year (sm3)	Oil income ($/year)	Water produced per year (sm3)	Water seperation cost ($/year)	Net cash flow ($)	Discounted factor	Discounted net cash flow ($)	NPV ($)	NPV (M$)
180810.5	120321.7	1	2023	180810.4688	91128476.25	120321.7109	1323538.82	89804937.43	0.930232558	83539477	83539477	83.5395
264119.4	416101	2	2024	83308.96875	41987720.25	295779.3203	3253572.523	38734147.73	0.865332612	33517921	117057398	117.057
314600.9	744394	3	2025	50481.5	25442676	328292.9688	3611222.656	21831453.34	0.80496057	17573459	134630857	134.631
351255.9	1087391	4	2026	36655	18474120	342996.75	3772964.25	14701155.75	0.74880053	11008233	145639090	145.639
380279.5	1438603	5	2027	29023.5625	14627875.5	351211.75	3863329.25	10764546.25	0.696558632	7498138	153137228	153.137

40-13 (10 - PROD)

OPT (cumu.) by 31/12/yea	WPT (cumu.) by 31/12/yea	Year number	Year	Oil produced per year (sm3)	Oil income ($/year)	Water produced per year (sm3)	Water seperation cost ($/year)	Net cash flow ($)	Discounted factor	Discounted net cash flow ($)	NPV ($)	NPV (M$)
162890.3	108294.8	1	2023	162890.25	82096686	108294.7578	1191242.336	80905443.66	0.930232558	75260878	75260878	75.2609
246870.7	403389.9	2	2024	83980.40625	42326124.75	295095.1172	3246046.289	39080078.46	0.865332612	33817266	109078144	109.078
297574	731418	3	2025	50703.34375	25554485.25	328028.125	3608309.375	21946175.88	0.80496057	17665806	126743950	126.744
334467.6	1074114	4	2026	36893.5625	18594355.5	342695.5	3769650.5	14824705	0.74880053	11100747	137844697	137.845
363530.8	1425272	5	2027	29063.1875	14647846.5	351158.75	3862746.25	10785100.25	0.696558632	7512455	145357152	145.357

ECLIPSE generated total oil production rate and total water production rate values over 2000 days are in the excel sheet

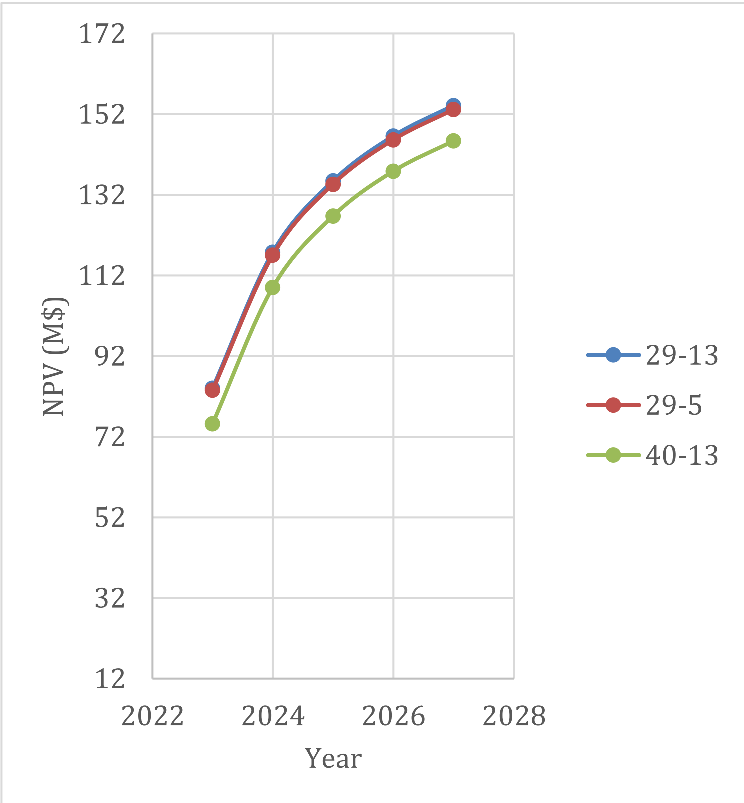

Appendix E: OLGA model for AICD and ICD for base case

AICD base case with 40 valves

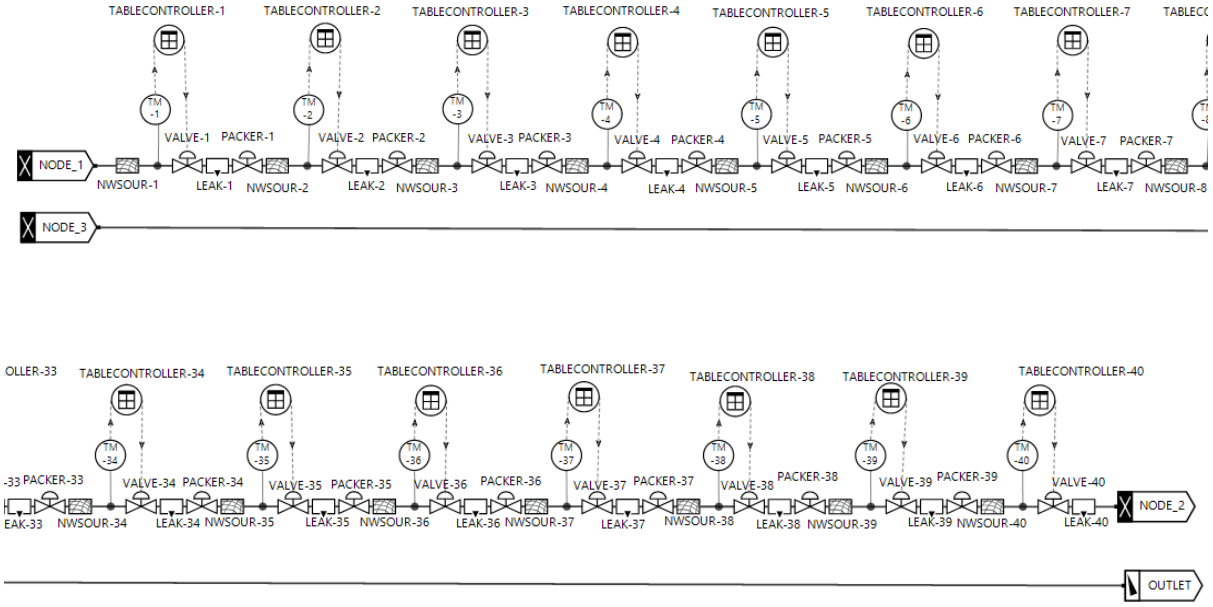

ICD base case with 40 valves

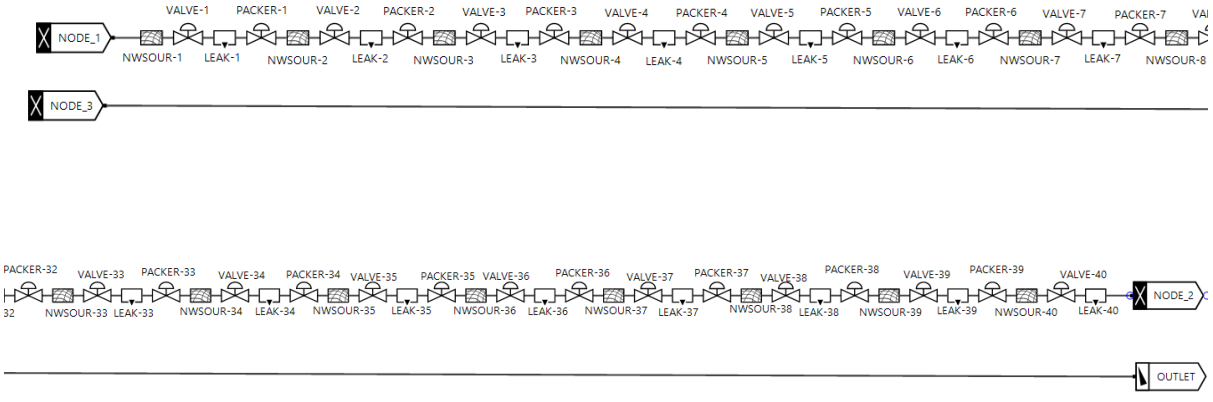

Appendix F: ECLIPSE model development for case 2

1) Reservoir grid

Main dimensions of the reservoir are given in table 1.

Table 1: Main dimensions of the reservoir.

Length of the reservoir (x)	1500 m
Width of the reservoir (y)	500 m
Height of the reservoir (z)	50 m

As discussed in section 3.6, each production joint has a length of 12.4 m. The horizontal well is positioned in the x-direction of the reservoir (length). Since the length is 1500 m, 120 ICDs can be placed along the well. But it is complex to simulate the real well with huge number of ICDs as it requires long simulation time. Therefore, one equivalent ICD is used to represent 4 real ICDs. Thus, 30 cells are considered in x direction and 30 ICDs are used along the well. In y and z directions, 10 and 5 cells are considered respectively. The grid settings in ECLIPSE including the number of cells and their sizes are given in table 2.

Table 2: Number of cells and their sizes for the grid setting in ECLIPSE.

Direction	**Number of cells**	**Size of the cells (m)**
x	nx = 30	50 m (constant)
y	ny = 10	50 m (constant)
z	nz = 5	10 m (constant)

In case 2 model, water in injected by horizontal well is positioned in the middle of (xi, 10, 5) cell row with 20 similaer injections along the well as shown in figure 1.

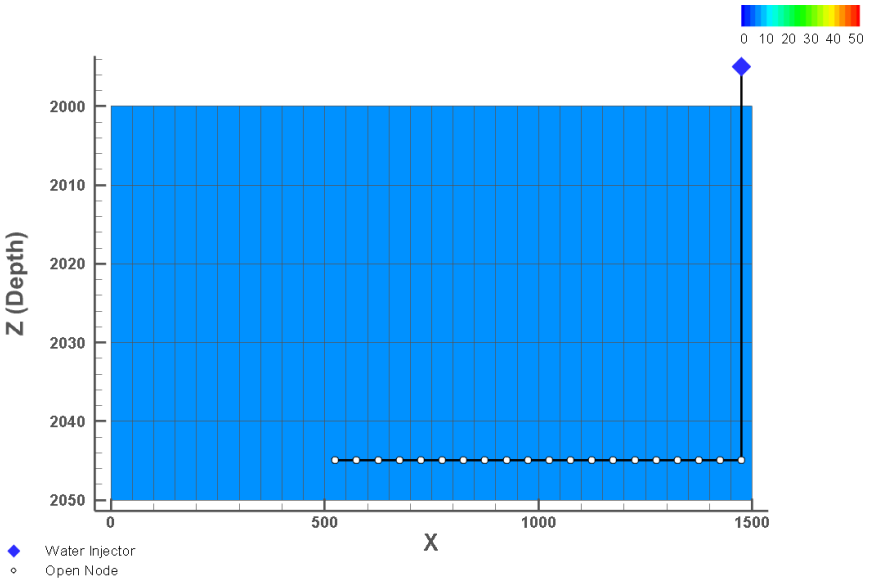

Figure 1: XZ plane of the reservoir through the 10th cell in y direction.

Figure 2 illustates the 3D view of the case 2model reservoir.

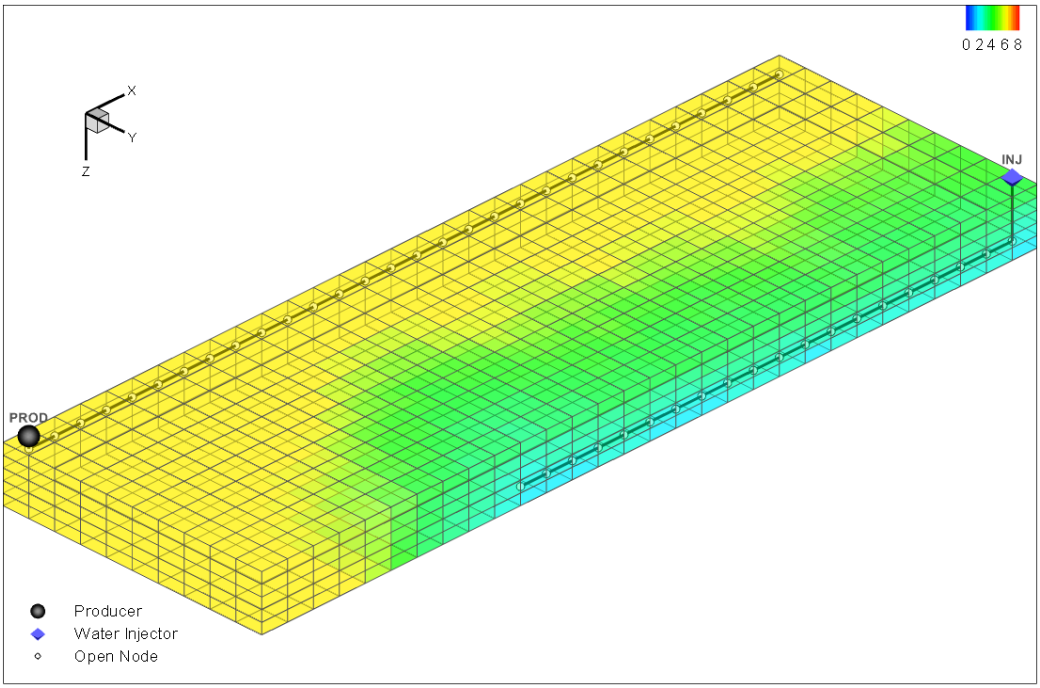

Figure 2: Reservoir geometry for case 2.

2) Reservoir fluid and rock properties

This reservoir has conditions similaer to the Troll field in the North Sea. It is assumed that the designed reservoir contains a viscous oil with 90cP viscosity. Therefore, the reservoir fluid can be considered as black oil type (viscosity is 2 to 3 – 100 and up). Reservoir fluid properties and some rock properties used for the OLGA/ECLIPSE model are listed in table 3.

Table 3: Fluids properties in reservoir.

Parameter	**Valve**
Solution GOR	50 Sm^3/Sm^3
Oil density	950 kg/m^3
Water density	1100 kg/m^3
Gas density	0.67 kg/m^3
Oil Viscosity	2.7 cP
Temperature	68°C
Mean porosity	0.25 (0.15-0.27)

Initial water saturation	0.12
Pressure	130 bara

In this study, oil is pushed towards the well by 20 similaer water in jections in a horisontal injection well as shown in figure.

The components of water drive feed and oil feed are listed in table 4.

Table 4: Water and oil feed components.

Feed	**Gas fraction**	**Water cut**
Oil	50 Sm^3/Sm^3 (GOR)	0.0001
Water	0.0001 Sm^3/Sm^3 (GLR)	0.99

3) Reservoir permeability

Reservoir permeabilities are in the similar ranges as base case.

4) Initial conditions

Initial oil, gas, and water satutations are similaer to base case. Initial temperature and pressure are 68℃ and 130 bar respectively.

5) Boundary conditions

It is assumed that the production well is controlled by a constant 115 bar Bottom Hole Pressure (BHP).

As the mean porosity of the reservoir is 0.21, the total void volume can be calculated as, $1500\text{m} \times 500\text{m} \times 50\text{m} \times 0.21 = 7875000\ \text{m}^3$. Assuming, the $^2/_3$ of the reservoir liquid is produced over 1000days, required water injection flow rate by one injection can be calculated as, $\frac{2/3 \times 7875000\ \text{m}^3}{1500\ \text{days}} = 3500\ \text{m}^3/\text{day}$. This water injection flow rate is impossible because of the limitation for maximum pressure allowed for the injection, which is 180bar according to practical injection rates in industry. Therefore, it is decided to inject water through 20 similar injections where each one with a water flow rate of $175\ \text{m}^3/\text{day}$.

6) Simulation setting

The ECLIPSE model is run with 1 day as the time step for 1500 days.

Appendix G: OLGA model development for case 2

1) Structure

The structure is similaer to base case.

2) Tables and curves

Based on the pressure drop 15 bar, the corresponding valve opening values with respect to WCs were generated in a MATLAB code and plotted in following figure 1.

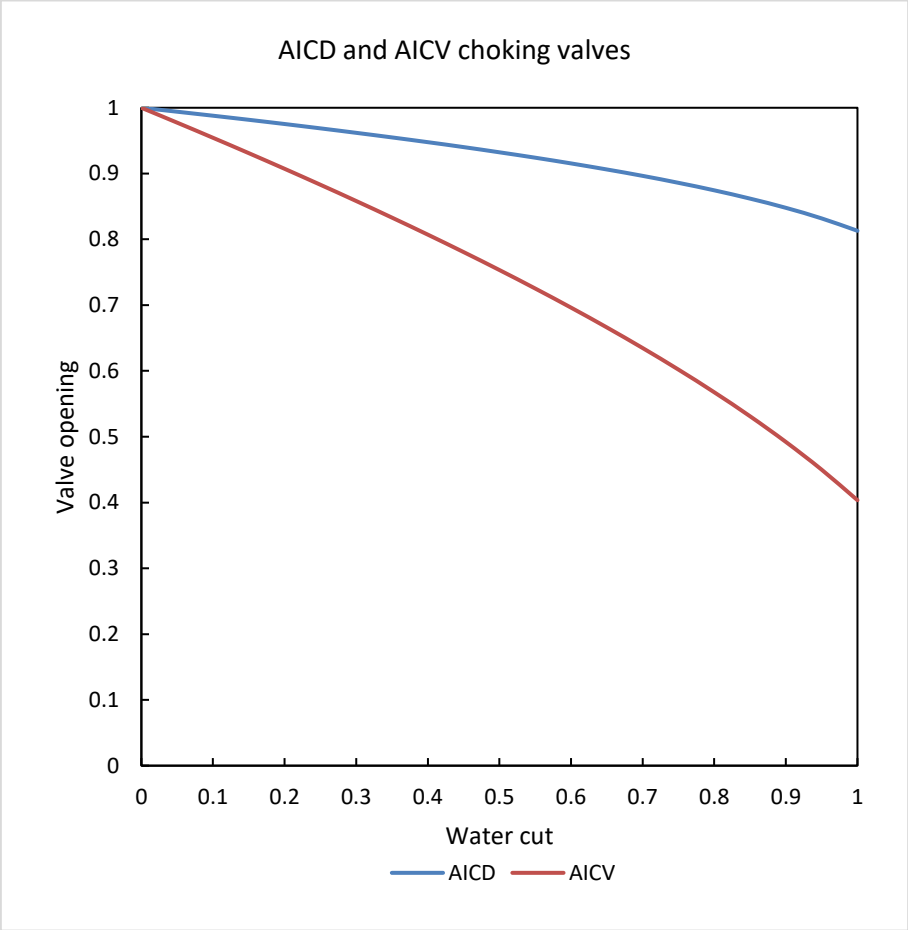

Figure 1: AICD and AICV choking valves for oil viscosity 2.7 cP for 15 bar pressure drop.

3) Case definition

The case 2 is set to run the basic model for 1500 days. Other settings are similaer to base case.

4) Compositional

Defined as simaler as ECLIPSE model for case 2 and setting are set according to the table 3 and 4 in Appendix E.

5) Flow conmponent

Wellbore and production tubing roughness and diameters as same as base case. It is assumed that oil is produced from 30 zones in the well, each of which contains two hypothetical sections as shown in figure 5.11. The production well has 30 valves. Since one valve is equvalant to 4 real valves, the diameter of one valve (AICD/AICV) is 0.0042 m considering CD as 0.85. Boundary conditions are set as following table 5.

Flow path name	Boundary Name	Boundary Type in OLGA
Wellbore	Inlet	Closed node
	Outlet	Closed node
Production tubing	Inlet	Closed node
	Outlet	Pressure node, Pressure =115 bar, Temp. = 68˚C

Appendix H: Case 2 water cut development & oil saturation

Just after OPENHOLE breakthrough

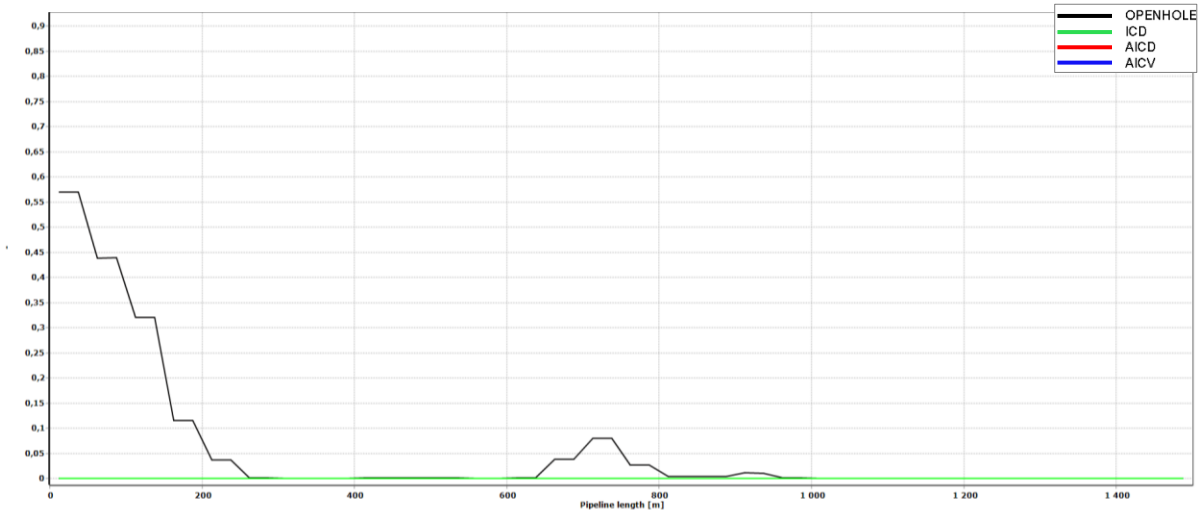

Just after FCD completions breakthrough

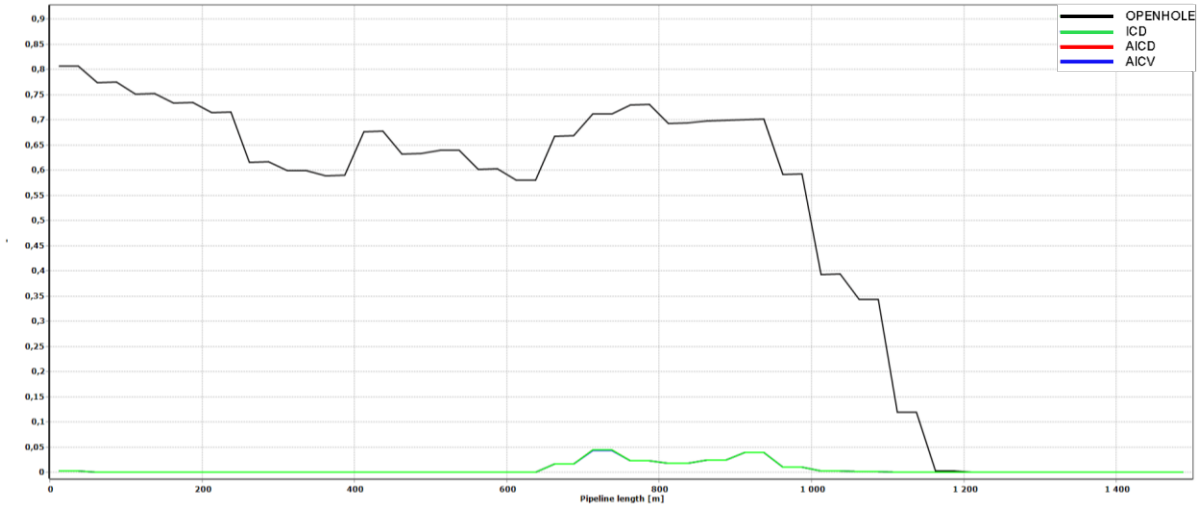

After 830days of production process.

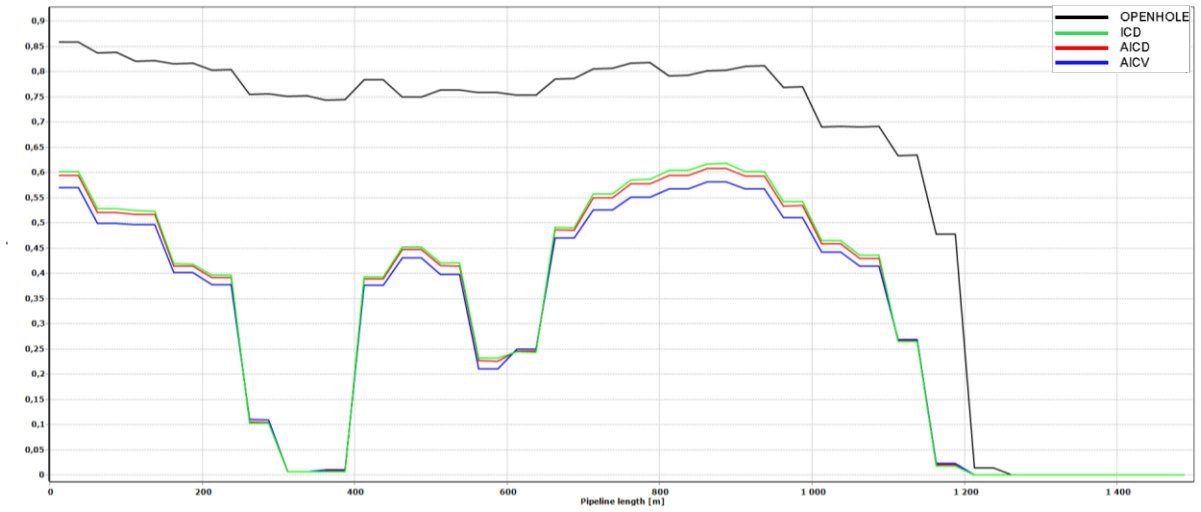

At the end of 1500days of oil production

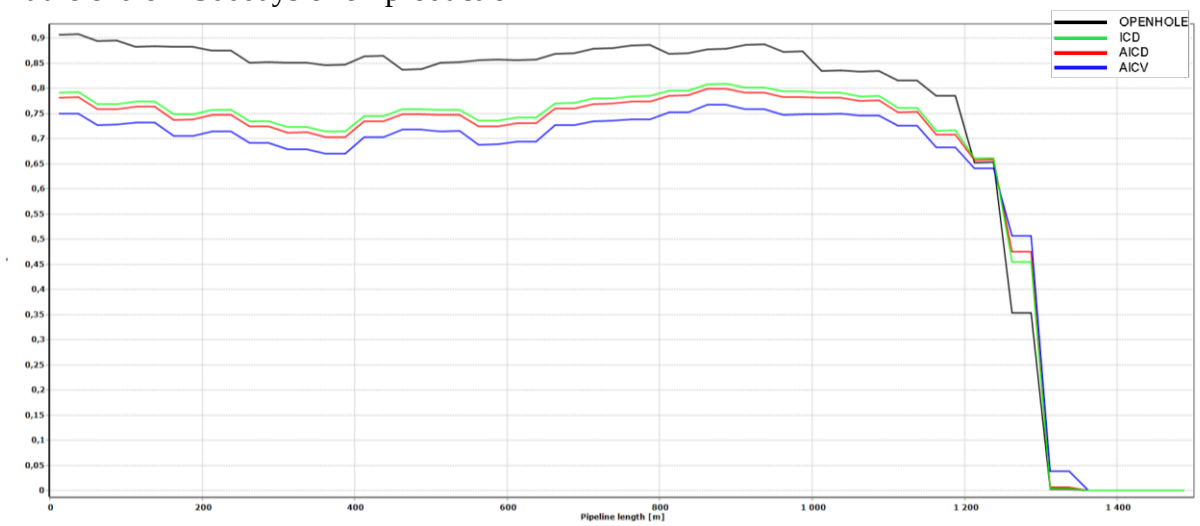

Oil saturation just after the water breakthrough

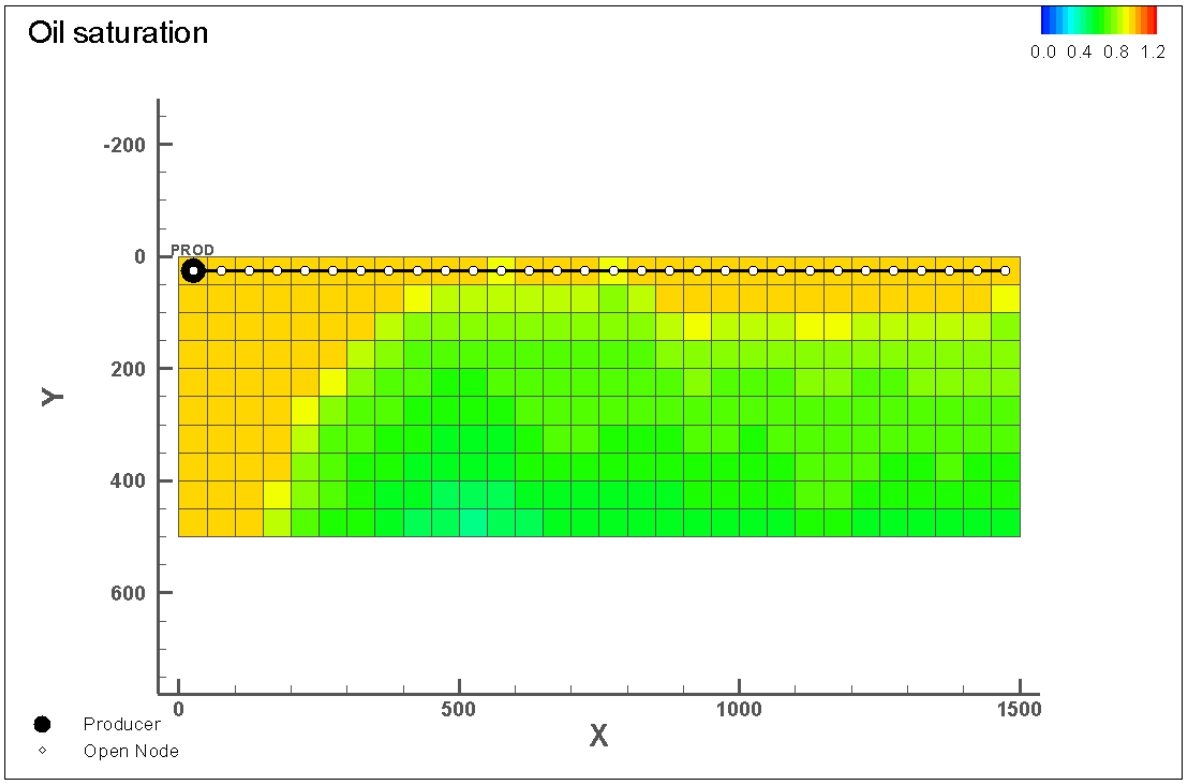

Appendix I: OLGA model for MLW case with two laterals